UNIVERSITÁ POLITECNICA DELLE MARCHE

DOCTOR OF PHILOSOPHY IN

"BIOMEDICAL SCIENCES"

Coordinator: Prof. Carlo Catassi

The Study of Malignant Melanoma Treatment on Various Platforms

Ph. D. dissertation by

Jiaojiao Zhang, B.Sc., M.Sc.

Supervisor: Prof. Maurizio Battino

Co-supervisor: Dr. Rongyi Chen

Co-supervisor: Dr. Francesca Giampieri

XXXIII Triennial Academic Cycle 2017-2020

To My Beloved Families

TABLES OF CONTENTS

ABSTRACT

With the medical improvement, the life expectancy has rocketed globally. Cancer as the main Noncommunicable disease (NCDs) is the major barrier to extend longevity, causing also a huge medical resource expense. Although innovative treatments as gene therapy, immunotherapy and classical treatments (i.e. chemotherapy, radiotherapy and surgical removal), there is no effective treatment to cure cancer, even because patients usually develop chemoresistance, radioresistance and some resist to gene therapy and immunotherapy as well. Skin is the largest organ first barrier of human body. The basal cell carcinoma, squamous cell carcinoma and melanoma are three common skin cancers Melanoma is a type of cancer that originally develops from melanocytes (pigment containing cells). Melanoma has dramatically increased during last 30 years with low five-year survival and prognosis rate. The current therapeutic approaches of melanoma not only could bring treatment assistance but also have serious side effects like vitiligo.

Under the setting of melanoma study, the current thesis investigated the melanoma suppression on different platforms. Firstly, resveratrol, a common bioactive compound, was used to target the potential biomarkers of melanoma. Secondly, through previous studies and then *in silico* research, certain biomarkers were furtherly targeted. Then *in vitro* melanoma-cell-culture models were investigated. We demonstrated that the melanoma cells were inhibited by protein-protein interaction. Third, after LC-MS/MS, the protein database was used to analyze and annotate the functions of the potential biomarkers. Forth, the rare case of amelanotic malignant melanoma (AMM) was reported that enlarged the understanding and supplement the phonotypes of melanoma.

Resveratrol (RSV) is a kind of phytoalexin that is widely distributed in Mediterranean diet, that as a bioactive natural product, could be a tumor suppressor. We evaluated the effects of RSV on melanoma cells (A375) and found that RSV could obviously inhibit the proliferation of melanoma cells by modulating cell cycle and triggering apoptosis; Cyclin D1 and PCDH9 were strongly affected by RSV duration

while RAC1 was not influenced. We furtherly explored the mechanism of these targeted genes of melanoma.

In silico and reference studies exhibited the PCDH9 would be the novel biomarker of melanoma. Therefore, the alteration of PCDH9 expression (overexpression and interference) were performed to explore the effects of PCDH9 on melanoma. The common matrix metalloproteinase (MMPs) is responsible for the extracellular matrix degradation. MMP2 -among the set of enzymes (MMPs)- has been demonstrated to play important roles in cell migration. The results of qRT-PCR exhibited that PCDH9 could suppress melanoma cells by affecting MMP2, CCND1 (Cyclin D1) and RAC1. The melanoma and healthy tissues were analogically analyzed to demonstrate the inhibition of melanoma cells by PCDH9. The methods of Co-IP and LC-MS/MS were used as well to deeply investigate the correlation between PCDH9 and its suppression effects of melanoma. We found that PCDH9 and RAC1 can predict the prognosis of malignant melanoma and hypothesized that PCDH9 can modulate melanoma progression through MMP2 and RAC1 by reducing RAC1-dependent ROS generation and enhancing NADPH oxidase activity complex.

The rare AMM firstly diagnosed as cutaneous squamous cell carcinoma (cSCC) was reported. According to the results of immunohistochemical examination (Ki67 (+++), Melan-A (+++), human melanoma black (HMB)45 (+), CD20 (-), cytokeratin (CK)7 (-) and CK5/6 (-) were found), the AMM was confirmed and the patient was applied surgical resection. This case showed the various phenotypes of melanoma. The main results are as follows:

(1) The bioactive investigation of RSV demonstrated that RSV strongly inhibited melanoma cells (A375 cells) proliferation, by decreasing cell viability, promoting apoptosis and arresting cell cycle. The double variance analysis of independent factors was operated after Bartlett's test for homogeneity by R project. The results clarified the major factor was duration nor concentration. In conclusion, RSV can inhibit A375 proliferation and trigger apoptosis by influencing cell cycle proteins; for these effects, treatment duration of RSV played more important role than concentration.

(2) The results of specimen investigation displayed lower PCDH9 expression in benign nevus tissue or/and normal skin than in malignant melanoma, and PCDH9 was mainly expressed in the cytoplasm rather than in nuclei. The results of a series of investigation on melanoma cells, and on human biopsy, revealed that PCDH9 could influence the expressions of MMP2, Cyclin D1 and RAC1. PCDH9 overexpression decreased cell viability, cell migration and increased apoptosis, but did not exert significant effects on cell cycle. This phenomenon indicated Cyclin D1 may affect melanoma cells by another approach. We hypothesized that Cyclin D1 might act as a transporter than cell regulator. The survival analysis showed that lower MMP2 expression could increase prognostic survival, presumably overexpression of PCDH9 might increase melanoma survival. RAC1 is involved in various cell biological processes and influences ROS generation that can trigger oncogenesis. PCDH9 negatively correlated with RAC1, whose character furtherly proved the suppressed mechanism of PCDH9 on melanoma cells. To be concluded, alteration of PCDH9 could influence melanoma cells viability. To make a further hypothesis, overexpression of PCDH9 suppressed melanoma cells and might increase prognostic survival.

(3) To map PCDH9-binding proteins, LC-MS/MS was applied to separate PCDH9-binding proteins and peptides, then protein data were processed by mainstreamed bioinformatic analyses. After performing KEGG pathway, Gene-Enrichment and Functional Annotation Analyses were done. We found most PCDH9-binding proteins in A375 cells were enriched in the terms of nuclear acid regulation, while in G361 cells were enriched in term of homeostasis control. However, the biological processes were similar in A375 and G361 cells. The PPIs in A375 were focused on regulation of nucleic acid, while in G361 on homeostasis. Therefore, we concluded that the analyses of PCDH9-binding proteins by bioinformatic platforms exhibited PPIs of PCDH9 to inhibit melanoma cells by different biological processes and suppress different melanoma cells by various pathways.

(4) The rare amelanotic malignant melanoma (AMM) initially diagnosed as cutaneous squamous cell carcinoma (cSCC) was reported. This AMM case showed the

various phenotypes of melanoma.

Key words: resveratrol (RSV); Protocadherins 9 (PCDH9); RAC1; CCND1; Cyclin D1; NADPH-oxidase; malignant melanoma (MM); ROS; PPI, mass spectrometry; PCDH9-binding protein; enrichment; annotation; bioinformatics servers; amelanotic malignant melanoma (AMM)

ITALIAN SUMMARY

Con il miglioramento della medicina, l'aspettativa di vita è aumentata vertiginosamente a livello globale. Il cancro rappresenta una delle principali cause di morte nel mondo, ma causa anche un enorme dispendio di risorse mediche. Sebbene negli ultimi anni siano stati sviluppati trattamenti innovativi come terapia genica, immunoterapia e trattamenti classici (cioè chemioterapia, radioterapia e rimozione chirurgica), ad oggi non esiste un trattamento efficace per curare questa patologia, anche perché i pazienti sviluppano spesso chemioresistenza, radioresistenza e alcuni resistono anche alla terapia genica e all'immunoterapia.

La pelle è l'organo più grande del corpo umano. Il carcinoma a cellule basali, il carcinoma a cellule squamose e il melanoma sono i tre tumori della pelle più comuni. Il melanoma si sviluppa originariamente dai melanociti (cellule contenenti pigmento) e la sua incidenza è aumentata notevolmente negli ultimi 30 anni con una bassa sopravvivenza a cinque anni e un basso tasso di prognosi. Gli attuali approcci terapeutici del melanoma non solo potrebbero essere inefficaci, ma anche avere gravi effetti collaterali come la vitiligine.

Nell'ambito dello studio del melanoma, l'attuale tesi ha studiato la soppressione del melanoma su diverse piattaforme. In primo luogo, il resveratrolo è stato utilizzato per identificare i potenziali biomarcatori del melanoma. In secondo luogo, attraverso studi precedenti e poi mediante studi in silico, alcuni biomarcatori sono stati ulteriormente valutati. Quindi sono stati studiati modelli di colture cellulari di melanoma *in vitro*. Abbiamo dimostrato che le cellule del melanoma erano inibite dall'interazione proteina-proteina. In terzo luogo, dopo analisi LC-MS/MS, il database delle proteine è stato utilizzato per analizzare e annotare le funzioni dei potenziali biomarcatori. Quarto, è stato riportato un raro caso di melanoma maligno amelanotico (AMM) che amplia la comprensione e integra i fonotipi del melanoma.

Il resveratrolo (RSV) è un tipo di fitoalessina ampiamente distribuita nella dieta

mediterranea che potrebbe agire anche da soppressore del tumore. Abbiamo valutato gli effetti dell'RSV sulle cellule di melanoma (A375) e abbiamo scoperto che l'RSV potrebbe inibire la proliferazione delle cellule di melanoma modulando il ciclo cellulare e innescando l'apoptosi; in particolare, l'espressione della Cyclin D1 e PCDH9 sono stati fortemente influenzati dalla durata del trattamento dell'RSV, mentre l'espressione di Rac1 non è stata affatto alterata. Abbiamo ulteriormente esplorato il meccanismo di questi geni mirati del melanoma.

Studi *in silico* hanno mostrato che il PCDH9 potrebbe rappresentare il nuovo biomarcatore del melanoma. Pertanto, l'alterazione dell'espressione di PCDH9 (sovraespressione e interferenza) è stata valutata per esplorare gli effetti di PCDH9 sul melanoma. La comune metalloproteinasi della matrice (MMP) è responsabile della degradazione della matrice extracellulare. È stato dimostrato che MMP2, tra l'insieme di enzimi MMP, gioca un ruolo importante nella migrazione cellulare. I risultati della qRT-PCR hanno mostrato che PCDH9 potrebbe sopprimere le cellule di melanoma influenzando MMP2, CCND1 (Cyclin D1) e RAC1. Il melanoma e i tessuti sani sono stati analizzati analogicamente per dimostrare l'inibizione delle cellule di melanoma da parte del PCDH9. I metodi di Co-IP e LC-MS/MS sono stati utilizzati anche per indagare in profondità la correlazione tra PCDH9 e i suoi effetti di soppressione del melanoma. Abbiamo scoperto che PCDH9 e RAC1 possono predire la prognosi del melanoma maligno e abbiamo ipotizzato che PCDH9 possa modulare la progressione del melanoma attraverso MMP2 e RAC1 riducendo la generazione di ROS dipendente da RAC1 e migliorando il complesso di attività dell'ossidasi NADPH.

Abbiamo anche riportato il raro caso di AMM diagnosticato per la prima volta come carcinoma cutaneo a cellule squamose (cSCC). L'AMM è stato confermato sulla base dei risultati dell'esame immunoistochimico (Ki67 (+++), Melan-A (+++), melanoma umano nero (HMB) 45 (+), CD20 (-), citocheratina (CK) 7 (-) e CK5 / 6 (-) sono stati trovati), e al paziente è stata applicata la resezione chirurgica. Questo caso mostra i vari fenotipi del melanoma. I risultati principali sono i seguenti:

(1) L'indagine bioattiva sull'RSV ha dimostrato che questo composto naturale ha

fortemente inibito la proliferazione delle cellule di melanoma (cellule A375), diminuendo la vitalità cellulare, promuovendo l'apoptosi e arrestando il ciclo cellulare. L'analisi della doppia varianza di fattori indipendenti è stata eseguita dopo il test di omogeneità di Bartlett da parte del progetto R. In conclusione, l'RSV può inibire la proliferazione dell'A375 e innescare l'apoptosi influenzando le proteine del ciclo cellulare; per questi effetti, la durata del trattamento dell'RSV ha giocato un ruolo più importante della concentrazione.

(2) I risultati dell'indagine sui campioni hanno mostrato un'espressione di PCDH9 inferiore nel tessuto del nevo benigno e nella pelle normale rispetto al melanoma maligno e il PCDH9 è stato espresso principalmente nel citoplasma piuttosto che nei nuclei. I risultati di una serie di indagini sulle cellule di melanoma e sulla biopsia umana hanno rivelato che PCDH9 potrebbe influenzare le espressioni di MMP2, Cyclin D1 e RAC1. La sovraespressione di PCDH9 ha ridotto la vitalità cellulare, la migrazione cellulare e aumentato dell'apoptosi, ma non ha esercitato effetti significativi sul ciclo cellulare. Questo fenomeno ha suggerito che la ciclina D1 può influenzare le cellule di melanoma con un' altra via. Abbiamo ipotizzato che la ciclina D1 possa agire più come trasportatore che come regolatore del ciclo cellulare. L'analisi di sopravvivenza ha mostrato che una minore espressione di MMP2 potrebbe aumentare la sopravvivenza prognostica, presumibilmente una sovraespressione di PCDH9 potrebbe aumentare la sopravvivenza del melanoma. RAC1 è coinvolto in vari processi biologici cellulari e influenza la generazione di ROS che possono innescare l'oncogenesi. PCDH9 è correlato negativamente con RAC1, dimostrando ulteriormente il meccanismo soppresso di PCDH9 sulle cellule di melanoma. Per concludere, l'alterazione della PCDH9 potrebbe influenzare la vitalità delle cellule di melanoma. Per fare un'ulteriore ipotesi, la sovraespressione di PCDH9 sopprime le cellule di melanoma e potrebbe aumentare la sopravvivenza prognostica.

(3) Per mappare le proteine leganti il PCDH9, analisi di LC-MS/MS sono state applicate a proteine e peptidi leganti PCDH9, quindi i dati sulle proteine sono stati elaborati mediante analisi bioinformatiche tradizionali. Dopo aver eseguito il percorso

KEGG, sino stati effettuati l' arricchimento genico e le analisi delle annotazioni funzionali. Abbiamo trovato che la maggior parte delle proteine leganti PCDH9 nelle cellule A375 sono arricchite in termini di regolazione dell'acido nucleare, mentre nelle cellule G361 sono omeostasi. Tuttavia, i processi biologici sono simili in entrambe le cellule A375 e G361. Gli IPP nelle cellule A375 si concentrano sulla regolazione dell'acido nucleico, mentre nelle cellule G361 si concentrano nel controllo dell'omeostasi. Pertanto, abbiamo concluso che le analisi delle proteine leganti PCDH9 da piattaforme bioinformatiche hanno mostrato PPI di PCDH9 per inibire le cellule di melanoma da diversi processi biologici e sopprimere diverse cellule di melanoma da vari percorsi.

(4) È stato riportato un raro melanoma maligno amelanotico (AMM) inizialmente diagnosticato come carcinoma cutaneo a cellule squamose (cSCC). Questo caso AMM mostra i vari fenotipi del melanoma.

Parole chiave: resveratrolo (RSV); Protocaderine 9 (PCDH9); RAC1; CCND1; Cyclin D1; NADPH-ossidasi; melanoma maligno (MM); ROS; PPI, spettrometria di massa; Proteina legante PCDH9; arricchimento; annotazione; server bioinformatici; melanoma maligno amelanotico (AMM).

LIST OF ABBREVIATIONS

Artificial intelligence (AI)

Acral lentiginous melanoma (ALM)

Adenosine monophosphate (AMP)

Amelanotic malignant melanoma (AMM)

American type culture collection (ATCC)

AMP-activated protein kinase (AMPK)

Angiotensin-1 (Ang-1)

Bovine serum albumin (BSA)

B rapidly accelerated fibrosarcoma (BRAF)

Cell Counting Kit-8 (CCK-8)

Complex immunoprecipitation (Co-IP)

Cutaneous squamous cell carcinoma (cSCC)

Dithiothreitol (DTT)

Gene Ontology (GO)

Hepatocellular carcinoma (HCC)

Immunohistochemical (IHC)

Malignant melanoma (MM)

Mass spectrometry (MS)

MEK (Mitogen-activated Protein Kinase)

Melanoma molecular disease model (MMDM)

Metalloproteinases (MMPs)

Molecular Disease Model (MDM)

Mucosal melanoma (MCM)

NCI (National Cancer Institute)

Nicotinamide adenine dinucleotide phosphate, reduce form (NADPH)

Noncommunicable disease (NCDs)

Photodynamic therapy (PDT)

Protein-protein interaction (PPI)

Protocadherins 9 (PCDH9)

RAF (Rapidly Accelerated Fibrosarcoma)

Ras-related C3 botulinum toxin substrate 1 (RAC1)

Reactive oxygen species (ROS)

Real time (RT)

Resveratrol (RSV)

Spatial Transcriptomics (ST)

Vascular endothelial growth factor (VEGF)

CHAPTER 1.

Chapter 1. General overview on melanoma

1 Epidemiology of melanoma

1.1 Recent conditions of cancer worldwide

Cancer has been expected as the major Noncommunicable disease (NCDs) that not only causes global deaths, but also is the most important barrier to extend life expectancy around the world [1-3]. It has become the main death factor before age 70, according to the statistic estimates of World Health Organization (WHO) in 2015. Since 2010 cancer has been the leading cause of mortality and become the main health problem also in China [4]. Currently, there is no effective therapy to cure cancer, and an increasing number of tumors resists to chemotherapy or/and radiotherapy, the so-called chemoresistance and radioresistance respectively [5], which represent the two major hurdles in cancer therapy.

1.1 Recent conditions of melanoma worldwide

Skin is the first barrier of human body [6], and skin cancers are common cancer types. Despite different therapeutic approaches (surgery, radiation and chemotherapy), the death incidence of skin cancer is continuous increasing [7]. There are three major categories of skin cancers: basal cell carcinoma, squamous cell carcinoma and melanoma [8]. Melanoma normally develops from the pigment-containing cells that are called melanocytes. Melanocytes are located in the basal layer of the epidermis and a type of cells that produce melanin, and melanocytes derived from neural crest stem cells (NCSCs) [9]. The origin of melanocyte could explain the melanoma migration to brain, lungs and other major organs [10]. According to research investigations, melanomas usually occur in the skin (cutaneous melanoma), sometime occur in eye, mouth and intestine [11, 12], but the occurrence of melanomas mostly happen in skin tissues [11, 12]. Therefore, melanoma is generally considered as one type of skin cancer, which

accounts for about 5% of all skin cancers [10]. Melanoma is not only the most malignant tumor, but also causes the major death of skin cancer among the other two types, which constitutes over 75% of all skin cancer deaths [10, 13]. Malignant melanoma (MM) has been considered as one of the most dangerous type of cancers in the world. The survival rate of this type of cancer (MM) is low [14]. According to the epidemiology data from World Health Organization (Source: Globocan 2018, International Agency for Research on Cancer): (1) The number of new cases in 2018 was 287,723 and the number of deaths in 2018 both sexes and all ages were 60,712; (2) The age standardized incidence rates of melanoma in females and males are represented in **Figure 1.1** and **Figure 1.2**; (3) The incidence, mortality and 5-year prevalence number of cutaneous melanomas in Europe population is shown in **Table 1.1**; (4) Overall, male are 1.2 times (3.5/2.9) more likely to develop melanoma than female, but the ratio of male to female is around 1 (1.01) in Europe, the same as in Asia (1.04) (**Figure 1.3 A**); (5) The incidence and mortality rates of cutaneous melanoma are higher in European than Asian population, which the rates of Europe are over the world average, while the rates of Asia are under the world average (**Figure 1.3 B**). The data of NCI (National Cancer Institute) present that the incidence of melanoma has rocketed over the last 30 years; estimated 7,230 deaths caused by melanoma in 2019 and its death rates have increased by 3.3% each year till 2009 [15, 16]. The investigation of Cancer Research 4 UK estimated that melanoma has an incidence rate of 3.1/10000 and a mortality rate of 0.8/10000 worldwide [17]. The five-year survival rate of patients with localized melanoma is 98%, while 64% for regional melanoma (**Table 1.2**) [10]. Unfortunately, the five-year survival rate of melanoma prognosis with distant metastasis still has been low (around 16%) [18, 19]. Meanwhile, in patients in stage IV, the five-year survival rate is as low as 23%, and they experienced metastasis to brain in over 60% diagnosed cases [20, 21]. The highest incidence of MM happened are in Queensland and Australia [22, 23]. The population incidence keeps increasing in Caucasian population, especially who are in United States, European countries [22, 23].

Table 1.1. The incidence, mortality and 5-year prevalence number of cutaneous

melanoma (Table was arranged from Globocan 2018, International Agency for Research on Cancer, World Health Organization)

Population	Incidence number	Mortality number	5-year prevalence number
Europe	144,209	27,147	494,111
North America	79,644	10,733	280,754
Asia	21,783	11,291	61,693
Latin America and the Caribbean	18,212	5,287	53,440
Oceania	17,246	2,111	61,500
Africa	6,629	4,143	14,125
Total	287,723	60,712	965,623

Table 1.2. The five-year relative survival rate of melanoma in different stages From the National Cancer Institute's Physician Data Query system

Stage at Diagnosis	Five-Year Relative Survival Rate
All Stages	90.5%
Stage 0	100%
Stage I-II (Localized)	97.6%
Stage III (Regional)	60.3%
Stage IV	16.2%

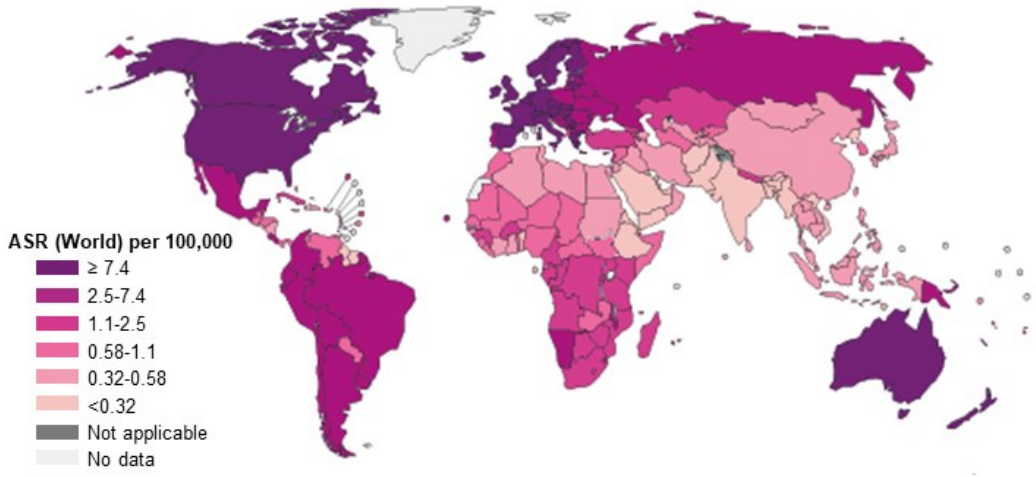

Figure 1.1. Age standardized (World) incidence rates, melanoma of skin, females, all ages (Data source: GLOBOCAN 2018, the graph produced by IARC http://gco.iarc.fr/today, World Health Organization)

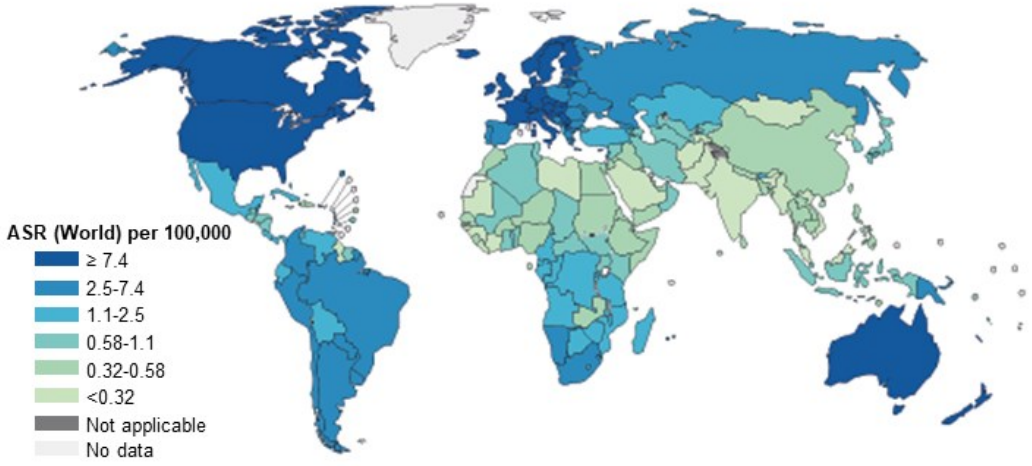

Figure 1.2. Age standardized (World) incidence rates, melanoma of skin, males, all ages (Data source: GLOBOCAN 2018, the graph produced by IARC http://gco.iarc.fr/today, World Health Organization).

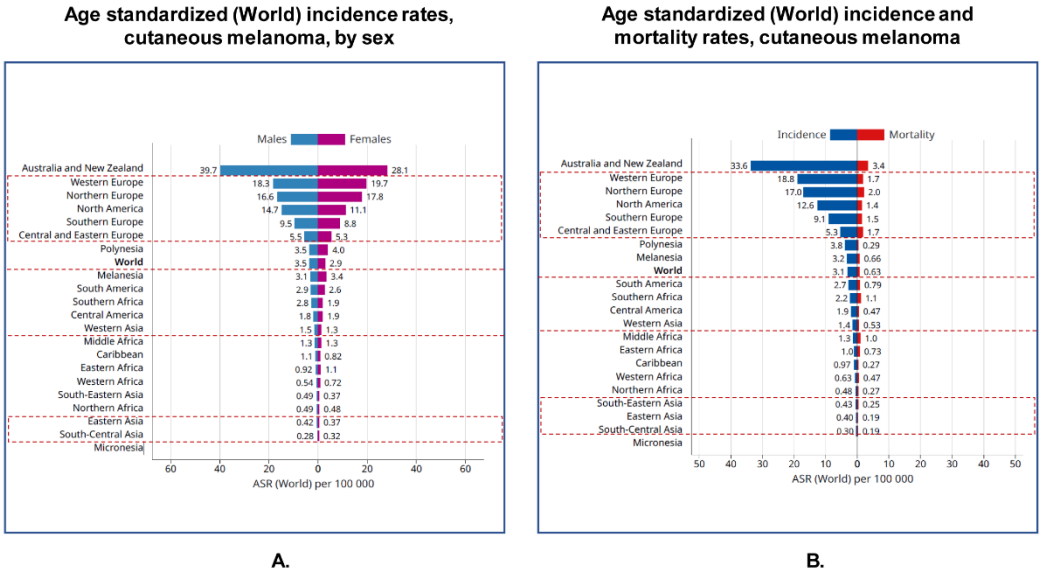

Figure 1.3. Aggregated pyramid of Age standardized (World) incidence rates, cutaneous melanoma by sex (A.); Age standardized (World) incidence and mortality rates, cutaneous melanoma (Data source: GLOBOCAN 2018, the graph produced by IARC http://gco.iarc.fr/today, World Health Organization).

2 Subtypes of melanoma

2.1 Phenotypes of melanoma

The percentages of cutaneous melanoma subtypes are different regarding population discrepancy. Acral lentiginous melanoma (ALM) has been popular – around 41.8% [24] - in Chinese malignant melanoma patients, while it only takes up 7-10% of malignant melanoma in Caucasian population [25, 26]; the second popular subtype is mucosal melanoma (MCM) in Chinese MM patients, while other subtypes are superficial spreading melanoma (SSM)) (around 70%), nodular melanoma (NM) (15-30%), lentigo malignant melanoma/lentigo maligna (4–10%) in western MM patients **(Figure 1.4.)** [27].

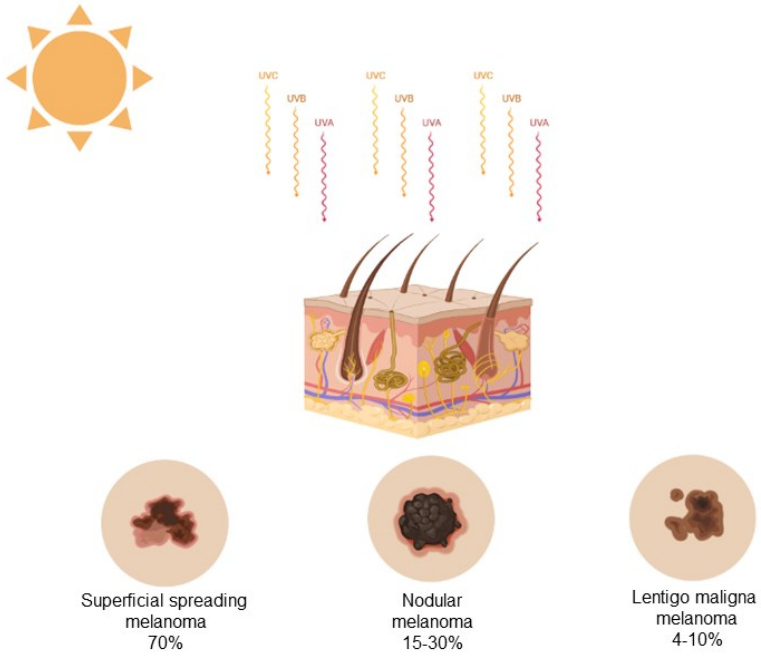

Figure 1.4. Subtypes of western MM patients are superficial spreading melanoma (around 70%), nodular melanoma (15-30%), lentigo maligna melanoma (4–10%), the figure is created in BioRender.com.

2.1.1 Superficial spreading melanoma

According to histologic study, superficial melanoma grows radially before their vertical growth into deeper tissue layers. Melanoma spreads are dispersed by single cell in radial growth phase, while melanoma is in vertical growth phase, once neoplastic melanocytes reach dermal layer [28]. The more frequency of this subtype occurs on women's lower extremities and men's back, and their lesions display various colors (i.e. black, blue, brown, white, gray, red), and irregular borders. Normally, the lesion's borders represent as asymmetric fare in advanced stage [28].

2.1.2 Nodular melanoma

Because of without the radial growth phase, nodular melanoma (NM) tends to grow more quickly in depth than in width compared to other melanoma subtypes [29], and NM may appear in spot without a lesion. Because NM looks similar to lesion, it usually

take longer time to determine melanoma, which leads to postpone therapy even gets worse prognosis. Commonly, nodular melanoma exhibits as darkly pigmented polypoid nodules [28], but some NM lesions can be multicolored as some are light-colored like light brown, even some are colorless. It is common that light-colored and non-pigmented NM lesions are ulcerated and/or bleeding [30].

2.1.3 Lentigo maligna melanoma

Lentigo maligna melanoma has evolved from a lentigo maligna that is the non-invasive skin growth [30], which is considered as a melanoma-in-situ [31, 32]. As soon as a lentigo maligna with melanoma cells invades the epidermis boundaries, it becomes a lentigo maligna melanoma [33], which is treated as an invasive melanoma. Mostly, lentigo maligna melanoma presents a small tanned asymmetric macule with irregular border at beginning, and then it enlarges into different colors.

2.2 Genetic subgroups of melanoma

There are four major genetic subgroups as follows: *(1)* activating $BRAF^{V600}$ mutations (around 50%) [34], *(2)* NRAS mutations (15–20%) [35], *(3)* inactivating mutations of NF-1 (around 10%, mutually exclusive with BRAF) [10], and *(4)* wild-type BRAF, NRAS and wild-type Kit (30–35% of patients) [36].

3 Signaling pathways of melanoma

According to different treatment, the signaling pathways could be classified into nine as follows: RAS/RAF/MEK/ERK (MAPK), AKT/PI3K/mTOR, c-KIT, WNT/β-catenin, CDK, GNAQ/GNA11, MITF, NRAS, and P53/BCL [37] **(Figure1.5)**.

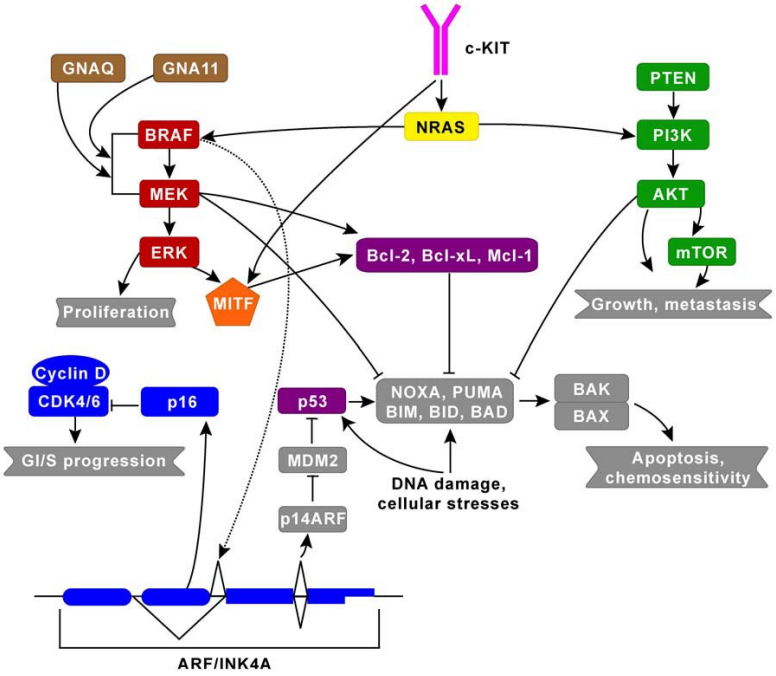

Figure 1.5. The signaling pathways could be classified into nine, among those, the two major signaling pathways implicated in melanoma are the MAPK and the mTOR pathway which regulate cell growth, proliferation and cell death [37].

3.1 MAPK and mTOR signaling pathways

Among mentioned pathways, MAPK and AKT/PI3K/mTOR pathways are major signaling pathways in melanoma, under whose regulation of cell growth, death, and proliferation, the balance of melanocyte differentiation and proliferation are coordinated by MAPK [37, 38]. These two main pathways are not separated, the pathways themselves and their downstream effectors have lots of cross talk. The MAPK pathway contains RAS, RAF, MEK and ERK, while RAS affect key regulators' transcription phosphorylation by triggering the RAF/MEK/ERK kinase complex formation [37]. Melanoma-triggered factors trigger wide-ranging intracellular signaling, most critical downstream events are triggered by extracellular factors, and furtherly those downstream events could activate MAPK-pathway [38]

3.2 WNT/β-catenin signaling pathway

While the conserved WNT/β-catenin pathway not only plays important part during the organism and even the whole life, overall, the role of WNT/β-catenin pathway is context-depended as it exhibits inhibition and enhancement of melanoma [39].

4 Study models of melanoma

4.1 *in vitro* study

4.1.1 Two-dimensional (2D) melanoma cell culture models

The classical in vitro studies are 2D models, also in the case of melanoma. They are relatively simple, but they are the first step in laboratory of targeted-based therapies for melanoma. Mostly, melanoma cells are grown on cell plates under high levels of oxygen and nutrients [40]. If the compounds have minor effects on melanoma cells, they usually have limited effects *in vitro* and *in vivo* models as well. So, 2D cell culture models have been the main investigated approach in study and utilized in beginning high-throughput screens of potential identifications [10].

4.1.2 Three-dimensional (3D) melanoma cell culture models (3D skin reconstruct, Spheroid)

Though lots of benefits in 2D models, there are some drawbacks of 2D melanoma models, such as the observed results could not represent the whole in vivo melanoma behavior. Besides, genetic drift could occur in long-term passaged cells that reduce reliability of results [10, 41]. 3D models could incorporate matrices and represent a contextual model to develop therapy against melanoma [42]. The 3D skin reconstruct comprises an “epidermis” (stratified, differentiated keratinocytes, a functional basement membrane) and a “dermis” [10, 42]. The “dermis” consists of fibroblasts embedded in the most prevalent extracellular matrix (ECM) found in the human skin,

collagen I [42]. In addition to the 3D skin reconstruct, spheroid is another 3D model that could intimate complex intracellular interactions as the *in vivo* conditions of melanoma patients [10]. Spheroids are aggregated cells that are adhered and invaded by outer cells, additionally, are embedded in collagen type I as "dermis" of 3D skin reconstruct [10]. Thus, 3D melanoma cell culture models display cellular condition, and they are complementary to conventional 2D models.

4.2 *ex vitro* study

Organoid is an *ex vivo* 3D model that similar to architecture of spheroids. The organoid platform could overcome limitation of spheroids by collecting organoid cultures from different areas of the same tumor or metastatic sites, which are present better tumor heterogeneity [10]. A study applied melanoma investigations in organoid platform and demonstrated the inhibition of TBK1/IKKε could increase the efficacy of PD-1 blockade with strong correlation with *in vivo* tumor response [43].

4.3 *in vivo* study

4.3.1 Non-murine *in vivo* melanoma models

White, R. M. et al. and Patton, E. E. et al. have used zebrafish for melanoma studies that made great progress [44, 45]. Non-murine *in vivo* melanoma models have advantages as high throughput that allow for investigate *in vivo* immune consequences.

4.3.2 Murine *in vivo* melanoma models

Traditionally, murine *in vivo* melanoma models comprise xenografting tumor cell stains. Firstly, human melanoma cells are cultured in cell plates and then engrafted into immunocompromised mice. Once xenograft melanoma models are established, murine stroma, lymphatic, and blood vasculature interact with melanoma cells that make melanoma dynamic *in vivo* possible [10].

5 Treatments of melanoma

5.1 Traditional treatments

The treatments of melanoma are various (i.e. surgery, radiation therapy, chemotherapy, electrochemotherapy, photodynamic therapy, hormone therapy, and/or immunotherapy). When patients are in early stage, mostly they could be cured by surgery and biopsies are combined. However, 10% cases are diagnosed as melanoma at late stage and exhibit visceral and brain metastases [46, 47]. Chemotherapy are used for progressed melanoma treatment [48].

5.2 Revolutionary therapies

FDA approved dacarbazine in 1974 for standard chemotherapy [49] and dacarbazine has been used as the sole care or combined with other chemotherapies as well as immunotherapies [50]. Dacarbazine's active metabolite, temozolomide (TMZ) has been used for advanced melanoma as well [50]. Electrochemotherapy (ECT) enhances the drug (normally cisplatin and bleomycin) delivery by high-intensity electric pulses [51, 52]. ECT has been applied to cutaneous and subcutaneous melanoma nodules with 85% response, without major negative reported adverse events [52, 53]. Photodynamic therapy (PDT)-a light-based therapy-has been used as an adjuvant treatment to stage III/IV cutaneous metastatic melanoma patients [54]. Because this method combined non-toxic compounds that generate reactive oxygen species (ROS) and photosensitizer, PDT is considered as a minimally invasive procedure [54, 55]. However, the efficacy of PDT is limited and needs to be improved [51]. Overcoming protective mechanisms as pigmentation and oxidative stress resistance could enhance PDT responses [56, 57]. Therefore, PDT has been combined with dacarbazine chemotherapy and this combined treatment displayed reduced resistance [58], meanwhile it can increase the eradicated effect and reduced melanoma recurrence [56].

5.2.1 Immunotherapy

Revolutionary therapies, like RAF (Rapidly Accelerated Fibrosarcoma) and MEK (Mitogen-activated Protein Kinase) inhibitors as well as anti-CTLA4 and anti-PD1, have been applied for patients in late stage [59, 60]. FDA has respectively approved targeted therapy and immunotherapy since 2011 and 2014. Although the combination of BRAF/MEK inhibitor was used in $BRAF^{V600}$ mutations patients with a response rate around 76% [61], over 80% patients would relapse on this treatment. While there hasn't been a targeted therapy that exhibited significant clinical efficacy in patients with wild type BRAF [62], MEK/CDK4/6 inhibitor cocktail has displayed pre-clinical activity and further clinical tests are under way [10]. The immune checkpoint PD-1 and CTLA-4 antibodies have demonstrated long responses in all subsets genotypes patients [60, 63], and anti-PD1 with anti-CTLA4 antibodies (ipilimumab, nivolumab and pembrolizumab) [64] as well as BRAF/MEK inhibitors (vemurafenib and trametinib) have displayed encouraging results in clinical trials [65-67]. However, there still are 60-70% melanoma patients who don't respond to immune checkpoint therapy [68], and other mutations like NRAS, NF1, CKIT, CDKN2A and PTEN have not been included in clinical practice yet [69].

5.2.2 Gene therapy

Additionally, FDA has approved fist virus-based melanoma drugs in 2015 [70]. Besides melanoma, in targeted cancers, like colon, cervix, glioblastoma and lung cancer viral vectors, as adenoviruses, alphaviruses, coxsackie viruses, herpes simplex viruses, have been applied to explore viral vector-based gene therapy [71, 72], whose research context is based on oncolytic viruses selective replication triggering tumor cell death and their vector spreading into neighboring cells [73]. Currently, non-viral vectors as well as viral vectors have been studies in gene therapy [69]. The delivery viral vectors are broad, including single-stranded (ss), double-stranded (ds) RNA, and DNA genome, meanwhile, they can express in short-term and long-term expression [74]. **Table 1.3** displays what virial vectors have been applied in gene therapy.

Table 1.3. Virial vectors applied in gene therapy

Virus vectors	References
SFV (Semliki forest virus)	[75]
SIN (Self-inactivating)	[76]
Reoviruses Reolysin	[77]
Newcastle disease virus	[78, 79]
Picornaviruses	[80]
HSV-1 (Herpes simplex sirus)	[81-83]
HSV T-VEC (Talimogene laherparepvec)	[84]
Reoviruses	[77]
Coxsackievirus	[81, 85]
Alphaviruses	[86]

Melanoma commonly afflicts the young and middle aged; however, people of all ages are at risk. It is the most common cancer in young adults aged 20-30 and is the leading cause of cancer death for women aged 25-30. Melanoma is significantly more prevalent among white populations than in blacks and Asians; the incidence of melanoma in blacks is approximately 1/20 than that of whites.

6 The purpose and significance of the study

Melanoma is one of the most dangerous cancer around world with low survival rate. For clarifying and understanding the mechanism of melanoma, a series of investigations were performed in this thesis project with various perspectives.

Firstly, resveratrol, a common bioactive compound, was used to target the potential biomarkers of melanoma. Secondly, through previous studies and then *in silico* research, certain biomarkers were furtherly targeted. Then *in vitro* melanoma-cell-culture models were investigated. Third, after LC-MS/MS analysis, protein database was used to analysis how PPI suppress melanoma. Forth, a rare case amelanotic malignant melanoma (AMM) was reported that enlarged the understanding and supplement the

phenotypes of melanoma.

Under the setting of melanoma study, the current thesis investigated the melanoma suppression on different platforms. We are attempting to provide prospect methods to overcome melanoma and increase survival rate.

7 Flow chart of this study

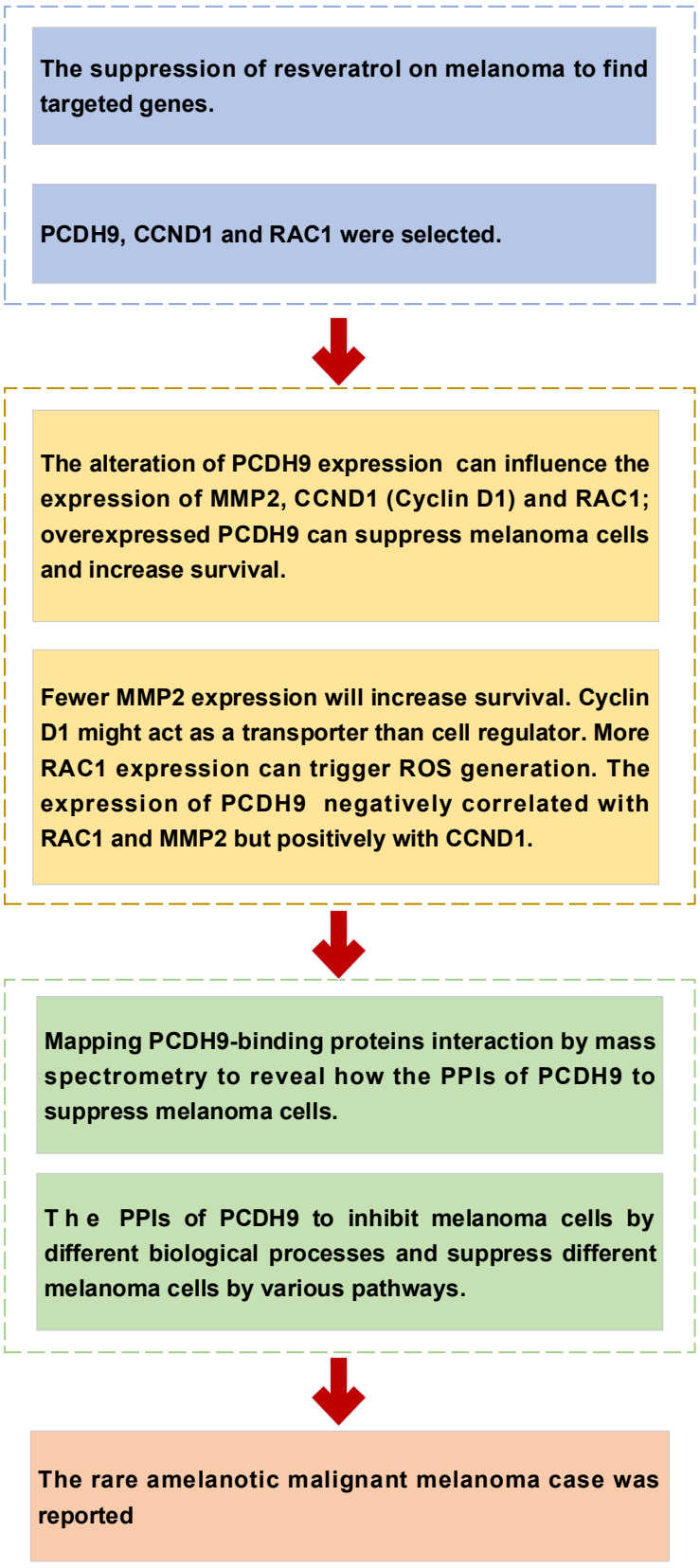

CHAPTER 2.

Chapter 2. Resveratrol inhibits the proliferation of melanoma cells by modulating cell cycle

1 Introduction

Bioactive natural products that are common in human diet have aroused interests in tumor suppression studies [87]. Resveratrol (RSV) is a kind of phytoalexin that is produced by plants when they are stimulated from environments (cutting, UV, pathogens as so on) [88]. The main plants that produce resveratrol are blueberries, raspberries, mulberries and grapes [89]. They all belong to main part of human diets, in other words human being can obtain RSV through daily diet. RSV has already been examined for its bioactivities by thousands of studies. Among them, lots have demonstrated that RSV can induce apoptosis and cell cycle arrest [5]. Specifically, RSV is a suppressor of A431 squamous carcinoma skin cancer cells [90, 91], both *in vitro* an in xenograft nude mice by downregulating protein expression [91]. Immunoblot and immunohistochemical analysis applied in SKH-1 nude-mouse models have revealed that RSV, through modulating essential cell cycle regulatory proteins, exerts anti-proliferative effects in skin cancer cells [92]. Therefore, we aimed to evaluate the effects of RSV on melanoma cells (A375).

The aim of this study was to evaluate the inhibitory effects of resveratrol (RSV) in A375 melanoma cells, by assessing cell viability (CCK-8 assay), apoptosis through flow cytometer and cell morphology, cell cycle assay by flow cytometer and western blot (Cyclin D1, Rac1 and PCDH9). Our results demonstrated that RSV strongly inhibited A375 cells proliferation, by decreasing cell viability, promoting apoptosis and arresting cell cycle. Besides, to clarify the main factor -duration or concentration of analyses Cyclin D1 and PCDH9 were strongly affected by RSV, duration while Rac1 was not influenced. In conclusion, RSV can inhibit A375 proliferation and trigger apoptosis by influencing cell cycle proteins; for these effects, treatment duration of RSV played more important role than concentration.

2 Materials and Methods

2.1 Chemical and reagents

DMEM and Fetal Bovine Serum (FBS) were purchased from Gibco (Thermo Fisher Scientific, shanghai, China); trans-RSV standard (trans-3,4,5-trihydroxystilbene), Triton X-100, and protease inhibitor cocktail were bought from Sigma-Aldrich (Shanghai, China); Cell Counting Kit-8 (CCK-8) were bought from Dongren Chemical Technology (Shanghai, China); BCA protein assay kit was purchased from Thermo Fisher Scientific (Shanghai, China); Antibodies (Cyclin D1 and Rac 1) and Beta-tubulin were purchased from Cell Signaling Technology (Shanghai, China), Antibodies (PCDH9) was purchased from abcam (Shanghai, China) while goat anti-rabbit immunoglobulin G-Peroxidase antibody was bought from Cell Signaling Technology (Shanghai, China); immobilon PVDF membranes and immobilon western chemiluminescent substrates were bought from Merck Millipore (Darmstadt, Germany); water was obtained from EPED-20TF (Nanjing, China).

2.2 Cell culture

A375 cell line (ATCC® CRL-1619™) was bought from the American Type Culture Collection (ATCC) (MD, USA), was grown in Dulbecco's Modified Eagle's Medium (DMEM) supplemented with 10% heat-inactivated fetal bovine serum as well as 100 IU/mL penicillin and 100 μg/mL streptomycin. Cells were maintained in a CO_2 incubator at 37°C under a humidified atmosphere (95% air, 5% CO2).

2.3 Cells' Lysates Preparation

After treatments with RSV for different hours (6, 12, 24, 48 and 72 hours) with different concentrations (0, 10, 50 and 100 μM), cells were lysed in a buffer containing 20 mM Tris–HCl (pH = 7.5), 0.9% NaCl, 0.2% Triton X-100, and 1% of the protease inhibitor cocktail. The analyses were conducted on cells between the third and the sixth

passages.

2.4 Cell viability: Cell Counting Kit-8 (CCK-8)

Cells were seeded into 96-well plates at a density of 2×10^5 cells/well and treated as explained above. RSV standards were directly dissolved in dimethyl sulfoxide (DMSO). After incubation, 10 μL of CCK-8 were added to each well, and cells were incubated for another 4 h at 37 °C. The level of colored formazan derivative was analyzed on Thermo Scientific Multiscan FC (Vantaa, Finland) at a wavelength of 450 nm [93, 94]. The viable cells were directly proportional to the formazan production and the percentage of viable ones was calculate. The following equations **(Equation1 and Equation2)** were utilized to determine the viability rate and inhibition rate respectively.

$$V\%=\frac{As-Ab}{Ac-Ab}\times100\% \quad \textbf{(Equation 1)}$$

$$I\%=\frac{Ac-As}{Ac-Ab}\times100\% \quad \textbf{(Equation 2)}$$

V%: the viability rate

As: the absorbing values of experimental wells (cells with medium, CCK-8, RSV)

Ab: the absorbing values of blank wells (medium, CCK-8)

Ac: the absorbing values of control wells (cells with medium, CCK-8)

I%: the inhibition rate

2.5 Apoptosis detection by flow cytometer and morphology investigation by EVOS XL Core Cell Imaging System

Apoptosis was measured using the flow apoptosis assay. Cells were seeded in 6-well plate at a density of 1×10^6cells/well and treated as explained above. At the end of the treatment, cells were centrifuged (1000 rpm for 10 min) and then cells were treated with Camptohtecin stock solution (1mM in DMSO) and incubated for 5 hours at 37°C. After that, the cells were washed twice by cold PBS and resuspended in 1X Binding Buffer 1 mL; to 100 μL of this solution 5 μL of FITC Annexin V (Bio-Rad) and 5 μL PI (Bio-Rad) were added. After vortexed gently and incubated for in the dark at room

temperature for another 15 min, the final solution was added 400 μL 1X Binding Buffer.

Finally, samples were analyzed using the BD FACSCanto II flow cytometer. Based on FITC Annexin V staining procedure, cells can be divided into three groups: *1)* viable cells not undergoing apoptosis as FITC Annexin V and PI both stain negative; *2)* cells in the early stages of apoptosis as FITC Annexin V positive and PI negative; *3)* dead cells and/or cells in the late stages of apoptosis that have damaged membranes as FITC Annexin V and PI both stain positive. The untreated cells were used to define the basal level of apoptotic and dead cells by subtracting the percentage of apoptotic cells in the untreated population from percentage of apoptotic cells in the treated population.

Besides, the morphological investigations of apoptosis were operated by Thermo Fisher Scientific EVOS XL Core Cell Imaging System (CA, USA), the magnification was 4×10. The cells with the common apoptotic features as cell shrinkage, membrane blebbing, chromatin cleavage, nuclear condensation and formation of pyknotic bodies of condensed chromatin were considered experiencing apoptosis [95].

2.6 Cell cycle assay by flow cytometer

Cell cycle was measured using the flow apoptosis assay. Cells were seeded in 6-well plate at a density of 1×10^6cells/well and treated as explained above. At the end of the treatment, cells were centrifuged (1000 rpm for 10 min) and then vortexed with 5 mL cold 75% ethanol, cells were incubated at -20°C for 2 hours, washed twice to remove ethanol (first washed in PBS and then washed in Stain Buffer) and centrifuged again (1000 rpm for 10 min); the cells were resuspended in 0.5 mL PI/RNase Staining Buffer (Bio-Rad) and after 15 min of incubation at room temperature, samples were analyzed using the BD FACSCanto II flow cytometer.

2.7 Western Blotting Analysis

Total protein concentration was detected by BCA protein assay kit. Equal amounts of protein (30 μg) of each sample were loaded and separated in a 10% acrylamide sodium dodecyl sulfate polyacrylamide gel electrophoresis (SDS/PAGE) and

transferred to immobilon PVDF membranes. Membranes were washed three times with PBS, blocked with 5% non-fat dry blocker, and incubated with the primary antibodies at 4℃ overnight. Next, membranes were washed with 5% Tween 20 in Tris HCl buffered saline and incubated with the secondary antibodies. Protein bands were visualized using Immobilon Western Chemiluminescent Substrate, and the protein signals were detected by Azure c500 Infrared Western Blot Imaging System from Azure Biosystems (CA, USA). Quantification of protein expression was made using the software Image J (Maryland, USA) and ggplot2 for visualization [96].

2.8 Statistical Analysis

The results are expressed as the mean values with standard deviations (SD) of three experiments and the statistical analysis was performed using the R Project for Statistical Computing [97]. After Bartlett's test for homogeneity of variances, the significant differences represented were obtained by double factor variance analysis ($p < 0.05$). For finding which factor has the main influence (treated concentration or duration) on inhibition, the double factor variance analysis of independent factors was performed by R project in different proteins separately. *gl() function* was used; and Bartlett's test was utilized for homogeneity of variances[98].

3 Results and Discussion

3.1 Inhibition effects of resveratrol on A375 cells' proliferation

To investigate whether RSV affected A375 cells' proliferation, Cell Counting Kit-8 (CCK-8) assay was performed. Cells were treated for 6, 12, 24, 48, and 72 hours with different concentrations (0, 10, 50, 100 μM) of RSV. **Figure 2.1A and 2.1B** show the viability and inhibition of cell percentage respectively. The inhibition was dose and duration dependent. The inhibition became stronger as the duration and concentration

increased. From the first 24 hours, the slope was very steep. Since then the inhibitory rate trend became very gently, and the trends were similar in different concentrations. In the other words, the inhibition increased with higher concentrations, but the tendency at 10, 50 and 100 µM were similar **(Figure 2.1 A)**. According to the results, the treatment time was very essential for cell viability. As time elapsed, the half maximal inhibitory concentration (IC_{50}) reduced a lot. For example, during the first 6 hours, the inhibition rate of 100 µM just reached 21.92%; after 12 hours the IC_{50} was around 100 µM; while 24 hours the IC_{50} was less than 50 µM. IC_{50} was less than 50 µM for duration of 48 and 72 hours **(Figure 2.1)**.

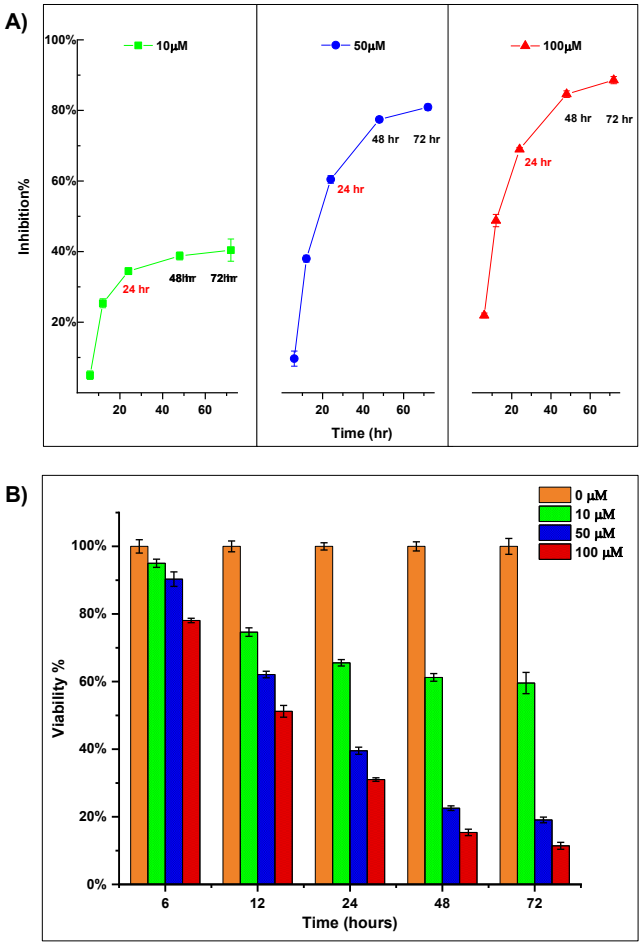

Figure 2.1. Inhibition of cell proliferation **(A)** and viability **(B)** by resveratrol in A375 cell line. A375 cells were treated with different concentrations of resveratrol (0, 10, 50 and 100 µM) for different time (6, 12, 24, 48, 72 hours). Cell viability was measured by using CCK-8 kit and results were expressed as a percentage (%) of inhibition and viability by Equation 1 and 2. Data are shown as the mean ± SD of three independent

experiments (n=3).

3.2 Apoptosis regulation by RSV on A375 cells

Apoptosis is a programmed cell death [99, 100], and it a highly regulated and controlled process during an organism's lifecycle. Since this process has the ability to modulate life or death of cell, it has been considered as therapeutic potential in pharmacy field [99]. Chemotherapeutic agents design and evaluation employ induction of apoptosis as an efficient strategy [101, 102]. We used flow cytometer to determine the percentage of live, dead cells and those in early apoptosis. A357 cells were treated with different concentration of RSV standards (0, 10, 50, 100 μM) with different time (24, 48, and 72 hours). The treatment durations were chosen according to the outcomes of inhibition analysis experiments, the IC_{50} with less than 50 μM was selected. The results showed that the effect of RSV treatment was duration and concentration dependent, with the higher concentration and longer time, the less cells lived, and more cells were through apoptosis to death **(Figure 2.2)**. The data in Figure 2 showed details folds of cells in different apoptosis stages as respect to control. The amounts of apoptotic cell population exhibited dependency on RSV treatment duration and concentration, with more treated time and higher concentration, the more cells had undergone through apoptosis to death **(Figure 2.2)**. Independently of concentrations, there were more cells in early apoptosis after 48 hours of treatment (Figure 2-B), while with 72 hours duration, there were more cells through apoptosis to death (Figure 2-C). In all treatments, there was no big difference in live cell amounts, especially in lower RSV concentration: when concentration was 10 μM, the folds respect to control were 0.96, 0.96 and 0.94 with durations 24 hours, 48 hours, and 72 hours respectively.

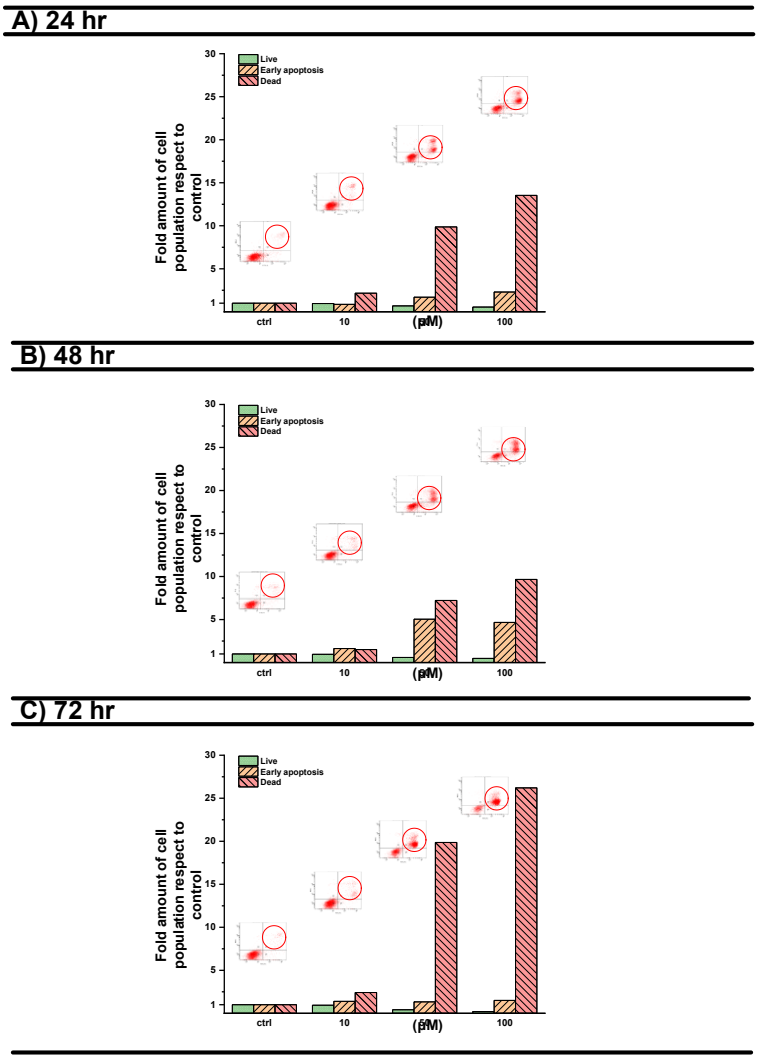

Figure 2.2. Resveratrol-induced apoptosis in A375 human melanoma cells, stained with annexin V-FITC and propidium iodide (PI) according to the manufacturers' instructions. (A) Cells treated with different concentrations of resveratrol for 24 hours. (B) Cells treated with different concentrations of resveratrol for 48 hours. (C) Cells treated with different concentrations of resveratrol for 72 hours. The viable cells are located in the lower left corner (negative for both annexin V-FITC and PI). Early apoptotic cells are in the lower right corner (annexin V-FITC positive). Late apoptotic cells showing signs of progressive cellular membrane and nuclear membrane damage are in the upper right corner (double positive). Necrotic cells lacking a cell membrane structure are in the upper left corner (PI positive).

As soon as cells underwent the apoptosis, they experienced morphological changes,

which include cell shrinkage, nuclear and chromosomal DNA fragmentation, and global mRNA decay. In order to further explore apoptosis in A357 cells, the morphological investigations were operated by Cell Imaging System (4 × 10) **(Figure 2.3)** from 12 to 72 hours. Results were similar to outcomes from flow cytometer: from 48 to 72 hours treatment cells got through early apoptosis to death. The best observation of apoptosis was after 48 hours RSV treatment, and since then more cells became dead. Figure 3 showed cells in apoptosis stage, the apoptosis morphology can be observed with RSV concentration at 50 μM after 12 hours, while after being treated for 24 hours, even at low RSV concentration (10 μM), the apoptosis was stronger. Although with increased treatment duration and concentration, the apoptosis became acuter **(Figure 2.3)**, the time factor influenced more than concentration factor to apoptosis morphological changes.

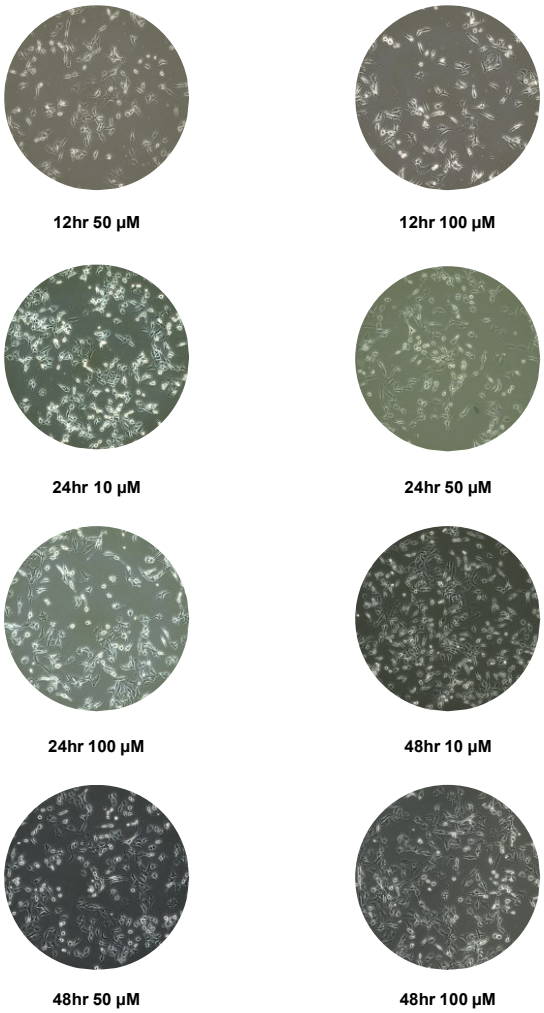

Figure 2.3. Cell morphology investigation by microscope after different treatment durations (24 and 48 hours) and concentrations (10, 50 and 100 μM). (The figures have not exhibited the cells without morphological changes.)

3.3 Cell cycle regulation by RSV on A375 cells

To further understand how RSV induced growth inhibition and apoptosis on melanoma cells, we performed cell cycle assay by flow cytometric methods **(Figure 4 A-C)**. The data of cells in different stages and the ratio of G2/G1 were collected for further analyses. G1 phase separates M from S, while G2 phase is between S and M [103, 104], both phases are checkpoints for cell proliferation, if they are activated and cause cells growth arrest, cells will be eliminated by apoptosis [104]. After 24 hours treatment with concentration of 50 μM and 100 μM, RSV induced most cell cycle arrest at the G1 checkpoint (50 μM-73.66% and 100 μM-78.03%) **(Figure 2.4 A, Table 2.1)** and for G2 phase there was no big difference between treatment with different concentrations (10 μM-5.89%, 50 μM-5.58% and 100 μM-4.35%), but as the RSV treatment duration increased, RSV didn't arrest more cells at G1. After 48 hours treatment we found 41.05%, 18.89% and 31.21% of cells in G1 phase at 10 μM, 50 μM and 100 μM, respectively, while 72 hours treatment led to 68.47%, 49.56% and 36.57% in G1 phase at 10 μM, 50 μM and 100 μM, respectively **(Figure 2.4 B-C, Table 2.2-2.4)**. Even when the duration time reached 48 and 72 hours with higher concentration, there was decreased cells amount in G1 period **(Figure 2.4, Table 2.2-2.4)**. The RSV associated G1 arrest was duration dependent.

Table 2.1. The percentage of A375 cells were arrested in G1 checkpoint by resveratrol with different concentration and duration.

	Resveratrol concentration (μM)			
Time (hours)	**0**	**10**	**50**	**100**
24	41.43%	24.13%	73.66%	78.03%
48	58.52%	41.05%	18.89%	31.21%
72	43.58%	68.47%	49.56%	36.57%

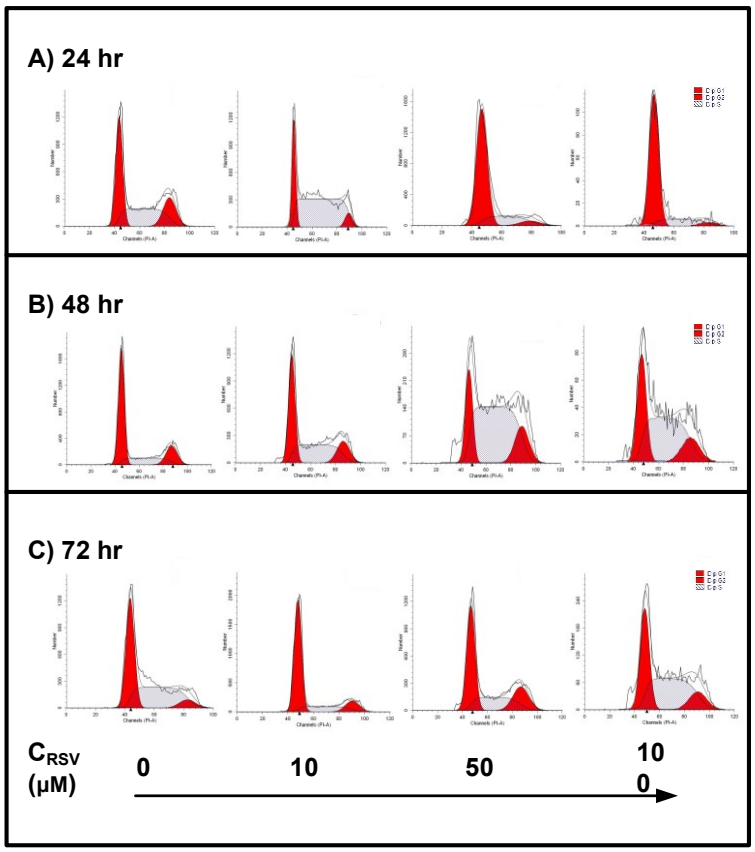

Figure 2.4. Effect of resveratrol on cell cycle progression in melanoma cells. A375 cells were exposed to the different concentrations (0, 10, 50 and 100 μM) and duration (24, 48 and 72 hours). Both adherent and non-adherent cells were harvested. Cell cycle distributions were analyzed by flow cytometry as described in the Materials and Methods.

Table 2.2. The percentage of A375 cells in different cell cycle by exposing to resveratrol with different concentration for 24 hours

Cell cycle	Resveratrol concentration (μM)			
	0	**10**	**50**	**100**
G1	41.43%	24.13%	73.66%	78.03%
G2	20.35%	5.58%	5.58%	4.35%
S	38.21%	69.98%	20.77%	17.62%
G2/G1	1.92	1.97	1.69	1.78

Table 2.3. The percentage of A375 cells in different cell cycle by exposing to resveratrol with different concentration for 48 hours

Cell cycle	Resveratrol concentration (μM)			
	0	**10**	**50**	**100**
G1	58.52%	41.05%	18.89%	78.03%
G2	18.56%	16.02%	14.72%	4.35%
S	22.92%	42.93%	66.39%	17.62%
G2/G1	1.92	1.91	1.91	1.84

Table 2.4. The percentage of A375 cells in different cell cycle by exposing to resveratrol with different concentration for 72 hours

Cell cycle	Resveratrol concentration (μM)			
	0	**10**	**50**	**100**
G1	46.65%	68.47%	49.56%	36.57%
G2	6.63%	12.56%	21.17%	12.26%
S	46.72%	18.97%	29.27%	51.18%
G2/G1	1.90	1.89	1.86	1.88

3.4 Cell cycle protein expressions by RSV on A375 cells

To explore whether the duration was the principle factor of RSV on A375 cells and how RSV affect A375 cell, three regulate cell cycle proteins, Cyclin D1, Rac1, Protocadherins 9 (PCDH9), have been chosen. Cyclin D1 protein is encoded by CCND1 gene that belongs to a highly conserved cyclin family. This cyclin family exhibits periodic characters in protein abundance through the cell cycle [105]; Rac1 encoded by the *RAC1* gene [106, 107], works with other RAC proteins to exert an essential role in cell growth and large-scale genomic researches make Rac1 has been considered as a target for melanoma [108]; PCDHs are the largest mammalian subgroup of the cadherin superfamily of homophilic cell-adhesion proteins [109], and PCDH9 is one of proteins of this family. Previous studies found the overexpression of cyclin D1 in breast carcinoma, therefore it has been considered as a biomarker [110] in cancer of *in vitro* researches; on the other hand, mutations in Rac1 are involved in melanoma [111-113] by large-scale genomic studies; recently studies have demonstrated that

PCDH9 can work as a suppressor to tumor by trapping cells at G0/G1 phase [114].

To clarify the main effect of RSV to cell cycle proteins, we analyzed the outcomes of western blot assays respectively to different proteins (Cyclin D1, PCDH9 and Rac1). First, we set two factors (duration (6, 12, 24, 48 and 72 hr) of RSV treatment as Factor A, concentration of RSV treatment as Factor B (0, 10, 50, and 100 μM)) and the data frame was 5×4. Second, the Bartlett's tests were utilized to check homogeneity. Finally, the double factor variances of independent factors were performed to find which factor affected more.

The Bartlett's test results of different cell cycle proteins are as following: Cyclin D1 (*p*-value of Factor A and B were 0.1147 and 0.5403), PCDH9 (*p*-value of Factor A and B were 0.1417 and 0.3418), Rac1 (*p*-value of Factor A and B were 0.1025 and 0.4133). All these values were over 0.05, in other words, the different levels of Factor A, B were homogenous in these proteins and Factor A, B can be operated double factor variances.

The outcomes of double factors variance analyses of independent factors are as following: Cyclin D1 (*p*-value = 0.0265 (Factor A) (< 0.05), while *p*-value (Factor B) = 0.7628 (> 0.05)), PCDH9 (0.0128 (Factor A) (< 0.05), while *p*-value (Factor B) = 0.6886 (> 0.05)), Rac1 (*p*-value = 0.0703 (Factor A), while *p*-value (Factor B) = 0.3103 (> 0.05), both values are over 0.5). On the basis of statistical results, Factor A (the RSV treatment duration) significantly affected expressions of Cyclin D1 and PCDH9, while the influence of Factor B (the RSV concentration) is not as vigorous as Factor A. Both factors haven't strongly influenced the expression of Rac1.

Also, the column graphs -which exhibited the protein expression tendency- were similar to the results of statistical analysis. **Figure 2.5 A-D** shows that RSV down-regulated the protein expression Cyclin D1 and PCDH9 in most treated time (6, 24 and 48 hours except 12 hours), while there was no obvious regularity of Rac1 expression. In particular, the amount of Rac1 increased in the first 6 hours, while the protein expressions of Cyclin D1 and PCDH9 decreased (**Figure 2.5 A)**. From 6 hours to 12 hours, RSV treatment increased all expressions of those proteins, except the PCDH9

that decreased at the concentration at 100 μM **(Figure 2.5 B)**. From 12 to 24 hours, Cyclin D1 and PCDH9 began decreasing, and Rac1 was reduced too. As concentrations increased from 50 to 100 μM, the protein expression didn't decrease a lot **(Figure 2.5 C)**. There was no significant difference between control and treatment groups in Rac1 (at concentration of 10 μM, the expression increased; at 50 μM, the expression hadn't changed; at 100 μM the expression decreased) after being treated 48 hours **(Figure 2.5 D)**. The schematic diagram displays how resveratrol effects on A375 **(Figure 2.6)**.

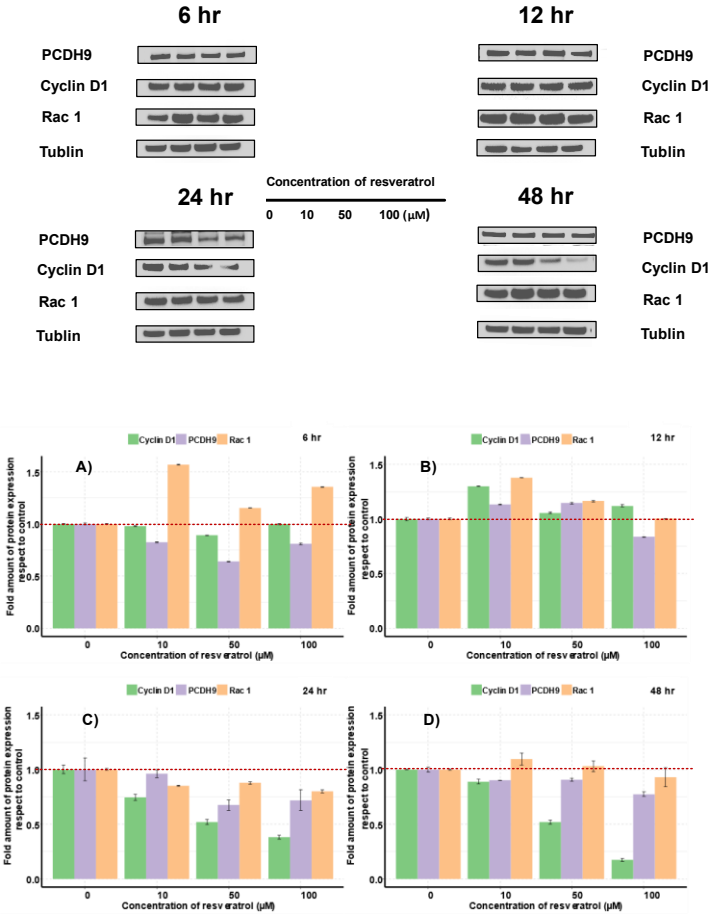

Figure 2.5. Proteins (Cyclin D1, Rac1 and PCDH9) expression in A375 cells after treatment with resveratrol for different concentrations (0, 10, 50 and 100 μM) and durations: (A) 6 hours, (B) 12 hours, (C) 24 hours, and (D) 48 hours.

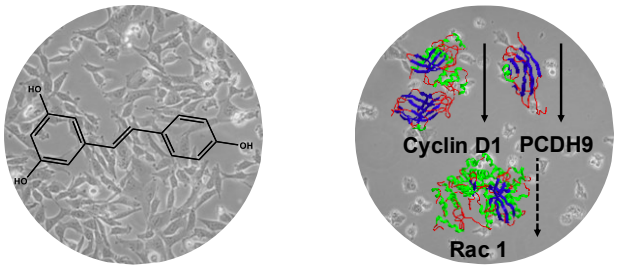

Figure 2.6. The schematic diagram of resveratrol effects on A375.

4 Conclusion

Malignant melanoma is a kind of highly malignant tumor [14], and A375 cell lines can be used to evaluate the therapy of melanoma and explore the mechanisms of how compounds influence this kind of tumor. RSV is a typical phytochemical that usually is a secondary metabolite of plant [115]. Previous studies have reported RSV has various biological functions including antitumor properties [116], especially on melanoma [117]. RSV has the ability to inhibit the proliferation of melanoma [118], by inducing cell-cycle disruption [119] and apoptosis as well [117, 119, 120]. We found similar results as those found in mentioned studies: RSV inhibited the proliferation capabilities of A375, and those effects were duration and concentration dependent, as these two factors increasing the rate become acuter. The two factors of RSV (duration and concentration) also influenced the degrees of RSV-induced apoptosis, being the treatment duration the principal factor **(Figure 2.2 and 2.3)**. RSV can influence A375 cells by affecting cell cycle: it downregulated Cyclin D1 and PCDH9, while the influence of RSV to Rac1 was not obvious **(Figure 2.5)**. Those results all pointed to treated time (duration) played more important role in influencing of A375 cells. Therefore, RSV may induce apoptosis of A375 cells and inhibit melanoma cells proliferation by modulating cell cycle, as previously reported [121] **(Figure 2.7)**.

This chapter represents a modified version of the paper already published: Yang H.Z. et al., Resveratrol inhibits the proliferation of melanoma cells by modulating cell cycle. International Journal of Food Sciences and Nutrition, 2020; 71:84-93. doi: 10.1080/09637486.2019.1614541.

Chapter 2 Conclusion

Background: Cancer is the major NCDs with global distribution. Malignant melanoma is one of the most dangerous caners with low survival rate. RSV has already been demonstrated that it could suppress tumor cells by inducing apoptosis and cell cycle arrest.

Methods: The inhibitory effects of RSV were evaluated by *in vitro* model that melanoma cells (A375) were chosen. RSV suppression were assessed by cell viability, apoptosis, cell cycle and cell morphology assay. Moreover, expressions of Cyclin 1, Rac1 and PCDH9 were also assessed by western blotting. The double variance analysis of independent factors was used to clarify the main factor by R project. Originlab 2018 was used for statistical analysis.

Results: RSV inhibited A375 proliferation; RSV could induce apoptosis; RSV could influence A375 cells by arresting cell cycle; RSV regulated cell cycle proteins in different effects as obviously downregulating Cyclin D1 and PCDH9 ($p<0.05$), Rac1 was not obvious ($p>0.05$). Our results demonstrated that RSV might induce apoptosis of A375 cells and inhibit melanoma cells proliferation by modulating cell cycle, which is similar to the previous study.

Conclusion: RSV can inhibit A375 proliferation and trigger apoptosis by influencing cell cycle proteins; for these effects, treatment duration of RSV played more important role than concentration **(Figure 2.7)**.

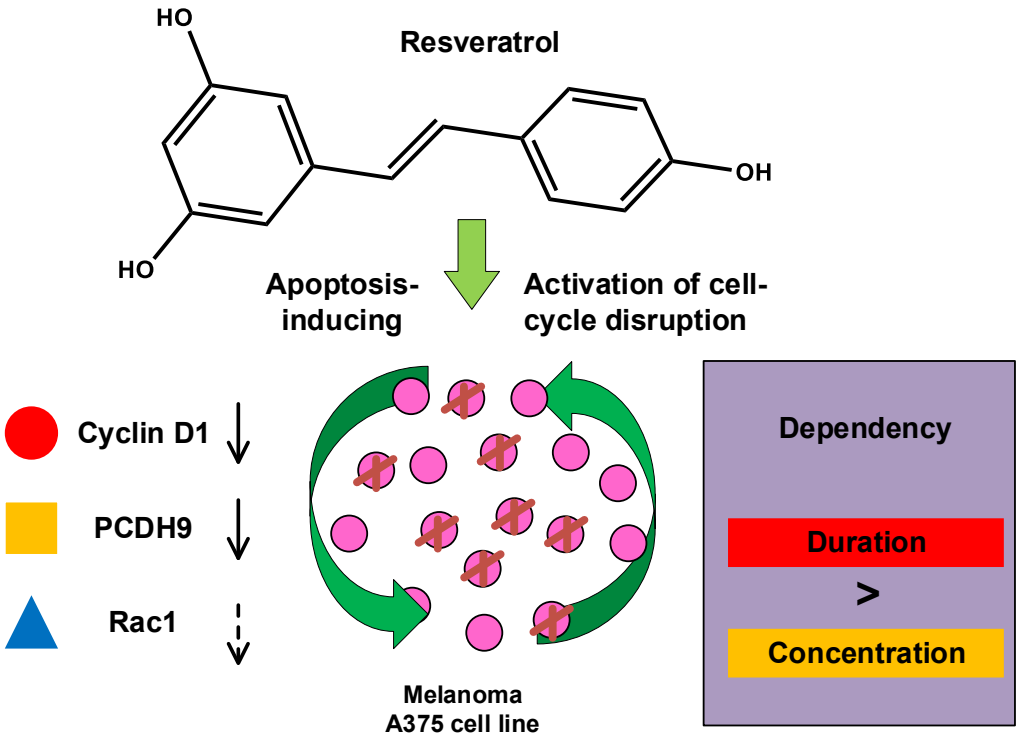

Figure 2.7. RSV may induce apoptosis of A375 cells and inhibit melanoma cells proliferation by modulating cell cycle, as previously reported

CHAPTER 3.

Chapter 3. Alteration of PCDH9 expression could influence melanoma cell viability

1 Introduction

Albeit numbers of validated biomarkers have been confirmed in melanoma, Chinese population has been demonstrated to gain different subtypes of melanoma from the Caucasian population [122], therefore the already-being biomarkers haven't predicted well in prognosis of Chinese melanoma patients. Hence, a novel biomarker, feasible is urgently needed. In order to figure out which genes could be relevant to Chinese population, bioinformatic technologies have been applied: PCDH9 has been chosen, while RAC1, PCDH9 and Cyclin D1 (CCND1) was found in our natural bioproduct against melanoma study [123, 124]. Besides, the result of PCDH9-expression evaluation by immunohistochemical (IHC) in patients' skin biopsy [125] exhibited that the positive percentage of PCDH9 expression is lower in human melanoma tissue than in normal skin or/and pigmented nevus tissue. PCDH9 belongs to Protocadherins, one of the largest subfamilies of calcium-dependent adhesion proteins [126]. Previous studies have demonstrated that the overexpression of PCDH9 could suppress different cancers [127, 128] and tumor cells by arresting cell cycle at G0/G1 phase [114, 129], it also can predict prognosis of cancer patients [127, 130]. Oppositely, RAC1 is a GTPase belonging to the RAS superfamily of small GTP-binding proteins. RAC1 functions as a molecule switch between active GTP-bound and inactive GDP-bound states through conformation changes closed to the nucleotide-binding site [126]. RAC1 could affect cellular adhesion, migration, and invasion [131], and it play important roles in tumor biology by modulating cell processes [132, 133]. Furtherly, activities of RAC1 have been reported of involving different stages of oncogenesis, such as initiation, progression, invasion and metastasis [134], even it was ranked as the third most frequently occurring mutation in melanoma induced by UV [135, 136]. Additionally, some reported ROS involving in tumor cell migration and

invasion [137, 138] and a key component of NAPDH-oxidase-complex formed by RAC1, one of the major enzymatic sources of ROS in various tissues [139]. While it's reported that RAC1 dependent NADPH-oxidase complex are involved in endothelial migration by mediation of angiotensin-1 (Ang-1) and vascular endothelial growth factor (VEGF) [140, 141]. As known, the endothelial migration is essential for tumor cell invasion, where RAC1-NADPH-oxidase complex induce expression of matrix metalloproteinases (MMPs) after growth factor and tumor promoter stimulation [142, 143]. Tumor-associated matrix metalloproteinase (MMPs) family has been studied for over half a century and are known as mediators in some cell processes [144]. Tumor-associated Matrix Metalloproteinase (MMP)s family has been studied for over half a century and are known as mediators in some cell processes [144]. Moreover, several studies demonstrated the important role of MMPs in melanoma [145]. Among them, MMP2 has been believed to act as a pro-tumorigenic and pro-metastatic factor in different cancers besides melanoma [146]. Therefore, MMP2 was chosen as tumor metastasis indicators of melanoma cells.

CCND1 encodes Cyclin D1 protein that belongs to highly conserved cyclin family. The members of cyclin family exhibit periodicity abundance throughout cell cycle. Cyclin D1-CDK4 complex regulates cell-cycle during G1/S transition. Cyclin D1 is the component of ternary complex (Cyclin D1/CDK4/CDKN18) and required for the Cyclin D-CDK4 complex translocation. Hence, CCND1 was selected to compare with the cell cycle assay.

The proteins that we chose (PCDH9, RAC1 and Cyclin D1) was according to our previous study, while MMP2 and MMP9 was usually used as tumor gene [145], but after dataset exploration (Human protein Altas, GEPIA), MMP9 represent cutaneous melanoma, hence we just chose MMP2 instead of both. Therefore, the main objective of this investigation was to clarify the role of PCDH9 in melanoma. After proceeding overexpression and interference of PCDH9 by GV358-PCDH9 lentivirus and GV358-SiRNA lentivirus in melanoma cell lines (A375 and G361), certain assays (cell viability, apoptosis and cell cycle assays, and PCR) were performed to explore the alteration-

influence of PCDH9 in melanoma cells. In current study, we evaluated that the alteration of PCDH9 had negative correlation with MMP2 and RAC1, while had positive with CCND1 (Cyclin D1) and apoptosis. Overexpression of PCDH9 could suppress melanoma cells and inhibit migration. Though the cell regulator protein, changes of Cyclin D1 (CCND1) altered with PCDH9, but did not exert significant effects on cell cycle. IHC showed lower PCDH9 expression in melanoma tissue and mainly expressed in the cytoplasm. It suggests that Cyclin D1 (CCND1) could affect tumorigenesis by mechanism of nuclear trafficking [147] nor via cell regulating. The result of IHC and survival analysis of MMP2 exhibited that PCDH9 would increase prognostic survival of melanoma. Taken together, our results reveal that alteration of PCDH9 expression could influence melanoma cells. Hence, we speculate that overexpression of PCDH9 suppressed melanoma cells and might increase prognostic survival.

2 Materials and Methods

2.1 Chemical and reagents

DMEM and Fetal Bovine Serum (FBS), PBS (pH=7.2) DEPC-treated water (Ambion) and TRIzol reagent (invitrogen) were purchased from Gibco (Thermo Fisher Scientific, Shanghai, China); ethanol (70%), Isopropyl alcohol, and Triton X-100 were bought from Sigma-Aldrich (Shanghai, China); Cell Counting Kit-8 (CCK-8) were bought from Dongren Chemical Technology (Shanghai, China); the primers (PCDH9, RAC1, CCND1, MMP2 and GAPDH) was designed and synthesized by Sangon Biotech (Shanghai, China); GV358-PCDH9 lentivirus and GV358-SiRNA lentivirus were designed by Genechem (Shanghai, China); SYBR® Premix Ex Taq™ Ex Taq ™ II and PrimeScript™ RT reagent Kit with gDNA Eraser were bought from Takara Bio Inc. (Beijing, China); water was obtained from EPED-20TF (Nanjing, China).

2.2 Cell culture

The same as Chapter 2-2.2.

2.3 Sample collection and Preparation

Tissues (human normal skin tissue (n=45), human pigmented nevus (n=30) and primary malignant melanoma tissue (n=30)) were collected and prepared as paraffin specimens until use. These tissues were ethically acquired from the outpatient clinic of the Affiliated Hospital of Guangdong Medical University with Chinese population (Han people) with personal identifiers redacted. The protocol of biopsy was proceeded according to the Ethical Committee of Guangzhou Medical University (PJ2015055KT).

2.4 Immunohistochemical (IHC) stains

IHC were performed on collected tissues (normal skin tissue, pigmented nevus and primary MM tissue) and 45 normal human skin tissues, 30 human pigmented nevus tissues, and 30 human malignant melanoma (MM) tissues were selected. These tissues were ethically acquired from the outpatient clinic of the Affiliated Hospital of Guangdong Medical University with Chinese population (Han people) with personal identifiers redacted. These MM tumor tissues were prepared as paraffin specimens. Deparaffinization included two 100% xylene changes (xylene I-10 min, xylen II-10 min) followed by rehydration with a graded series of ethanol (anhydrous ethanol I-5min, anhydrous ethanol II-5 min, 95% ethanol-5 min, 85%-5 min, 75%-5 min) and then rinsed under distilled running water for 3-5 min. Antigen retrieval consisted of a two-minute incubation of slides in citric acid retrieval solution heated to 98°C with a commercial steamer following a cool down step to room temperature (cold water and ice pack were added), slides were transferred into a wet box and were then rinsed three times by PBS. After protein blocking, primary antibodies (1:200) (Anti-PCDH9, Sigma-Aldrich; LOT #; HPA015581) were incubated at 4℃ overnight. After being in room temperature for 30 min, the slides were washed 3 times for 3 min each by PBS. After removing PBS and protein blocking, secondary antibodies (1:1000) were added

at room temperature for 1 h. The slides were then washed 3 times for 3 min each by PBS. After removing PBS, 1 drop of prepared DAB solution (1 ml A:1 drop B:1 drop C) for DAB staining was added and the slides were observed under microscope. After being rinsed in running water for 10 min, hematoxylin was added for 1 min and then the slides were washed by water for 5 min. The slides were then dehydrated in a series of ethanol (75%, 85%, 95%, 100%) and 100% xylene changes, and mounted with a coverslip with dry neutral resin.

2.5 Evaluation of various protein expression in MM

Evaluation of various protein expressions in MM were evaluated by semi-quantitative analysis, according to the staining intensity and the percentage of positive cells. The score standards of staining intensity were: no coloration-0, low intensity (light yellow)-1, medium intensity (light brown)-2, and high intensity (dark brown)-3. Five fields of view were randomly selected under microscope (400×), and 500 cells were counted as one unit, meanwhile the percentage of positive cells was calculated. The percentage scores were as follows: <5%-0, 6% to 25%-1, 26~50%-2; 51%~75%-3, >75%-4. The score standards were the product of staining intensity and percentage of positive cells: 0-negative (-), 1 to 4 -positive (+), 5 to 8 - moderately positive (++), and 9 to 12 - strongly positive (+++).

2.6 Survival analysis

Gene Expression Profiling Interactive Analysis (GEPIA) is web server for comprehensive expression analyses [148]. This web-based tool is based on the Cancer Genome Atlas (TCGA) [149] and Genotype-Tissue Expression (GTEx) [150]. The GEPIA web server provides survival analysis. GEPIA was used to analysis the tumor metastasis indicators of this study-MMP2.

2.7 Overexpression by Lentivirus Infection

Before experimental process, cells were divided into three groups: blank group (no

lentivirus), control group (lentivirus with empty plasmid) and PCDH9 group (lentivirus with overexpressed PCDH9 plasmid).

Different parameters of lentiviral infections were determined for optimizing the experimental conditions: (i) cell seeding density at 0.5×10^6 cell/mL, (ii) infectious time course at 12 hr post-infection, (iii) observed time at 72 hr post-infection, (iv) lentivirus titer of control group of 2×10^8 TU/mL, (v) lentivirus titer of transfected group of 1×10^9 TU/mL and (vi) MOI (Multiplicity of Infection) of 20.

Briefly, after seeding cells at an appropriate density in 2 ml in 6 well plates (1×10^5 cell/well), they were incubated for one day for 30%-40% adherence. They were then centrifuged for 30 sec under slow speed. After the inclusion of viruses (MOI=20), the fresh media with polybrene was added to maintain 1mL each, while the blank groups contained 1mL culture medium with 10% FBS. After being incubated for 12 hr, the media with lentiviruses was changed with culture medium with 10% FBS (2 mL). Cells were observed by fluorescent inverted microscope 72 hr post-infection and were screened by puromycin for post-infection assay.

2.8 Interference by Lentivirus Infection

Before the experimental process, cells were divided into three groups: blank group (no lentivirus), control group (lentivirus with empty plasmid) and PCDH9-SiRNA group (lentivirus with siRNA plasmid).

Different parameters of lentiviral infections were determined for optimizing the experimental conditions: (i) cell seeding density at 0.5×10^6 cell/mL, (ii) infectious time course at 12 hr post-infection, (iii) observed time at 72 h post-infection, (iv) both lentivirus titers of control group and transfected group of 1×10^9 TU/mL, (v) MOI (Multiplicity of Infection) was of 20.

After seeding cells at the appropriate density in 2 mL in 6 well plates (1×10^5 cell/well), they were incubated for one day for 30%-40% adherence. They were then centrifuged for 30 sec under slow speed and after including the viruses (MOI=20), the fresh media with polybrene was added to maintain 1 mL each, while the blank groups

contained 1 mL culture medium with 10% FBS. After being incubated for 12 h, the media with lentiviruses was changed with culture medium with 10% FBS (2 mL). Cells were observed by fluorescent inverted microscope 72 h post-infection. and were screened by puromycin for post-infection assay.

2.9 Cell viability by Cell Counting Kit-8 (CCK-8)

The same as Chapter 2-2.4.

2.10 Apoptosis detection by flow cytometer

The same as Chapter 2-2.5.

2.11 Cell cycle assay by flow cytometer

The same as Chapter 2-2.6.

2.12 Wound-healing assay

Cells were seeded onto six-well plates at a density of 1.5×10^5 cells/well and were incubated under cell culture conditions for 24 h till confluent condition. The scratched wounds were created by a sterile 10 μL pipette tip. The suspension cells were washed twice by PBS, then DMEM (10% FBS) were added for incubation at 0h, 24h, and 48h after which DMEM were discarded. The cells were fixed 3.7% formaldehyde in PBS for 30 min and stained with 0.1% toluidine blue at room temperature for another 30 min. The wounds were viewed using an inverted microscope DMI3000B (Leica, Germany). The image J (Maryland, USA) was applied to measure the wound space. The wound closure rates were determined at 0 h, 24 h and 48 h.

2.13 TRIzol RNA Isolation and Purity determination

Cells were rinsed by cold PBS and lysed by TRIzol Reagent, after which they were thoroughly vortexed, centrifuged for 5 min (300×*g*) and supernatant was discarded and

refreshed with cold PBS; after spinning for 5 min (300×*g*), TRIzol was repetitively added and after a five-minute incubation at room temperature, the sample was centrifuged to remove debris. According to the amount of TRIzol, chloroform was added (0.2 mL chloroform to 1 mL TRIzol); after being vortexed vigorously (15 sec) and after a three-minute incubation at room temperature, the sample was spun at 4℃ for 15 min (12,000×*g*); aqueous phase was taken. RNA was precipitated by isopropyl alcohol (0.5 mL isopropyl alcohol to 1 mL TRIzol in homogenized step), after ten-minute incubation at 20℃. The supernatant was discarded and then the RNA, which was at the bottom of tube, was washed by 75% ethanol (1 mL ethanol to 1 mL TRIzol in homogenized step). The sample was centrifuged at 4℃ for 5 min (7,500×*g*) several times till all ethanol was removed. After being dried for eight-minutes, the RNA sample was dissolved in DEPC-treated water by pipette tip (1 μL RNA to 39 μL DEPC-treated water, 1:40 dilution). the A_{260}/A_{280} of RNA which was extracted was above 1.6.

2.14 Quantitative Real-Time PCR analysis

Each frozen pellet of melanoma cells (A375 and G361) treated in different experimental conditions were homogenized in a lysis buffer. Total RNA was isolated through the TRIzol Reagent Total RNA isolation system (Thermo Fisher Scientific, United States) according to the manufacturer's reference guide. Total RNA was quantified by nanodrop, was reverse transcribed by PrimeScript RT reagent kit TaKaRa referred to SYBR Green qPCR assay introduction (SYBR® Premix Ex TaqTM II kit) by MasterCycler Gradient PCR (Thermo Fisher Scientific, United States). The reaction mixture (20μL) was taken and incubated for three minutes at 95°C. Quantification of genes was performed with the $2^{-\Delta\Delta CT}$ method, as described previously [151]: the sample was cycled (95°C-10 sec and 60°C-20 sec) for 40 times by ABI7500Fast Real-time PCR System Amplifier (Thermo Fisher Scientific, United States). The primers designed for selected genes (PCDH9, CCND1, MMP2, RAC1 and GAPDH) and amplicon sizes are shown in **Table 3.1**.

Table 3.1. Primers designed for the amplifications of selected genes and amplicon sizes.

Name	Sequences (5'→3')	Sizes (bp)
PCDH9	F: TCCCAACTCTGATGGGCCTTTGGG R: GGCTCTGGTCAGGGTGTGCC	217
CCND1	F: AGGAGAACAACTCTGACAACCACAATC R: GCTCTTGATCGTCCTCTGACCAATAC	93
MMP2	F: TTTGACGGTAAGGACGGACTC R: TACTCCCCATCGGCGTTC R: TCAGGGCGAGGACCATAGAG	146
RAC1	F: ACAAGCCGATTGCCGATGTGTTC R: TGCCGCACCTCAGGATACCAC	97
GAPDH	F: TAAAAGCAGCCCTGGTGACC R: CCACATCGCTCAGACACCAT	88

2.15 Statistical Analysis

Data are presented as the mean ± SD from at least 3 independent experiments. Statistical comparisons between two groups were made using Student's t tests. Differences among three or more groups were compared by one-way ANOVA followed by least significant difference post hoc tests (Originlab 2020, Northampton, MA, USA), $p<0.05$ was considered as statistically significant, while $p<0.01$ was considered as highly statistically significant.

3 Results and discussion

3.1 PCDH9 protein expressed differences in normal skin, pigmented nevus and melanoma tissue tested by IHC stains

IHC results showed that the positive percentage of PCDH9 expression was lower in human melanoma tissue than in normal skin or/and pigmented nevus tissue; additionally, PCDH9 was mainly expressed in the cytoplasm, while a small amount was expressed in the nuclei. The positive percentage of PCDH9 was expressed in normal skin or/ and pigmented nevus tissue, while only 23.3% (7/30) in melanoma tissue, which was lower than non-tumor tissue **(Table 3.2, Figure 3.1).**

Table 3.2. The positive percentage of PCDH9 expression in normal skin, pigmented nevus and melanoma tissues.

Time (hours)	Total	PCDH9(-)	PCDH9(+)	Positive Percentage
Normal skin	45	0	45	100.0%
Pigmented nevus	30	0	30	100.0%
Melanoma	30	23	7	23.3%

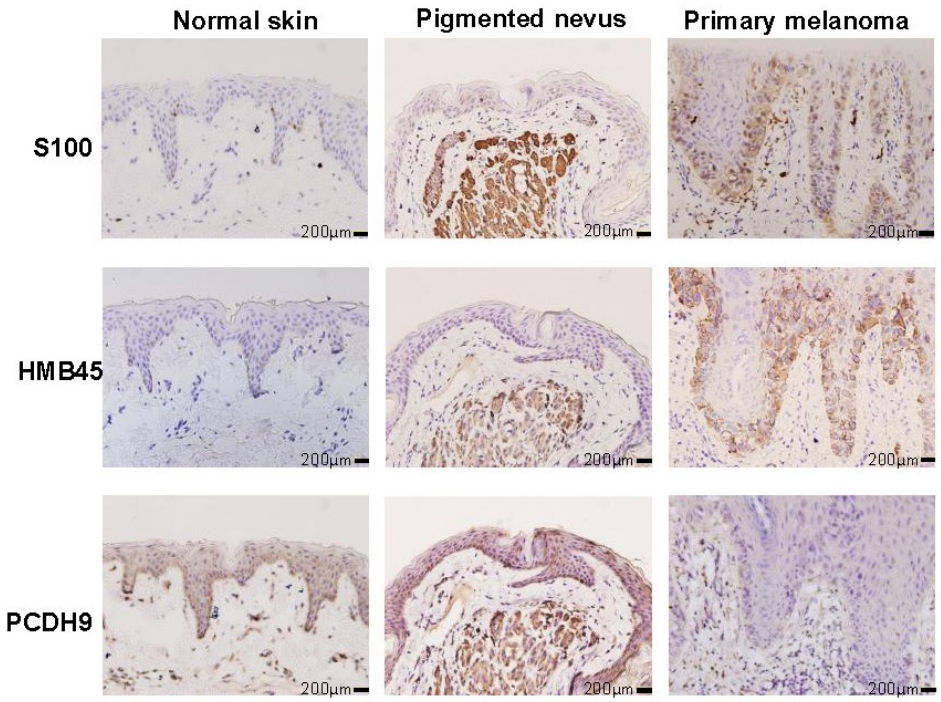

Figure 3.1. Immunohistochemical analyses of PCDH9 expression in normal skin, pigmented nevus and melanoma tissue. Positive percentage of PCDH9 expression was lower in human melanoma tissue than normal skin or/and pigmented nevus tissue. PCDH9 was mainly expressed in cytoplasm, while a small amount in nuclei. S100 and HMB45 are melanoma markers. The scale bar represents 200 μm.

3.2 The survival analysis of MMP2

GEPIA was used for survival analysis of MMP2: the cutoff was set as median;

calculate the hazards ratio based on Cox PH Model; Cancer datasets was SKCM (Skin Cutaneous Melanoma); Multiple Datasets were selected. The survival rate of highly expressed MMP2 is poorer than lowly expressed MMP2, and the HR is 1.5 (p<0.05) **(Figure 3.2).**

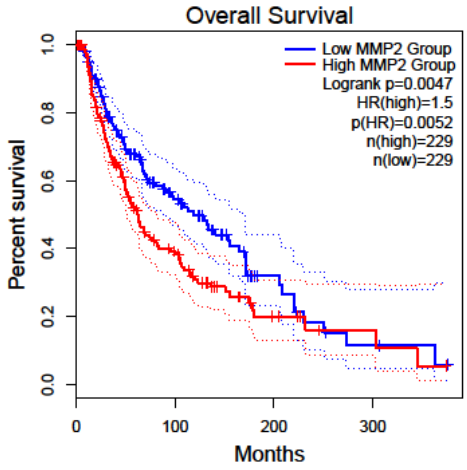

Figure 3.2. Survival curves of MMP2 in normal and Skin Cutaneous Melanoma (SKCM) tissues based on TCGA data in GEPIA. Red line represents the samples with MMP2 highly expressed (n=229), while blue line exhibits lowly expression (n=229) (Logrank p=0.0047). HR represents hazard ratio. The p value of HR is less 0.05 (p=0.0052).

3.3 PCDH9 expression affected selected gene expressions and protein expressions

PCDH9 was overexpressed by lentivirus with PCDH9 plasmid **(Figure 3.3 A)** and interfered by lentivirus with siRNA **(Figure 3.3 D, E)**. The relative expression of selected genes (CCND1, MMP2, RAC1) varied with PCDH9 expression, but the effectiveness on them was different. PCDH9 and CCND1(Cyclin D1) exhibited positive correlation **(Figure 3.3 B, C, D, E)**, while RAC1, MMP2 exhibited negative in both melanoma A375 and G361 cells **(Figure 3.3 B, C, D, E)**.

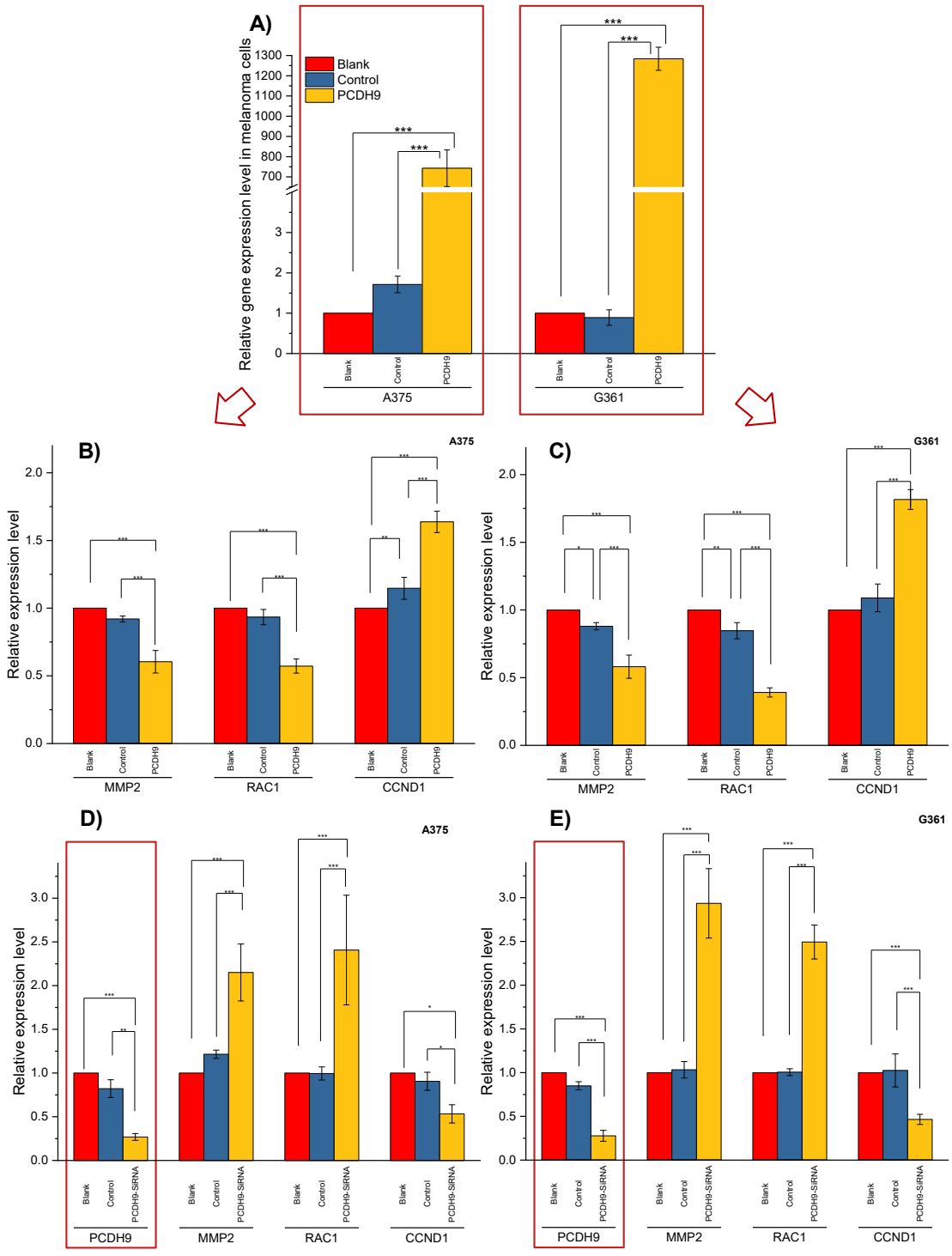

Figure 3.3. Effects of overexpressed and interfered PCDH9 in melanoma cells measured by PCR analysis (**A**). The expressions of PCDH9 were significantly upregulated by lentivirus infection. Overexpressed PCDH9 significantly upregulated CCND1 and downregulated RAC1, MMP9 in both cells (A375-**B**, G361-**C**). Interfered PCDH9 downregulated CCND1 and upregulated RAC1, MMP2 in both cells (A375-**D**,

G361-**E**). *p<0.05, **p<0.01, ***p<0.001 compared in groups by using one-way ANOVA followed by least significant difference post hoc tests.

3.4 Effects of overexpressed PCDH9 on cell viability

The overexpression of PCDH9 reduced the proliferation of melanoma cells. Overexpressed PCDH9 groups showed indeed a lower viability than control groups **(Figure 3.4)**. As time passed, the viability of melanoma cells tended to stabilize, but PCDH9 overexpressed groups had less viable cells than control groups in different durations **(Figure 3.4 C, D)**, and the differences between PCDH9 and control groups were significant (24, 48, 72 and 96 hours) **(Figure 3.4 A, B)**.

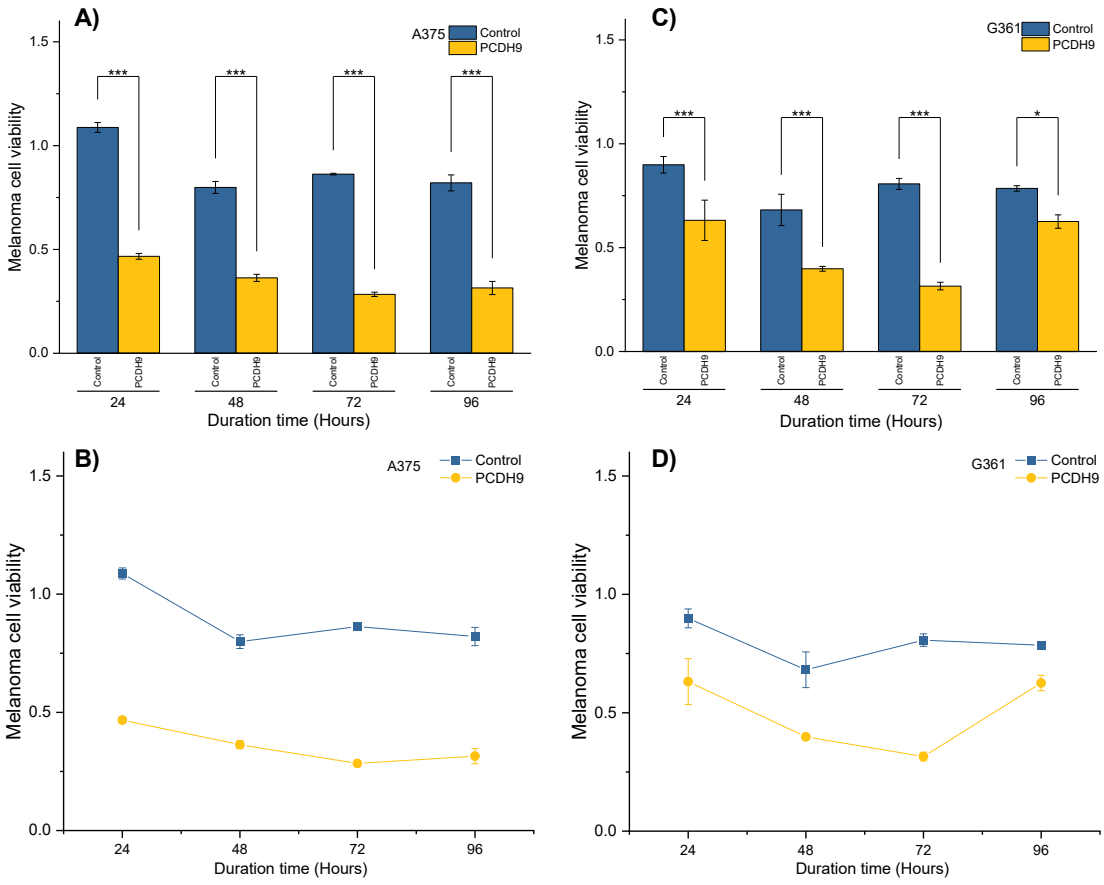

Figure 3.4. The viability of melanoma cells significantly was reduced by overexpressed PCDH9 in A375 (**A**, **B**) and G361 (**C**, **D**) cells. * p<0.05, **p<0.01, ***p<0.001 compared with control groups by using Student's t tests. The alteration of PCDH9 expression significantly affected the apoptosis of melanoma cells.

3.5 Effects of PCDH9 alteration on apoptosis

The overexpression of PCDH9 promoted the apoptosis in both melanoma cells **(Figure 3.5 C)**, the apoptosis percentage of PCDH9 overexpression was exhibited by **Figure 3.5 A** (A375) and **B** (G361). While the interfered PCDH9 reduced the apoptosis in both cell lines **(Figure 3.6 C),** the apoptosis percentage of PCDH9 interference was exhibited by **Figure 3.6 A** (A375) and **B** (G361). The alteration of PCDH9 and apoptosis exhibited positive correlation **(Figure 3.5, 3.6)**.

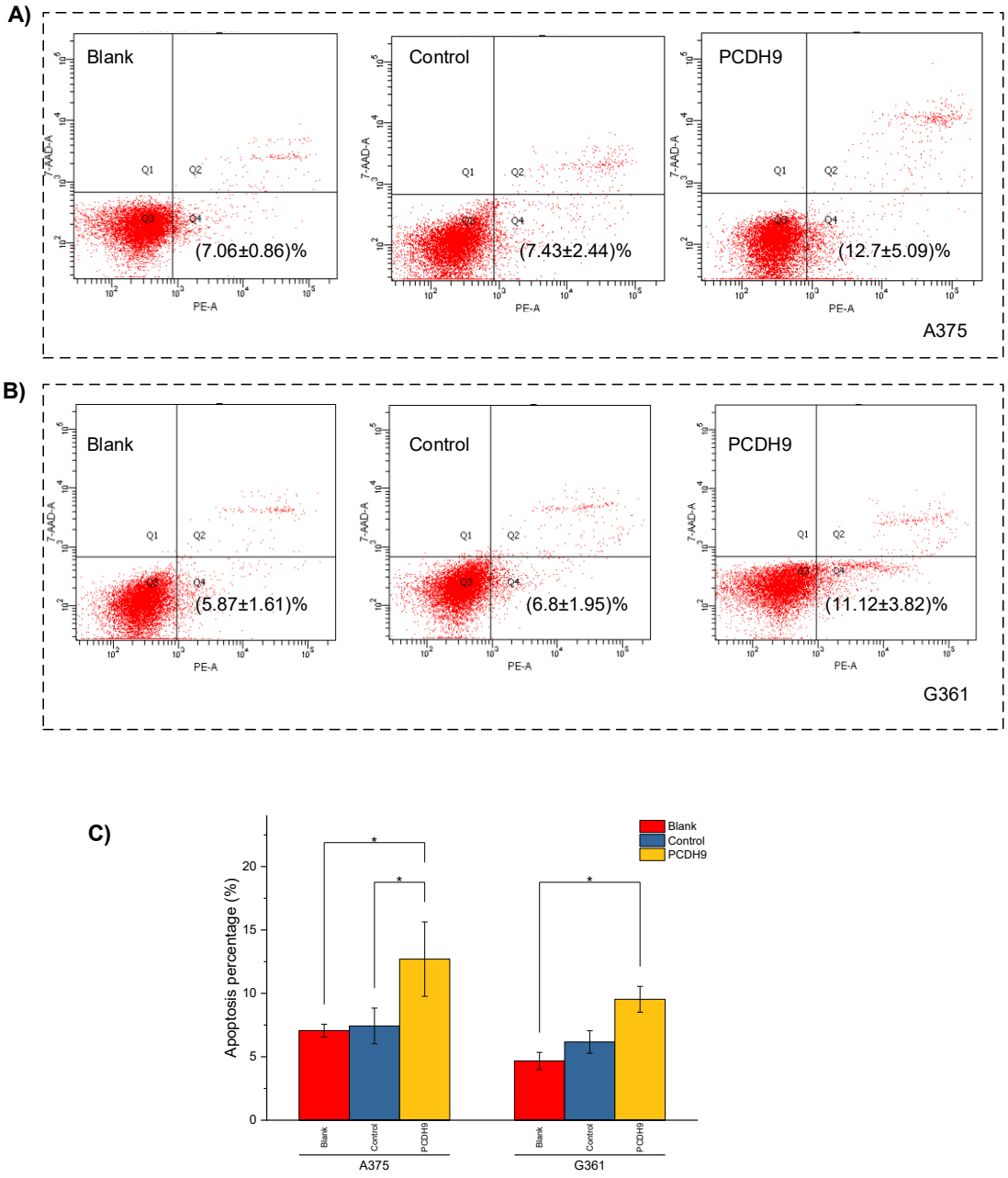

Figure 3.5. The apoptosis percentage of PCDH9 overexpression was exhibited by **A** (A375) and **B** (G361). The overexpression of PCDH9 significantly promoted apoptosis in both cell lines (**C**). * $p<0.05$, ** $p<0.01$, *** $p<0.001$ compared in groups by using one-way ANOVA followed by least significant difference post hoc tests.

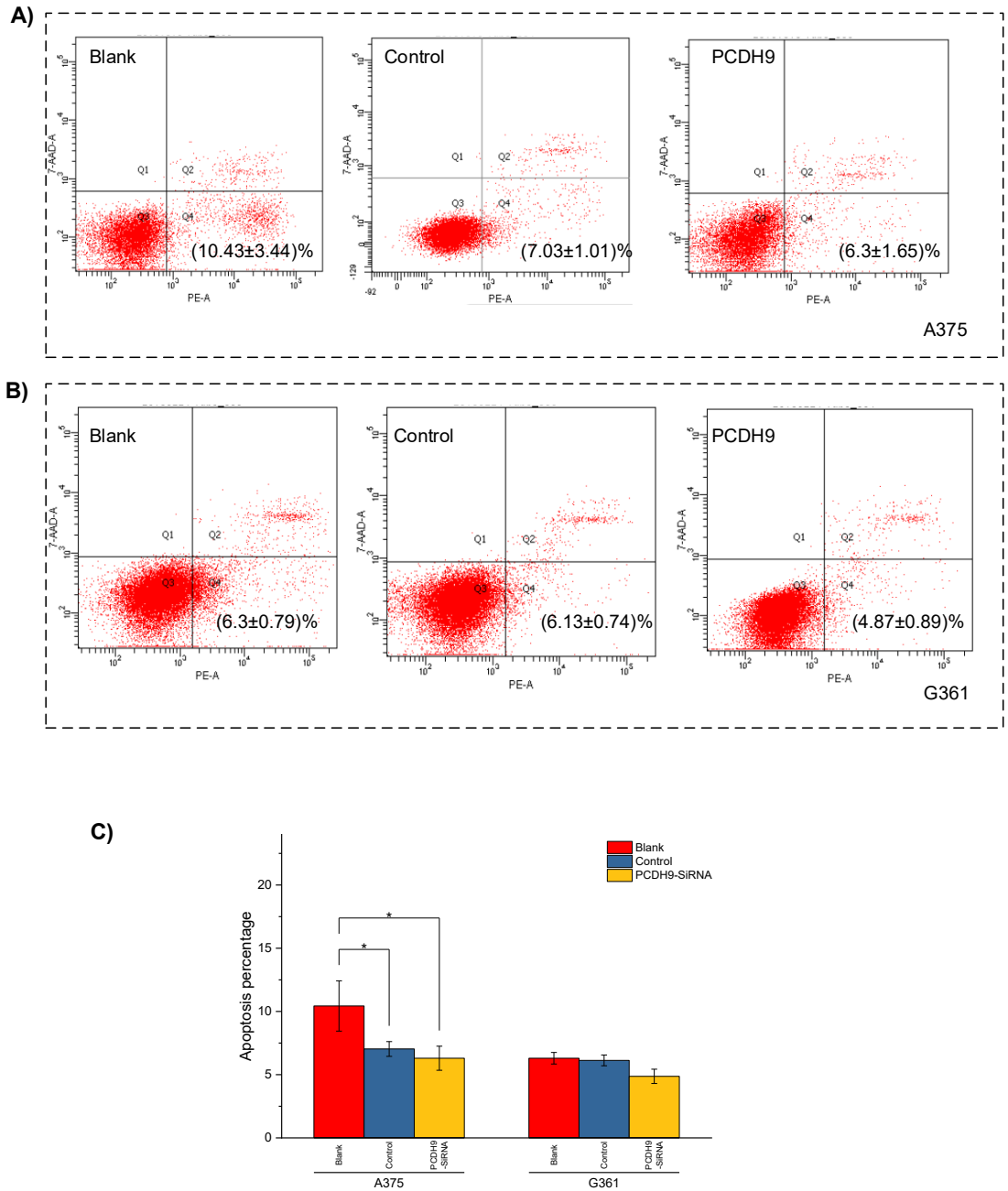

Figure 3.6. The apoptosis percentage of PCDH9 interference was exhibited by **A** (A375) and **B** (G361). The interference of PCDH9 reduced apoptosis in A375 cell line and in a more modest manner in G361 cell lines (**C**). * $p<0.05$, ** $p<0.01$, *** $p<0.001$ compared in groups by using one-way ANOVA followed by least significant difference post hoc tests.

3.6 Effects of overexpressed PCDH9 on cell cycle

Regarding the cell cycle arrest, there was no discrepancy between overexpressed PCDH9 or interfered PCDH9 groups and other groups (blank and control groups) in both cell lines (A375 and G361) **(Figure 3.7 A-D)**. Therefore, the changes in PCDH9 did not affect melanoma cell regulation and the cell cycle regulator Cyclin D1 (CCND1) modulation revealed no significant effect on cell cycle.

A)

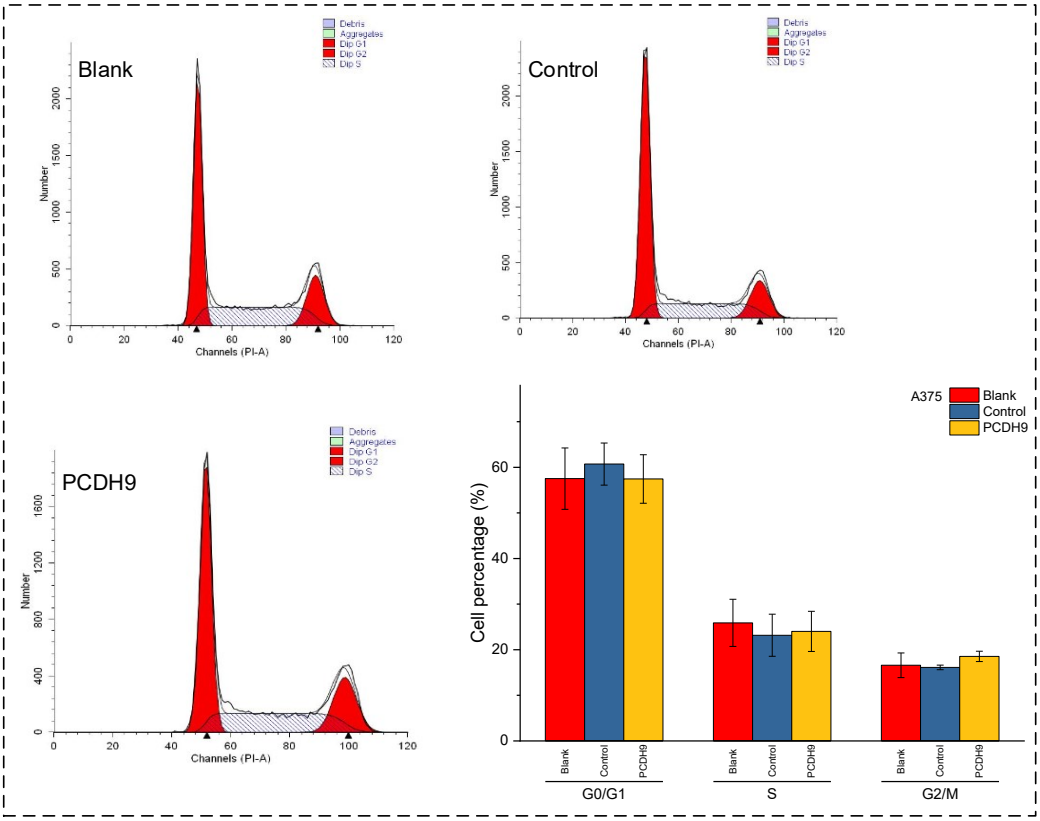
Blank
Control
PCDH9
Debris
Aggregates
Dip G1
Dip G2
Dip S
Number
Channels (PI-A)
A375
Blank
Control
PCDH9
Cell percentage (%)
G0/G1
S
G2/M

B)

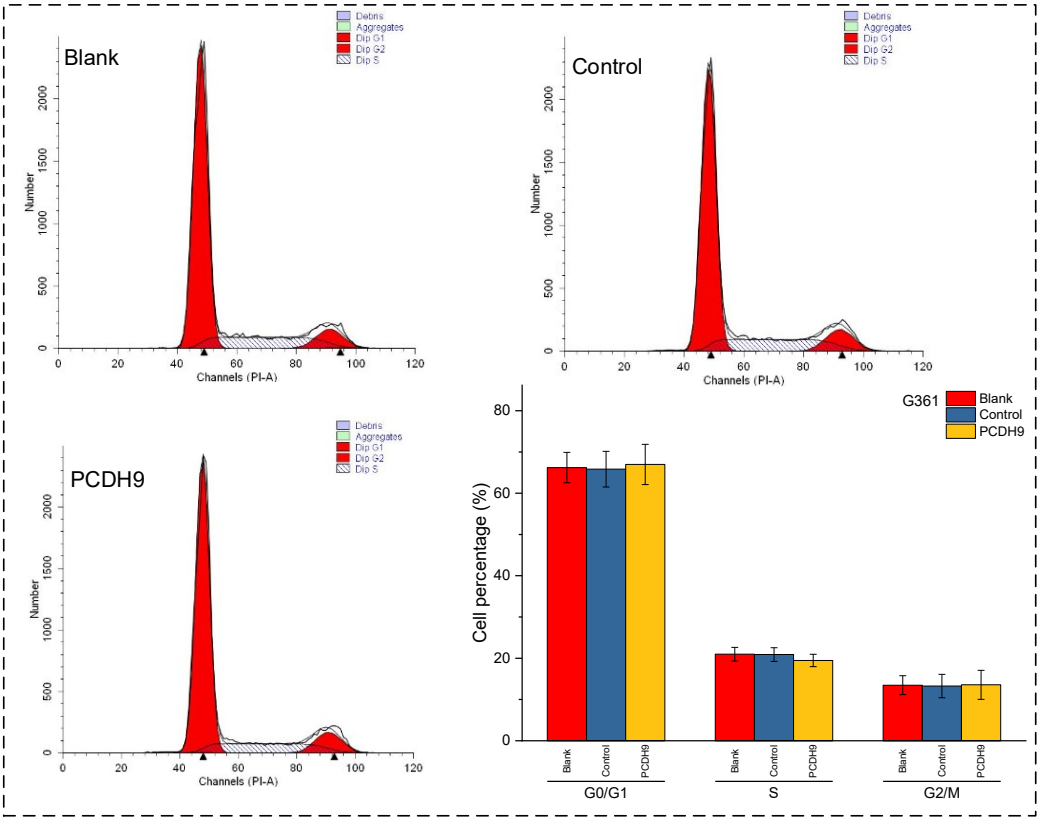
Blank
Control
PCDH9
Debris
Aggregates
Dip G1
Dip G2
Dip S
Number
Channels (PI-A)
G361
Blank
Control
PCDH9
Cell percentage (%)
G0/G1
S
G2/M

C)

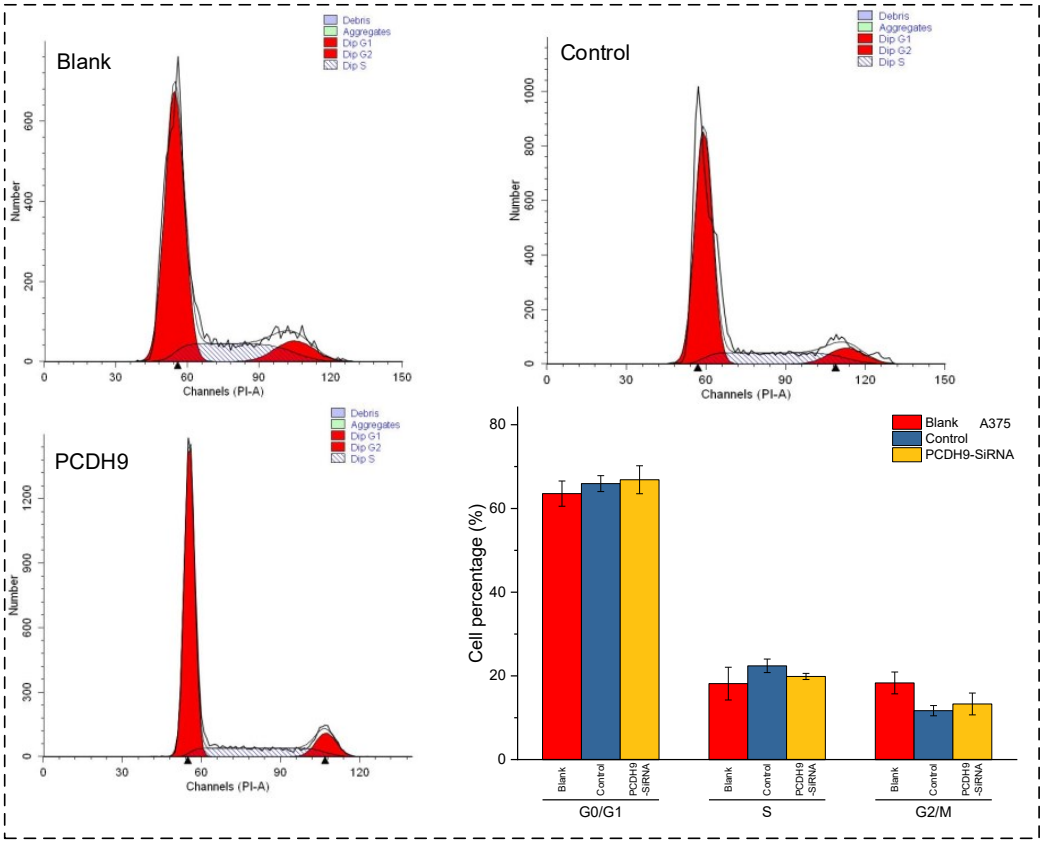
Blank
Control
PCDH9
Debris
Aggregates
Dip G1
Dip G2
Dip S
Number
Channels (PI-A)
Blank A375
Control
PCDH9-SiRNA
Cell percentage (%)
G0/G1
S
G2/M

D)

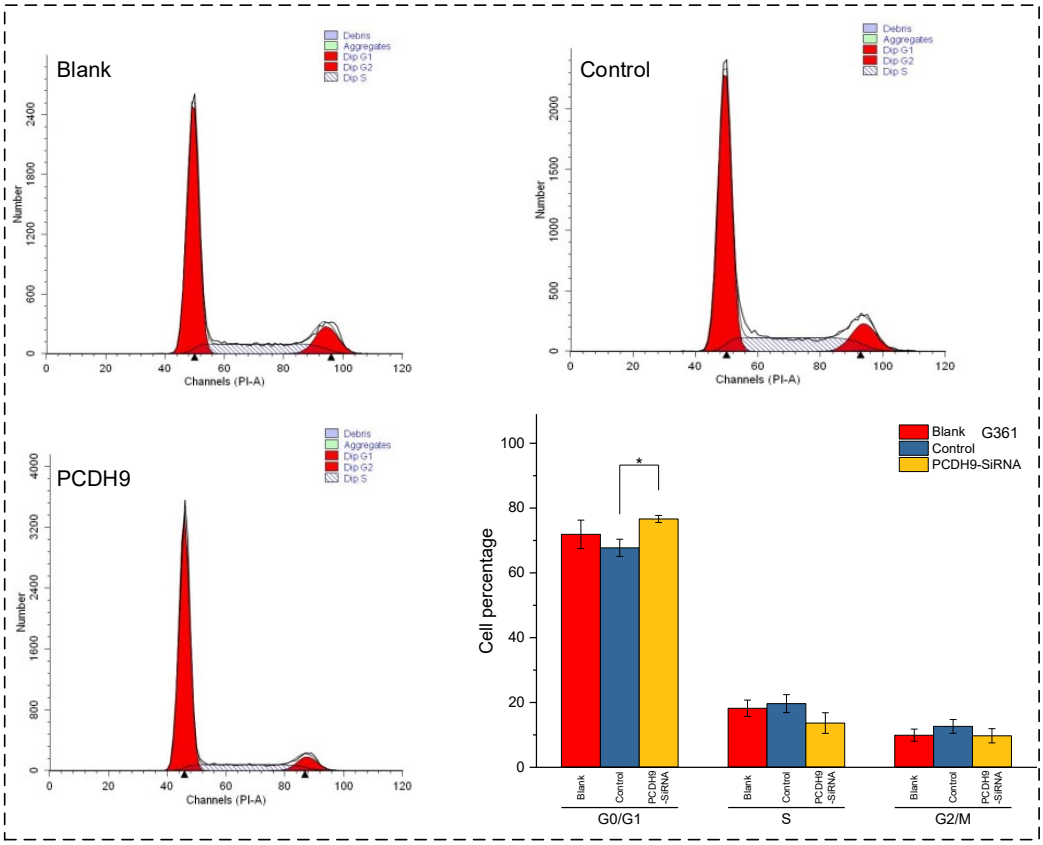
Blank
Control
PCDH9
Debris
Aggregates
Dip G1
Dip G2
Dip S
Number
Channels (PI-A)
Blank G361
Control
PCDH9-SiRNA
Cell percentage
*
G0/G1
S
G2/M

Figure 3.7. The varieties of PCDH9 expression didn't significantly affect melanoma cell regulation. The cell percentage of melanoma cells affected by overexpressed PCDH9 in different cell period time in A375 (**A**) and G361 (**B**) cell lines. The cell percentage of melanoma cells in A375 (**C**) and G361 (**D**) cell lines. * $p<0.05$, ** $p<0.01$, *** $p<0.001$ compared in groups by using one-way ANOVA followed by least significant difference post hoc tests.

3.7 Effects of overexpressed PCDH9 on wound healing

With respect to cell migration, after quantifying the scratched boundary by Image J **(Figure 3.8 A, D)**, the results revealed that the relative density decreased with the duration of cell culture in blank and control groups ($p<0.001$), while the relative wound density did not change in a marked way in overexpressed PCDH9 groups ($p>0.05$) **(Figure 3.8 B, E)**. The relative wound density of scratched boundary was significantly different in overexpressed PCDH9 groups compared with blank and control groups after 24 hours and 48 hours ($p<0.001$) **(Figure 3.8 C, F)**.

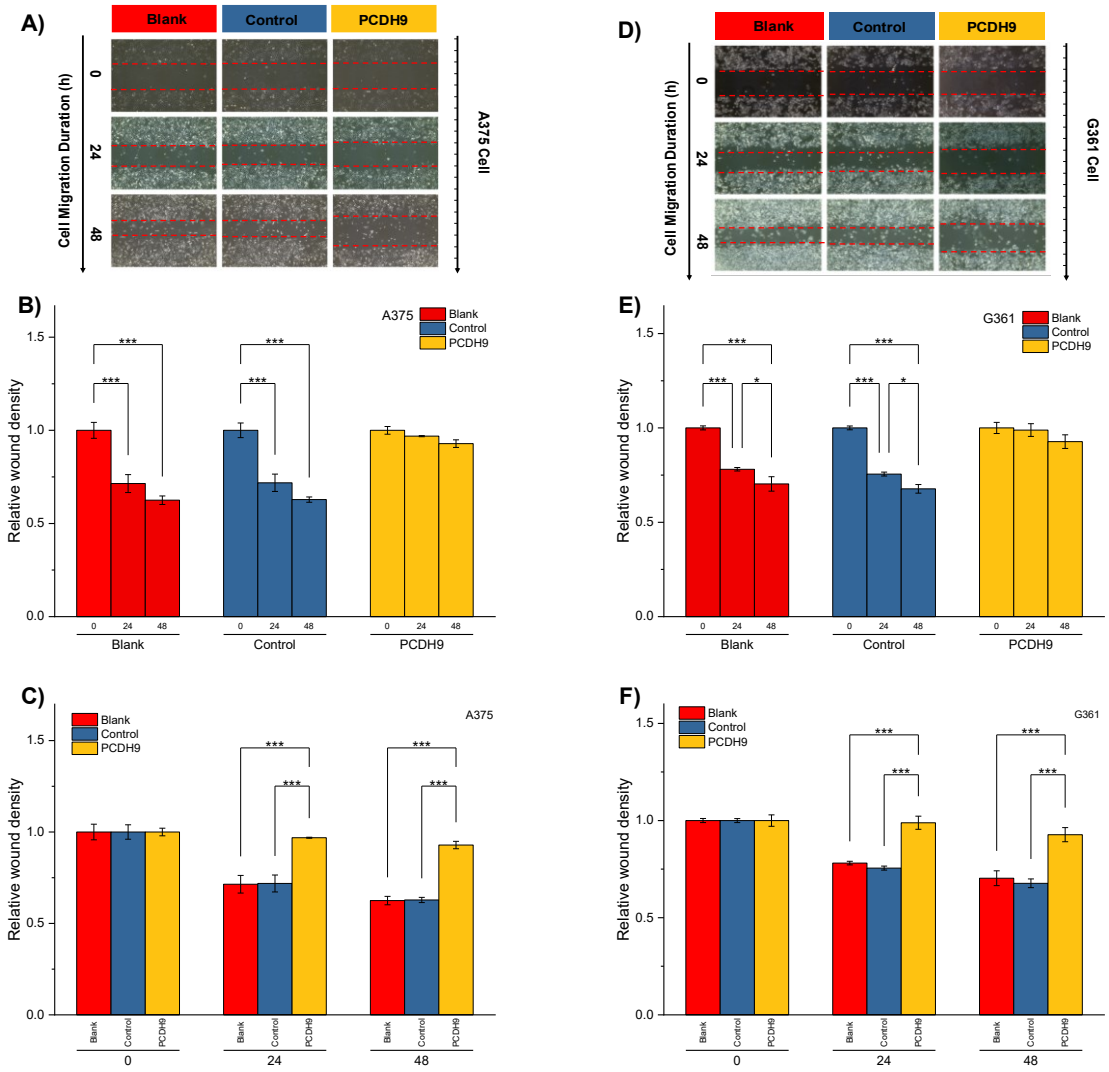

Figure 3.8. The scratched boundary of migrator cells was observed by inverted microscope DMI3000B (Leica, Germany). Representative image of melanoma cells invaded from the scratched boundary in A375 (**A**) and G361 (**D**) cell lines. Relative density of scratched boundary wasn't altered in overexpressed PCDH9 groups comparing with blank and control groups in A375 (**B**) and G361 (**E**) cell lines. Relative density of scratched boundary was significant different in overexpressed PCDH9 groups after 24 and 48 hours in A375 (**C**) and G361 (**F**) cell lines. * $p<0.05$, ** $p<0.01$, *** $p<0.001$ compared in groups by using one-way ANOVA followed by least significant difference post hoc tests.

4 Discussion

Specimen investigations of IHC assay exhibited lower PCDH9 expressions in malignant melanoma specimens than in benign nevus tissue or/and normal skin. Moreover, our study revealed that PCDH9 was mainly expressed in the cytoplasm rather than in nuclei. The survival analysis of MMP2 associated the highly expression with lower survival rate, while the low expression with higher survival rate. The HR was 1.5 (p<0.05). Our study agreed with previous investigations that MMP2 can represent a biomarker of malignant melanoma [146], and downregulating MMP2 expression would increase prognostic survival. We explored and performed a series of investigations, including cell viability assay, apoptosis assay, PCR, of overexpression and interference of PCDH9 by GV358-PCDH9 lentivirus and GV358-SiRNA lentivirus respectively in melanoma A375 and G361 cell lines. According to our results, overexpressed PCDH9 triggered upregulated expressions of CCND1, while RAC1 and MMP2 were downregulated. Interfered PCDH9 induced downregulation of CCND1, while RAC1and MMP2 were upregulated. The alteration of PCDH9 exhibited positive correlation with apoptosis. The apoptosis was promoted with overexpressed PCDH9, while decreased with interfered PCDH9. The overexpression of PCDH9 reduced the viability of melanoma cells. RAC1-NADPH-oxidase complex induce expression of matrix metalloproteinases (MMPs) after growth factor and tumor promoter stimulation [142, 143], the alteration of RAC1 has positive correlation with MMP2 that agreed with our results. Our results agreed with recent studies that found low PCDH9 expression in various cancer types [130, 152, 153]. The PCDH9 could suppress melanoma by reducing the activity of RAC1-NADPH-oxidase complex to generate ROS and induce MMPs expression. The alteration of PCDH9 affected CCND1 (Cyclin D1), the cell regulator protein. Previous investigations of hepatocellular carcinoma (HCC) found that PCDH9 suppresses HCC cells by inducing cell cycle arrest at G0/G1 phase [114]. However, the alteration of PCDH9 expression did not affect melanoma cell regulation in a significant manner (p>0.05). This result suggests that PCDH9 and Cyclin D1 (CCND1) could affect melanoma cell by different mechanisms. Cyclin D1 (CCND1)

could affect tumorigenesis via nuclear trafficking [147], which resulted in PCDH9 mainly expressed in the cytoplasm nor in nuclei. The results of wound healing assay revealed that overexpression of PCDH9 could inhibit the cell migration or the duration, which similar to PCDH9 affecting on HCC [154]. To conclude, increase of PCDH9 suppress NADPH oxidase activity, decreased ROS generation and ROS-induced angiogenesis. PCDH9 can target complex-bound Rac1 to weaken angiogenesis by regulating NADPH oxidase, ROS production and DNA damage susceptibility through cyclin D1 trafficking. VEGF binding to VEGFR2 leads to activating and translocating RAC1 into the plasma membrane, while ROS-dependent signaling events may trigger angiogenesis (i.e. cell migration, proliferation, etc.) and influence MMP2, that affect growth factor, tumor promoter stimulation and prognostic survival as well **(Figure 3.9)**. Therefore, alteration of PCDH9 could affect melanoma cell proliferation.

This chapter represents a modified version of the paper that was pre-printed. But after duplicated experiments of Co-IP besides other data analyses, the phenomenon was not obvious. Therefore, we rearranged and modified this chapter. ZHANG J.J. et al., PCDH9 target RAC1/ROS-NADPH-oxidase complex with the assistance of Pyk2 interaction through Cyclin D1 trafficking, https://www.researchsquare.com/article/rs-95026/v1.

Chapter 3 Conclusion

Background: Melanoma has dramatically increased during last 30 years with low five-year survival and prognosis rate.

Methods: Melanoma cells (A375 and G361) were chosen as *in vitro* model. The immunohistochemical analysis and bioinformatics mining exhibited the suppression of PCDH9 on melanoma. The interference and overexpression of PCDH9 were infected by lentivirus. The effects of PCDH9 on melanoma cells were assessed in terms of alteration of PCDH9 such as cell viability, apoptosis, cell cycle and wound-healing assay. Moreover, expressions of PCDH9 with other genes (MMP2, CCND1, and RAC1) were also assessed by PCR. Originlab 2020 was used for statistical analysis.

Results: The alteration of PCDH9 has negative correlation with MMP2 and RAC1, while had positive with CCND1 (Cyclin D1) and apoptosis. Increase of PCDH9 could suppress melanoma cells and inhibit migration, but not exert significant effects on cell cycle. IHC showed lower PCDH9 expression in melanoma tissue with main expression in cytoplasm.

Conclusion: Our results suggested that increase of PCDH9 suppresses NADPH oxidase activity, decreased ROS generation and ROS-induced angiogenesis. PCDH9 can target complex-bound RAC1 to weaken angiogenesis by regulating NADPH oxidase, ROS production and DNA damage susceptibility through cyclin D1 trafficking. VEGF binding to VEGFR2 leads to activating and translocating RAC1 into the plasma membrane, while ROS-dependent signaling events may trigger angiogenesis (i.e. cell migration, proliferation, etc.) and influence MMP2, that affect growth factor, tumor promoter stimulation and prognostic survival as well. In conclusion, alteration of PCDH9 affect melanoma cell viability. To make a further hypothesis, overexpression of PCDH9 suppressed melanoma cells and might increase prognostic survival.

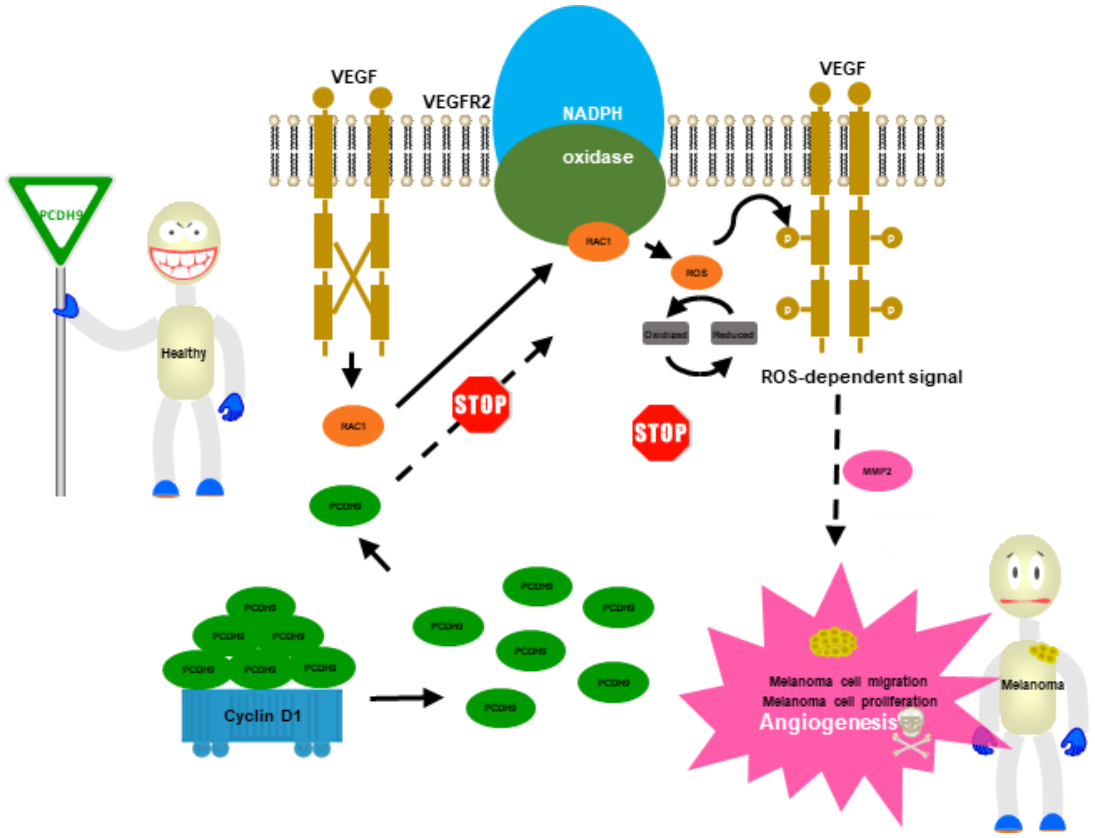

Figure 3.9. Proposed model for the role of PCHD9 regulates melanoma. Increase of PCDH9 suppressed NADPH oxidase activity, decreased ROS generation and ROS-induced angiogenesis. PCDH9 can target complex-bound Rac1 to weaken angiogenesis by regulating NADPH oxidase, ROS production and DNA damage susceptibility through cyclin D1 trafficking. VEGF binding to VEGFR2 leads to activating and translocating RAC1 into the plasma membrane. While ROS-dependent signaling events may trigger angiogenesis (i.e. cell migration, proliferation, etc.) and influence MMP2 that affect growth factor and tumor promoter stimulation as well.

CHAPTER 4.

Chapter 4 Mapping PCDH9-binding proteins interaction by mass spectrometry

1 Introduction

As known that proteins are a kind of biomacromolecules, their structure seriously influences biological functions. Moreover, proteins hardly work alone, most of which tend to form complexes and perform concerted activities by interacting with other proteins. The number of those multiprotein complexes range from two to over 81 [155, 156]. PPIs formed multiprotein complexes are space-dependent or/and time-dependent ways, and proteins do not randomly bind [157], and most PPIs are found in signaling mechanisms. Mapping PPIs is essential for protein-function understandings.

To clarify binding proteins of PCDH9, we used PCDH9 as a bait protein. After processing in-gel digestions, LC-MS/MS were applied to separate proteins and peptides. Then Proteome Discovery 2.2 (Thermo Fisher) and the uniport data were used for MS data analysis. Finally, we investigated and mapped PCDH9-binding proteins. The signal pathways studies were applied by bioinformatics and then bioinformatics platforms have been used to furtherly analyze the proteomics, which were performed in mainstreamed servers (GO, KEGG, Reactome, David and Metascape), pathview and clusterProfiler of Bioconductor were used for pathway and cluster analyses, then visualization [158, 159]. PPIs of PCDH9 were analyzed through Gene-Enrichment and Functional Annotation. According to our previous studies, we assumed that PCDH9 might contribute to melanoma inhibitions by PPIs. It is vital to analyze PCDH9-binding proteins to utterly unravel its melanoma-inhibition mechanism at molecular level.

2 Materials and methods

2.1 Chemicals and reagents

DMEM and Fetal Bovine Serum (FBS), PBS (pH=7.2) DEPC-treated water (Ambion) and TRIzol reagent (invitrogen) were purchased from Gibco (Thermo Fisher Scientific, Shanghai, China); ethanol (70%), Isopropyl alcohol, and Triton X-100 were bought from Sigma-Aldrich (Shanghai, China); Cell Counting Kit-8 (CCK-8) were bought from Dongren Chemical Technology (Shanghai, China); BCA protein assay kit was purchased from Thermo Fisher Scientific (Shanghai, China); antibodies were purchased from Cell Signaling Technology (Shanghai, China); the primers PCDH9 was designed and synthesized by Sangon Biotech (Shanghai, China); GV358-PCDH9 lentivirus was designed by Genechem (Shanghai, China); SYBR® Premix Ex Taq™ Ex Taq ™ II and PrimeScript™ RT reagent Kit with gDNA Eraser were bought from Takara Bio Inc. (Beijing, China); antibodies (PCDH9) and protease inhibitor cocktail was purchased from abcam (Shanghai, China) while goat anti-rabbit immunoglobulin G-Peroxidase antibody was bought from Cell Signaling Technology (Shanghai, China); immobilon PVDF membranes and immobilon western chemiluminescent substrates were bought from Merck Millipore (Darmstadt, Germany); water was obtained from EPED-20TF (Nanjing, China). NH_4HCO_3, ethanol, Dithiothreitol (DTT), Acetonitrile Trypsin and Trifluoroacetic acid (TFA) were bought from Sigma-Aldrich (Shanghai, China); ZipTip C18 were purchased from Merck Millipore (Darmstadt, Germany) while Trap column，100um*20mm (RP-C18 ,thermo Inc.)，100um*20mm (RP-C18) were bought from Thermo Fisher Scientific Inc. (San Jose, CA, USA).

2.2 Cell culture

The same as Chapter 2-2.2.

2.3 PCDH9 Overexpression by Lentivirus Infection

The same as Chapter 3-2.3.

2.4 TRIzol RNA Isolation and Purity determination

The same as Chapter 3-2.9.

2.5 Reverse Transcription and Real-Time PCR

The same as Chapter 3-2.10.

2.6 Cell harvest and extract preparation

All procedure were performed at 4℃. The process of cells' lysates preparation was same as Chapter 2-2.6. Collecting cell lysate and then clarifying it through preparative centrifugation for 30min at 20,000*g* to yield a crude extract. PCDH9 were immunoblotted by anti-FLAG antibody to verify its (bait) presence.

2.7 Protein extraction and Protein complex immunoprecipitation

2.7.1 In-gel digestion

2.7.1.1 Cutting and bleaching

The precipitate obtained in Co-IP experiment and the cell lysate were provided in the state of protein test strips. (i) After washing the gel twice with ultrapure water, the strips were cutted with a scalpel into 1 mm^3 size and placed in 1.5 mL Eppendorf tube; (ii) a dye bleaching solution 1 mL (containing 25mM NH_4HCO_3ON of 50% ethanol-water) was added and vortexed 15-20 minutes (repeating the process couple times till all colors were bleached); (iii) the supernatant was discarded and vacuum- dried for 10 minutes.

2.7.1.2 Alkylation reduction

(i) An appropriate amount (without strips) of DTT solution (10mM DDT in 25 mM NH_4HCO_3 solution for alkylation reduction) was added and put in a 56 ℃ water-bath incubation for 1 hour; (ii) the supernatant was cooled to room temperature, and the appropriate amount of IAA solution (55mM IAA in 25Mm NH_4HCO_3 solution) was added and incubated in the dark at room temperature for 45 min, then the supernatant was discarded; (iii) 1 mL of 50 Mm NH_4HCO_3 solution was added to wash for 10 min with shaking, and 1 mL of water wash for 10 min with shaking; (iv) After removing the supernatant, a1 mL acetonitrile was added and vortexed to mix, after washing for 5 min, the supernatant was removed and vacuum-dried for 10 min.

2.7.1.3 Digestion

(i) appropriate amounts of Trypsin (sequencing grade) was added and placed on ice for 10 minutes, then enzyme was added to be sure to immerse the gel pieces completely, until the solution completely absorbed; (ii) then reading 10-20 μL, 50 mM $(NH_2)_4HCO_3$, then 16-20 hours digestion on 37 ℃.

2.7.1.4 Peptide extraction

(i) the enzymolysis was aspirated into a new Eppendorf tube, and added 2-3 times amount of 50% acetonitrile-water solution (containing 5% trifluoroacetic acid), shaked at room temperature for 15 min with one-minute centrifuge, supernatant was aspirated; (ii) 2-3 times amount of the gel was added to 75% acetonitrile-water solution (containing 0.1% trifluoroacetic acid), shacked at room temperature for 10 min with one-minute centrifuge, then the supernatant was aspirated; (iii) 2-3 times amount of acetonitrile was added to the gel, and shacked at room temperature for 5 minutes with one-minute centrifuge, then the supernatant was aspirated; (iv) the extracts were combined and dried in vacuum, then stored at -20 ℃ for future use.

2.7.1.5 Desalination

(i) Desalting was performed by using the Zip Tip C18 micro desalting column (Millipore, Merck KGaA, Darmstadt, German) with acetonitrile, 90% acetonitrile (0.1% trifluoroacetic acid) and water (0.1% trifluoroacetic acid); (ii) the vacuum-dried sample was dissolved in 10 μL 0.1% trifluoracetic acid-water, and pipetting 15-20 times in the Eppendorf tube. (iii) Rinsing the Zip Tip three times with 0.1% trifluoracetic acid-water and pipetting 10 μL 0.1% trifluoroacetic acid-water (containing 0.1% trifluoroacetic acid) 15-20 times to elute the peptide; (xvi) After vacuum drying, the samples were loaded (0.1% formic acid-water), then analyzed.

2.8 Hydrolysates LC-MS/MS

A Thermo Scientific™ EASY-LC™ 1000 Liquid Chromatography system (Thermo Fisher Scientific Inc., San Jose, CA USA) and a Thermo Scientific LTQ Orbitrap Velos Pro mass spectrometer (Thermo Fisher Scientific Inc., San Jose, CA USA) were used. The liquid chromatography separations were performed on trap column (100μm ×20mm; RP-C_{18}; Thermo Fisher Scientific, USA) and analysis column (75μm×150mm; RP-C_{18}; Thermo Fisher Scientific, USA) at room temperature. The mobile phase consisted of solvent A (0.1% FA in water) and solvent B (0.1% FA in methanol). A linear gradient with a flow rate of 300nL/min was applied in the following manner: A100% (0 min) → B 1% (0 min) → 5% (2 min) → 26% (50 min) → 40% (61 min) → 100% (66-70 min). The injection volume was 10 μL. The mass spectrometer was interfaced with an electrospray ion source and operated in the positive MRM mode. The ion transfer capillary temperature was held at 275 °C; the electrospray capillary voltage was optimized to1.9 kV; and the parent ion scan ranged from 350-1800 m/z. The mass-to-charge ratio of polypeptides and polypeptide fragments were collected the strongest fragment patterns (data-dependent scanning mode). The fragmentation mode was as following ways: normalized energy was 35%; *q*-value was 0.25; activation time was 30 ms; dynamic exclusion time was 30s (collision Induced dissociation). The resolution of MS^1 at M/Z 400 was 60,000; and the MS^2 in the ion trap was unit mass

resolution. (The first level of MS-profile mode, and the second level of MS-profile centroid mode).

2.8 ESI mass spectrometry data analysis

The data were collected and processed by using the Proteome Discovery 2.2 software (Thermo Fisher Scientific Inc., San Jose, CA USA). The search engine was set SEQUEST. Database were downloaded from the UniProt database (uniprot-human-173324-20180828.fasta; uniprot-human-169671-20190315.fasta), the decoy database was used to calculate the false positives rate of proteins (FDR, false discovery rate). The main parameters were set as follows: Enzyme Name: trypsin (Full); Max Missed cleavage (2); Min. Peptide length (6 amino acids); maximum peptide length (144 amino acids); minimum precursor mass (350 Da); maximum precursor mass (5000Da); precursor mass tolerance (10 ppm); fragment mass tolerance (0.6 Da); database： uniprot-human-173324-20180828.fasta; fixed modification: Carbamidomethyl (C); variable modification: Oxidation (M), Acetyl (Protein N-term); peptide FDR: 0.01; protein FDR: 0.01.

2.9 Bioinformatics analysis

Bioconductor packages was used: pathview [158] was for KEGG pathway, while clusterProfiler [159] was to analyze and visualize functional profiles (GO and KEGG) of gene and gene clusters. Additionally, data analyses were performed in different popular bioinfomation platforms as well for Gene-Enrichment and Functional Annotation Analysis, the main websites and databases that applied as follows: GO, KEGG, Reactome, David and Metascape.

2.9.1 Pathway and process enrichment analysis

For given list of A375 and G361 cells, pathway and process enrichment analyses have been carried out with the ontology sources like KEGG Pathway, GO Biological Processes, Reactome Gene Sets, Canonical Pathways and CORUM. All proteins in the

list have been used as the enrichment background. Terms are collected and grouped into clusters based on their membership similarities (p-value<0.01, count⩾3, enrichment factor>1.5, Kappa scores>0.3; p-values - accumulative hypergeometric distribution [160], and q-values - Benjamini-Hochberg procedure to account for multiple testing [161]. Kappa scores [162]- hierarchical clustering on the enriched terms).

2.9.2 Network analysis

To capture PPIs, enriched terms were selected as a network plot and the similarity of terms>0.3 are connected by edges. The least p-values 20 clusters network was visualized by Cytoscape with "force-directed" layout and with edge bundled for charity, where each node represents an enriched term and is colored first by its cluster ID and then by p-value. One term from each cluster is selected to have its term description shown as label.

2.10 Statistical Analysis

Data are presented as the mean ± SD from at least 3 independent experiments. Statistical comparisons between two groups were made using Student's t tests. Differences among three or more groups were compared by one-way ANOVA followed by least significant difference post hoc tests (Originlab 2020, Northampton, MA, USA), p<0.05 was considered as statistically significant, while p<0.01 was considered as highly statistically significant. The overrepresentation analysis of Reactome: A statistical (hypergeometric distribution) test that determines whether certain Reactome pathways are over-represented (enriched) in the submitted data. This test produces a probability score, which is corrected for false discovery rate using the Benjamani-Hochberg method. A binomial test is used to calculate the probability shown for each result, and the p-values are corrected for the multiple testing (Benjamini–Hochberg procedure) [163]. When members of two independent groups can fall into one of two

mutually exclusive categories, Fisher's Exact test is used to determine whether the proportions of those falling into each category differs by group. The false discovery rate (FDR) of adjusted p-values for approximate control of false discovery rate [164].

3 Results and discussion

3.1 The results of PCDH9 overexpression by Lentivirus

After PCDH9 was overexpressed by lentivirus, RNA was extracted and reversed into cDNA. The expressions of PCDH9 were significantly upregulated by lentivirus. infection.

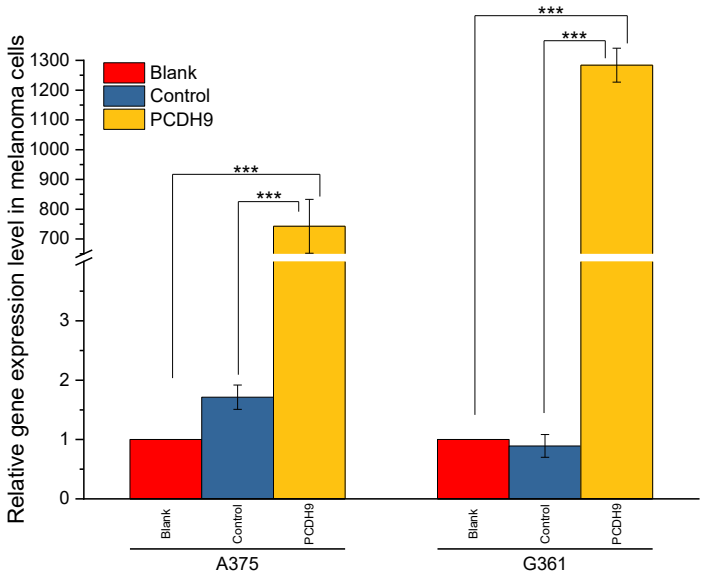

Figure 4.1. Effects of overexpressed PCDH9 in melanoma cells measured by PCR analysis. The expressions of PCDH9 were significantly upregulated by lentivirus infection. * p<0.05, **p<0.01, ***p<0.001 compared in groups by using one-way ANOVA followed by least significant difference post hoc tests.

3.2 The results of Chromatography-mass spectrometry

A375 **(Figure 4.2)** and G361-basepeak Chromatography-mass spectrometry (**Figure 4.3)** exhibited the interactions of PCDH9 and other proteins were separated well in both cells (A375 and G361). The amount of binding proteins and peptides has been showed in **Table 4.1** and **Table 4.2**, and they were separated into groups.

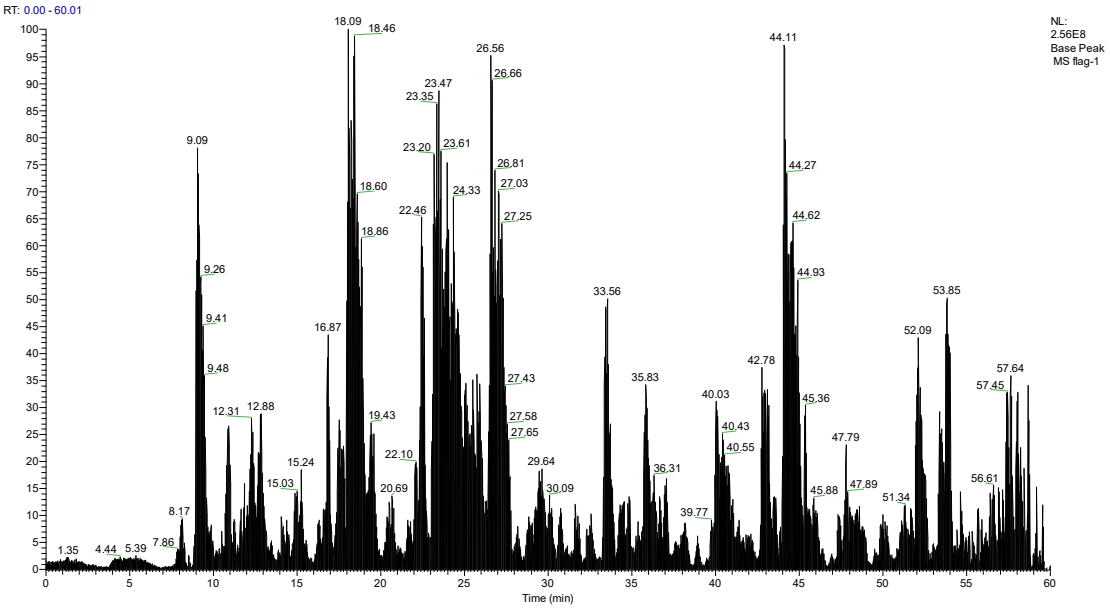

Figure 4.2. A375-basepeak Chromatography-mass spectrometry

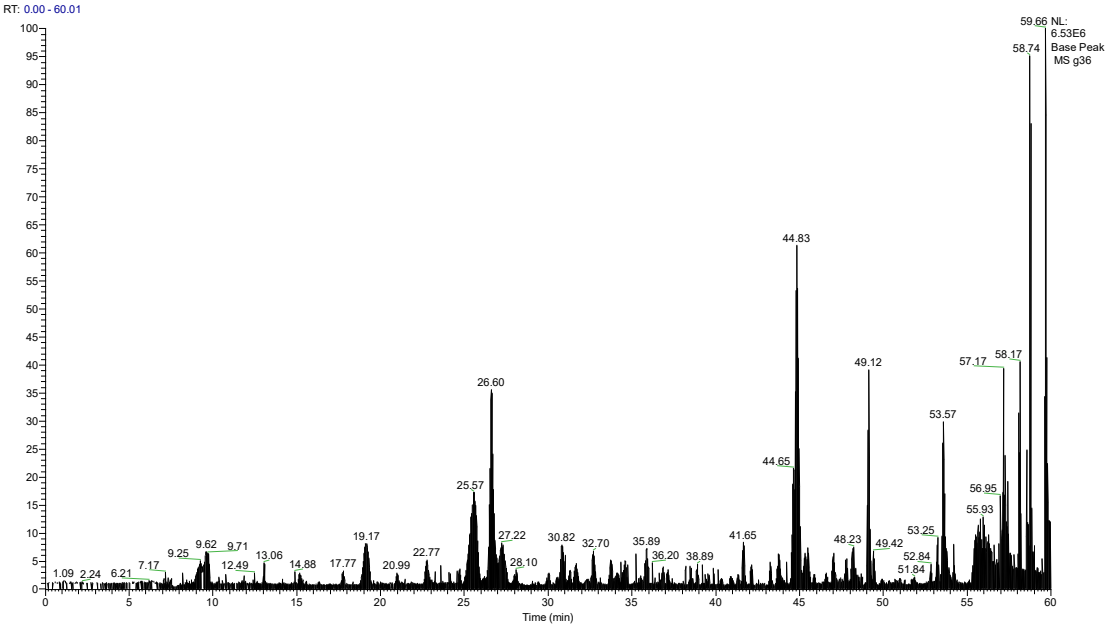

Figure 4.3. G361-basepeak Chromatography-mass spectrometry

Table 4.1. The results of A375 LC-MS/MS

	Amount
Protein groups	687
Proteins	656
Peptide groups	3496

Table 4.2. The results of G361 LC-MS/MS

	Amount
Protein groups	98
Proteins	98
Peptide groups	348

3.3 The results of proteomics analyses by bioinformatics.

Database were downloaded from the UniProt, the screening was used by FDR. The UniProt accession were transfer into gene ID then be analyzed. The enrichment analysis processes were as follows: firstly, the statistically enriched terms were identified, then filtered according to the calculation of accumulative hypergeometric p-values and enrichment factors; the 0.3 kappa score was applied as the threshold to cast clusters, the significant terms were remained as enrichment.

3.3.1 Biological process and pathway enrichment

The enriched terms of PCDH9-binding proteins in A375 cells are as follows: Metabolism of RNA; ribonucleoprotein complex biogenesis; rRNA processing in the nucleus and cytosol; regulation of mRNA metabolic process; nuclear transport; translation; ribonucleoprotein complex subunit organization; rRNA modification in the nucleus and cytosol; cell cycle; 17S U2 snRNP; positive epigenetic regulation of rRNA expression; chromatin remodeling; chromatin assembly or disassembly; purine ribonucleoside monophosphate biosynthetic process; regulation of chromosome organization; H2AX complex; isolated from cells without IR exposure; maturation of 5.8S rRNA; muscle contraction; positive regulation of gene expression; epigenetic; PID MYC ACTIV PATHWAY (Figure 4.4-A). The enriched terms of PCDH9-binding proteins in G361 cells are as follows: platelet degranulation; cornification; regulation of peptidase activity; humoral immune response; blood coagulation, fibrin clot formation; Scavenging of heme from plasma; receptor-mediated endocytosis; 40S

ribosomal subunit, cytoplasmic; supramolecular fiber organization; Glycolysis, core module involving three-carbon compounds; Amyloid fiber formation; anatomical structure homeostasis; interaction with symbiont; response to toxic substance; aute-phase response; Pyruvate metabolism; Staphylococcus aureus infection; Iron uptake and transport; Neutrophil degranulation; maintenance of location (Figure 4.4-B). Most enriched terms of PCDH9-binding proteins in A375 cells are focused on nuclear acid regulations with more count (Table 4.3), while in G361 cells are focused on homeostasis with less count (Table 4.4). The following biological processes are PCDH9-binding proteins in A375 cells: cellular component organization or biogenesis; metabolic process; multi-organism process; negative regulation of biological process; localization; regulation of biological process; positive regulation of biological process; multicellular organismal process; immune system process; response to stimulus; cellular process; developmental process; signaling; rhythmic process; biological regulation; biological adhesion; cell killing; locomotion (Figure 4.5-A). The following biological processes are PCDH9-binding proteins in G361 cells: localization; developmental process; immune system process; biological regulation; negative regulation of biological process; multicellular organismal process; response to stimulus; cellular component organization or biogenesis; cellular process; metabolic process; biological adhesion; multi-organism process; positive regulation of biological process; cell killing; signaling; locomotion (Figure 4.5-B). The biological processes of PCDH9-binding proteins are similar in both melanoma cells (A375 and G361) (Figure 4.5.).

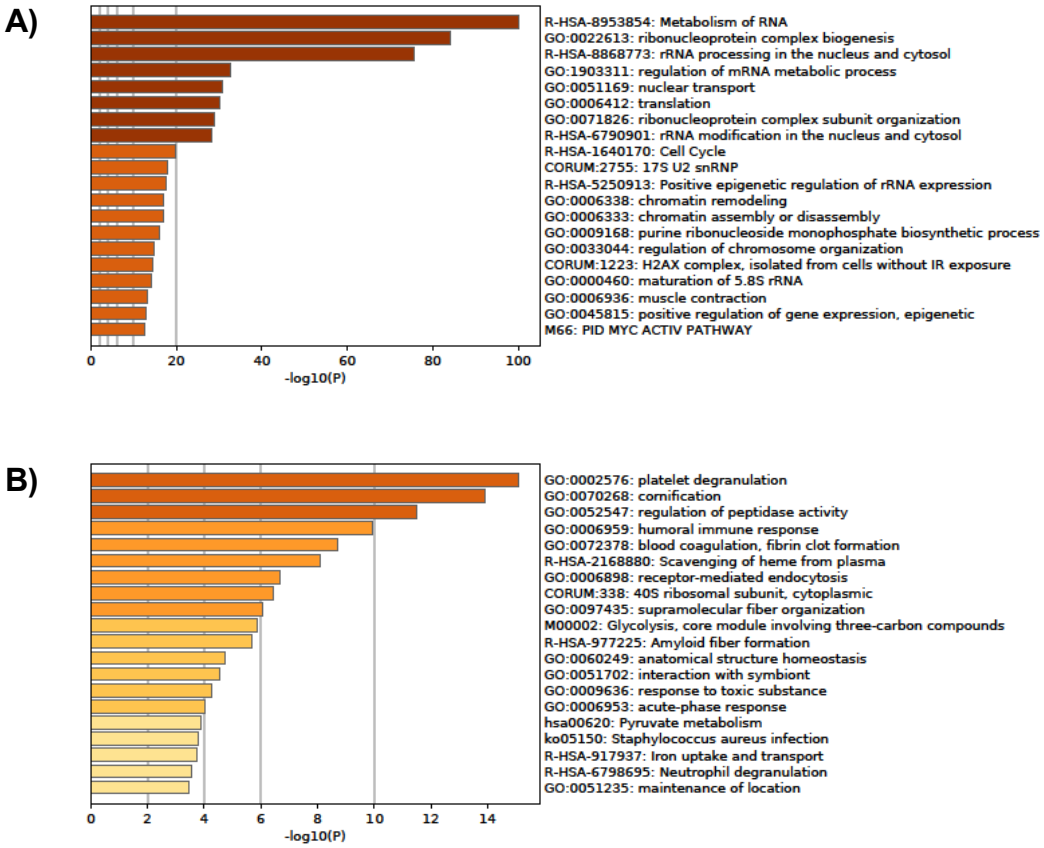

Figure 4.4. Bar graph of enriched terms across PCDH9-binding proteins (A. A375, B. G361), the top 20 clusters was visualized by Metascape [165], colored by *p*-values.

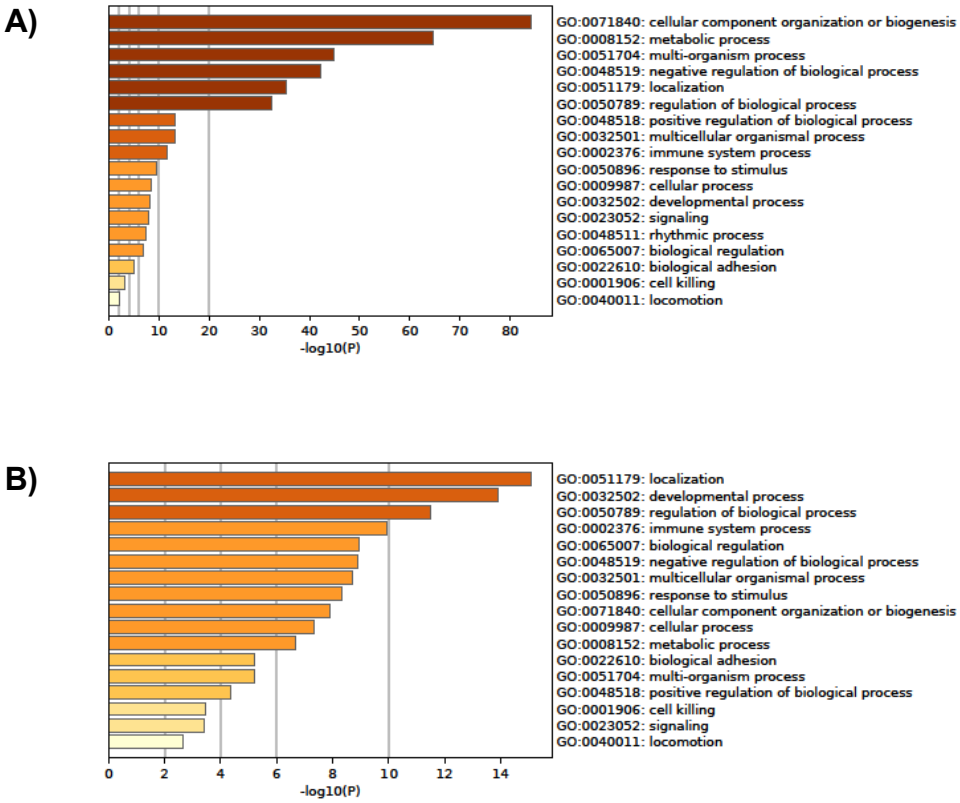

Figure 4.5. The top-level Gene Ontology biological processes of PCDH9-binding protein (A. A375, B. G361) was visualized by Metascape [165].

Table 4.3. Top 20 clusters with PCDH9-binding proteins of A375 enriched terms.

GO	Category	Description	Count	%	Log10 (P)	Log10 (q)
R-HSA-8953854	Reactome Gene Sets	Metabolism of RNA	140	30.3	-100	-95.65
GO:0022613	GO Biological Processes	ribonucleoprotein complex biogenesis	106	22.94	-84.09	-80.05
R-HSA-8868773	Reactome Gene Sets	rRNA processing in the nucleus and cytosol	71	15.37	-75.61	-71.74
GO:1903311	GO Biological Processes	regulation of mRNA metabolic process	51	11.04	-32.51	-29.95
GO:0051169	GO Biological Processes	nuclear transport	50	10.82	-30.66	-28.14
GO:0006412	GO Biological Processes	translation	68	14.72	-30.26	-27.75

GO:0071826	GO Biological Processes	ribonucleoprotein complex subunit organization	45	9.74	-28.97	-26.49
R-HSA-6790901	Reactome Gene Sets	rRNA modification in the nucleus and cytosol	25	5.41	-28.14	-25.68
R-HSA-1640170	Reactome Gene Sets	Cell Cycle	53	11.47	-19.84	-17.48
CORUM:2755	CORUM	17S U2 snRNP	15	3.25	-17.94	-15.62
R-HSA-5250913	Reactome Gene Sets	Positive epigenetic regulation of rRNA expression	22	4.76	-17.5	-15.19
GO:0006338	GO Biological Processes	chromatin remodeling	27	5.84	-16.94	-14.65
GO:0006333	GO Biological Processes	chromatin assembly or disassembly	27	5.84	-16.88	-14.6
GO:0009168	GO Biological Processes	purine ribonucleoside monophosphate biosynthetic process	26	5.63	-16.15	-13.89
GO:0033044	GO Biological Processes	regulation of chromosome organization	33	7.14	-14.7	-12.49
CORUM:1223	CORUM	H2AX complex, isolated from cells without IR exposure	9	1.95	-14.35	-12.15
GO:0000460	GO Biological Processes	maturation of 5.8S rRNA	13	2.81	-14.03	-11.85
GO:0006936	GO Biological Processes	muscle contraction	31	6.71	-13.13	-10.99
GO:0045815	GO Biological Processes	positive regulation of gene expression, epigenetic	15	3.25	-12.95	-10.83
M66	Canonical Pathways	PID MYC ACTIV PATHWAY	16	3.46	-12.71	-10.61

Count: the number of genes in PCDH9-binding proteins of G361 with membership in the given ontology term

%: the percentage of PCDH9-binding proteins in G361 cells that are found in the given ontology term

P: the *p*-value

q: is the multi-test adjusted *p*-value

Table 4.4. Top 20 clusters with PCDH9-binding proteins of G361 enriched terms.

GO	Category	Description	Count	%	Log10 (P)	Log10 (q)
GO:0002576	GO Biological Processes	platelet degranulation	11	20.75	-15.08	-11.03
GO:0070268	GO Biological Processes	cornification	10	18.87	-13.89	-10.15
GO:0052547	GO Biological Processes	regulation of peptidase activity	13	24.53	-11.5	-8.05
GO:0006959	GO Biological Processes	humoral immune response	11	20.75	-9.95	-6.72
GO:0072378	GO Biological Processes	blood coagulation, fibrin clot formation	5	9.43	-8.72	-5.73
R-HSA-2168880	Reactome Gene Sets	Scavenging of heme from plasma	4	7.55	-8.09	-5.19
GO:0006898	GO Biological Processes	receptor-mediated endocytosis	8	15.09	-6.67	-3.92
CORUM:338	CORUM	40S ribosomal subunit, cytoplasmic	4	7.55	-6.46	-3.76
GO:0097435	GO Biological Processes	supramolecular fiber organization	10	18.87	-6.07	-3.43
M00002	KEGG Pathway	Glycolysis, core module involving three-carbon compounds	3	5.66	-5.86	-3.32
R-HSA-977225	Reactome Gene Sets	Amyloid fiber formation	5	9.43	-5.7	-3.21
GO:0060249	GO Biological Processes	anatomical structure homeostasis	7	13.21	-4.73	-2.45
GO:0051702	GO Biological Processes	interaction with symbiont	4	7.55	-4.53	-2.31
GO:0009636	GO Biological Processes	response to toxic substance	7	13.21	-4.25	-2.08

GO:0006953	GO Biological Processes	acute-phase response	3	5.66	-4.01	-1.91
hsa00620	KEGG Pathway	Pyruvate metabolism	3	5.66	-3.9	-1.81
ko05150	KEGG Pathway	Staphylococcus aureus infection	3	5.66	-3.78	-1.71
R-HSA-917937	Reactome Gene Sets	Iron uptake and transport	3	5.66	-3.74	-1.67
R-HSA-6798695	Reactome Gene Sets	Neutrophil degranulation	6	11.32	-3.54	-1.54
GO:0051235	GO Biological Processes	maintenance of location	5	9.43	-3.44	-1.46

Count: the number of genes in PCDH9-binding proteins of G361 with membership in the given ontology term

%: the percentage of PCDH9-binding proteins in G361 cells that are found in the given ontology term

P: the *p*-value

q: is the multi-test adjusted *p*-value

3.3.2 Biological interpretation of the interaction network

The network is visualized with Cytoscape (v3.1.2) with "force-directed" layout and with edge bundled for clarity. Selected terms were shown as label. The terms of PCDH9 PPI in A375 cells are Metabolism of RNA, ribonucleoprotein complex biogenesis, mRNA processing, DNA repair, regulated exocytosis, protein localization to nucleus, PID BARD1 PATHWAY, Spliceosome, regulation of mRNA processing, regulation of adaptive immune response, ribonucleoprotein complex assembly, negative regulation of interleukin-1 beta production, DNA-templated transcription elongation, circadian regulation of gene expression, positive regulation of type I interferon production, Cell Cycle, RNA transport, positive regulation of histone modification, Unfolded Protein Response (UPR), antigen processing and presentation of peptide antigen (Figure 4.6. A); while in G361 are platelet degranulation, cornification, regulation of peptidase activity, Complement and coagulation cascades, Scavenging from plasma , response to wounding, receptor-mediated endocytosis, 40S ribosomal subunit, cytoplasmic, Glycolysis core module involving three-carbon comp, Amyloid fiber formation,

anatomical structure homeostasis, interaction with symbiont, acute-phase response, response to toxic substance Staphylococcus aureus infection, Iron uptake and transport, Neutrophil degranulation, Bacterial invasion of epithelial cells, Signaling by MET, response to nutrient levels (Figure 4.6. B). The PPI in A375 are focus on regulation of nucleic acid, while in G361 homeostasis.

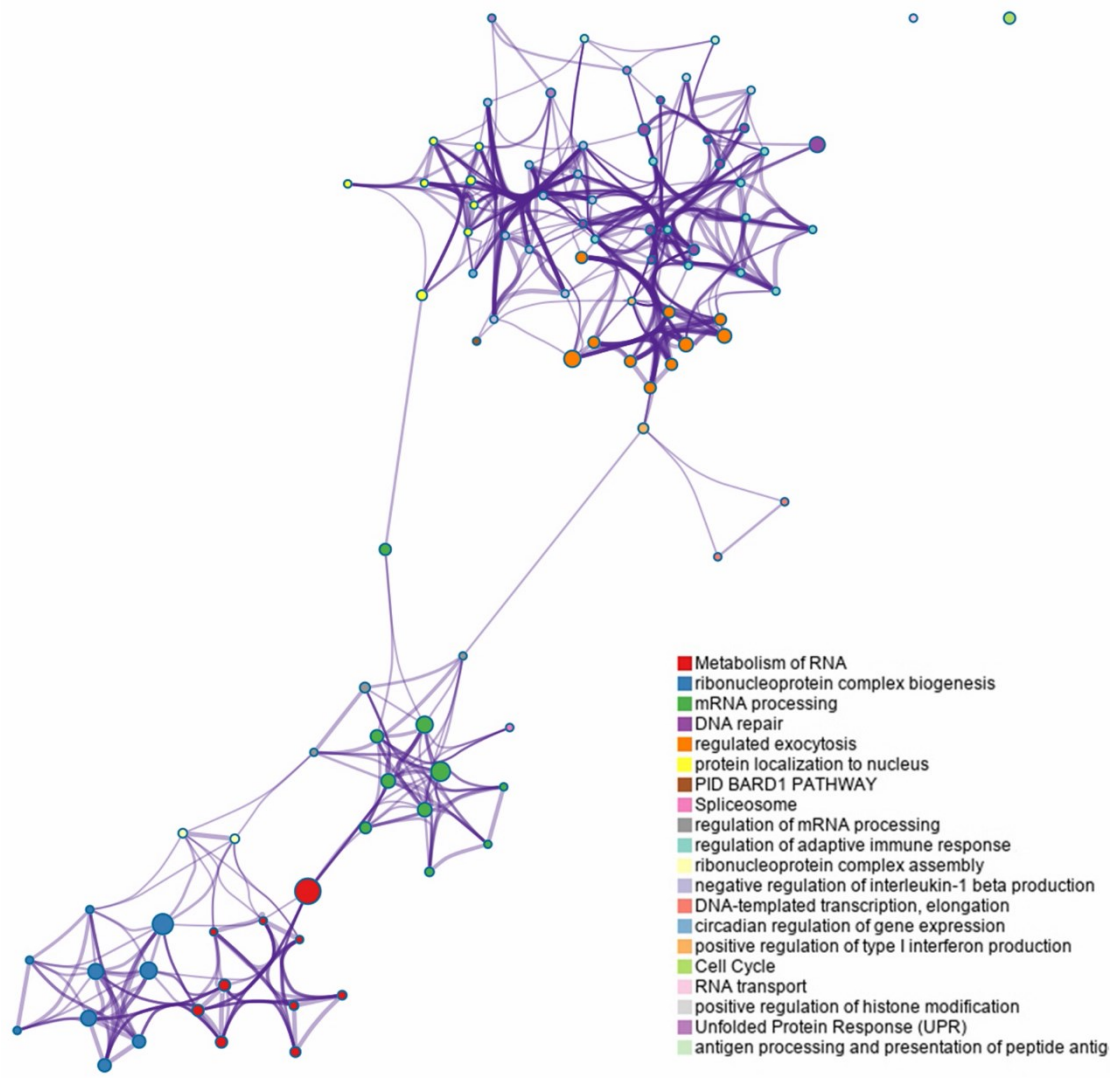

A.

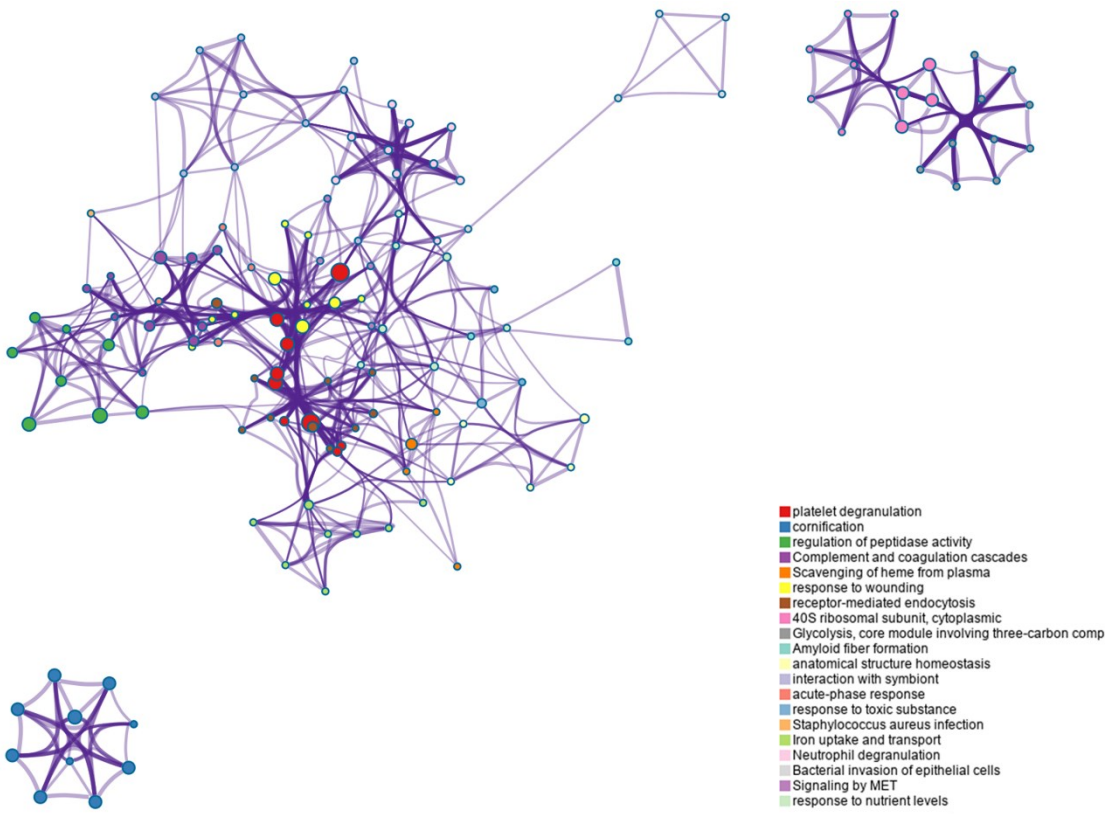

B.

Figure 4.6. PPI networks of PCDH9 in melanoma cells (A-A375, B-G361)

4 Conclusion

After LC-MS/MS, PCDH9-binding proteins and peptides were separated then proteins data were processed for mapping analysis, various bioinformatics platforms were used. KEGG pathway, Gene-Enrichment and Functional Annotation Analysis were performed. Most PCDH9-binding proteins in A375 cells are enriched in nuclear acid regulation, while in G361 cells are homeostasis. The biological processes are similar in two cells (A375 and G361 cells). The PPIs in A375 are focus on regulation of nucleic acid, while in G361 homeostasis. The analyses of PCDH9-binding proteins exhibited PPIs of PCDH9 to inhibit melanoma cells by different biological processes and suppress different melanoma cells by various pathways. The results suggested that PCDH9 may suppress different melanoma cell lines by different ways.

Chapter 4 Conclusion

Background: Proteins hardly work alone, most of which tend to form complexes to perform concerted activities by interacting with other proteins. We have assumed PCDH9 contributing to melanoma suppression by protein-protein interactions (PPIs). Therefore, we processed mapping PCDH9-binding proteins interaction by mass spectrometry to unveil the suppressed mechanism of PCDH9.

Methods: LC-MS/MS were applied to separate and analyze PCHD9-binding proteins and peptides. Proteome Discovery 2.2 and the uniport data were used to determine MS data. Mainstreamed bioinformatics servers (GO, KEGG, Reactome, David and Metascape), pathview and clusterProfiler of Bioconductor were used for pathway and cluster analyses, then visualization as well. The binding proteins of PCDH9 were analyzed through Gene-Enrichment and Functional Annotation.

Results: PCDH9 was though binding with other proteins to suppress melanoma cells growth. There were 656 proteins that were separated in A375 cells while 98 proteins in G361 cells. Enrichment of PCDH9-binding proteins were in terms of nuclear acid regulation in A375, while in G361 cells they were in terms of homeostasis control . Both cells experienced the similar biological processes when being suppressed.

Conclusion: Most PCDH9-binding proteins in A375 cells are enriched in nuclear acid regulation, while in G361 cells are in homeostasis control. PPIs experienced similar biological processes to inhibit A375 and G361 cells. PPIs of PCDH9 inhibit melanoma cells by various biological processes and suppress different melanoma cells by various pathways.

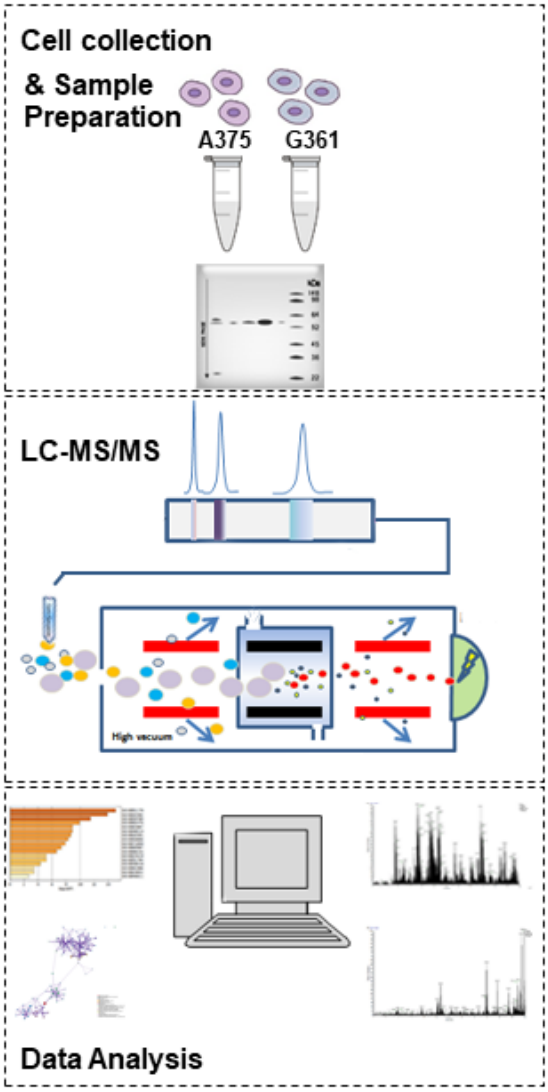

Figure 4.7. The Pipeline of Chapter 4. After cell collection and sample preparation, LC-MS/MS was used for separating and analyzing PCHD9-binding proteins and peptides. Proteome Discovery 2.2 and the uniport data were used to determine MS data. Mainstreamed bioinformatics platforms (GO, KEGG, Reactome, David and Metascape), pathview and clusterProfiler of Bioconductor were used for pathway and cluster analyses, then visualization as well. The binding proteins of PCDH9 were analyzed through Gene-Enrichment and Functional Annotation

CHAPTER 5.

Chapter 5. Primary acral amelanotic melanoma: A rare case report

1 Introduction

Due to the high propensity for metastasis and poor prognosis of MM, early diagnosis and timely treatment are crucial. Amelanotic MM (AMM) is a rare clinical type of melanoma that comprises 2-8% of all MM cases [2, 3]. AMM is a clinically diverse entity and its clinical characteristics are non-specific; hence, the diagnosis of AMM is difficult, and it can easily be misdiagnosed as other cutaneous diseases and/or tumors, such as benign ulcerations or squamous cell carcinoma [166, 167]. The aim of the present study was to report a rare case of primary acral AMM that was initially misdiagnosed as cutaneous squamous cell carcinoma. The aim of the present study was to present a rare case of primary acral amelanotic malignant melanoma (AMM). A 61-year-old man developed an aggressive tumor in the front part of the sole of his left foot, which continued to increase in size for >1 year. The biopsy results revealed epidermis loss, ulcer formation, and the presence of abundant allotropic tumor cells throughout the dermis, with deeply stained nuclei, light reddish cytoplasm, and visible multinucleated giant cells with heterogeneous nuclear division. The tumor cells exhibited partial formation of nests and bundled distribution, and there were no observed pigment particles. The diagnosis was confirmed as AMM based on the findings of the histopathological examination and immunohistochemical staining for Ki67 (+++), Melan-A (+++), human melanoma black (+), CD20 (-), cytokeratin (CK)7 (-) and CK5/6 (-).

2 Case report

On January 1st, 2019, a 61-year-old man presented to the Dermatology Clinic at the Affiliated Hospital of Guangdong Medical University with a painful pinkish tumor on the sole of his left foot that had been enlarging over the last 3 months. Approximately

1 year before the patient presented at the Dermatology Clinic of the Affiliated Hospital of Guangdong Medical University, he observed an ulcerated mass with exudate in the sole of the left foot, sized ~2×3 cm, that developed after an injury. The ulcerated wound was treated local povidone iodine and oral cefuroxime axetil for 2 months at a local clinic, but without obvious improvement. After 3 months, the mass in the left foot gradually increased in size to 7×6×5 cm **(Figure. 5.1)**. Macroscopically, the mass was cauliflower-like, with a pinkish color and no pigmentation. The mass appeared to be locally infiltrative with poorly defined boundaries and was adherent to the subcutaneous tissue with poor mobility **(Figure. 5.1)**.

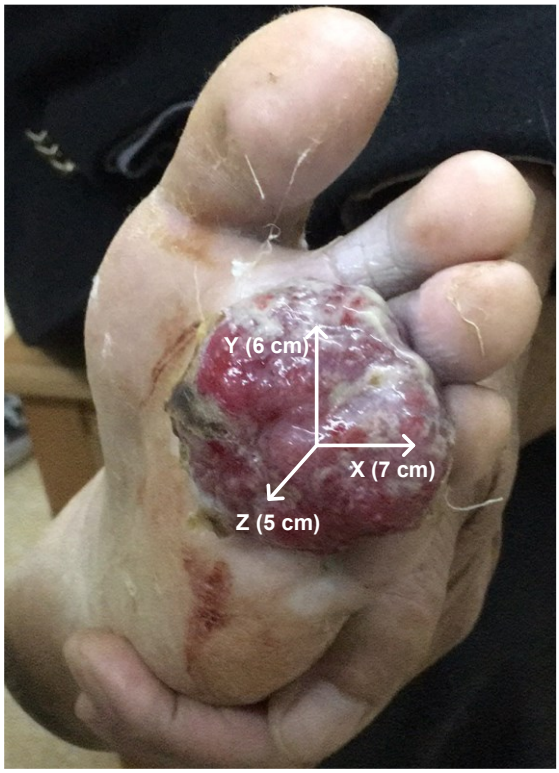

Figure 5.1. The dimensions of the mass were 7×6×5 cm. Macroscopically, the mass was cauliflower-like, with a pinkish color and no pigmentation. The mass appeared to be locally infiltrative with poorly defined boundaries and was adherent to the subcutaneous tissue with poor mobility.

The findings of the chest X-ray, electrocardiogram and abdominal B-ultrasound were normal. A biopsy was performed in previous hospital and the lesion was originally

diagnosed as squamous cell carcinoma. The mass was surgically resected, and histopathological examination revealed loss of epidermis with ulcer formation, abundant tumor cells throughout the whole thickness of the dermis (characterized by deeply stained nuclei, reddish cytoplasm and visible multinucleated giant cells), heterogeneous nuclear division, partial formation of nests and bundled distribution, and lack of pigment particles **(Figure. 5.2)**.

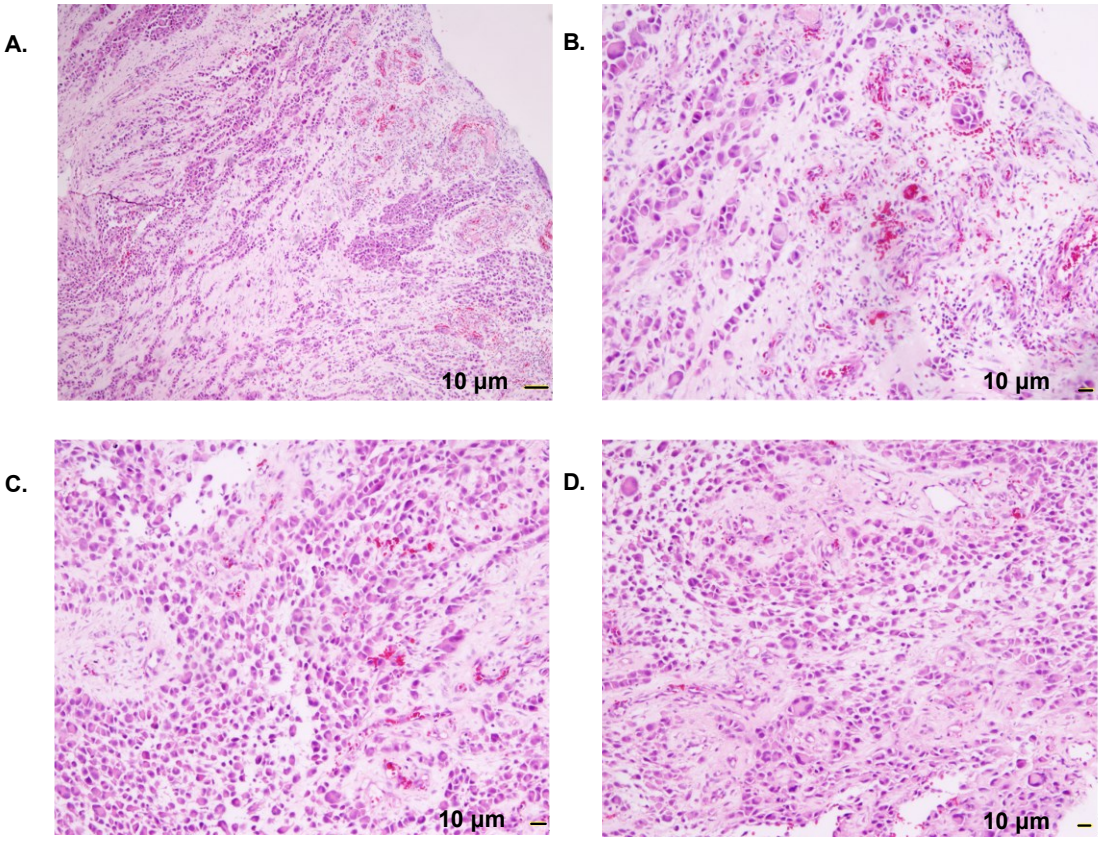

Figure 5.2. The findings on histopathological examination were as follows: (A) Loss of epidermis with ulcer formation, (B) with abundant tumor cells in the whole dermis, (C) heterogeneous nuclear division, (D) partial nest formation and bundled distribution, without pigment particles. Hematoxylin and eosin staining; all magnifications, × 10.

The results of immunohistochemical examination were as follows: Ki67 (+++), Melan-A (+++), human melanoma black (HMB)45 (+), CD20 (-), cytokeratin (CK)7 (-) and CK5/6 (-) **(Figure. 5.3)**.

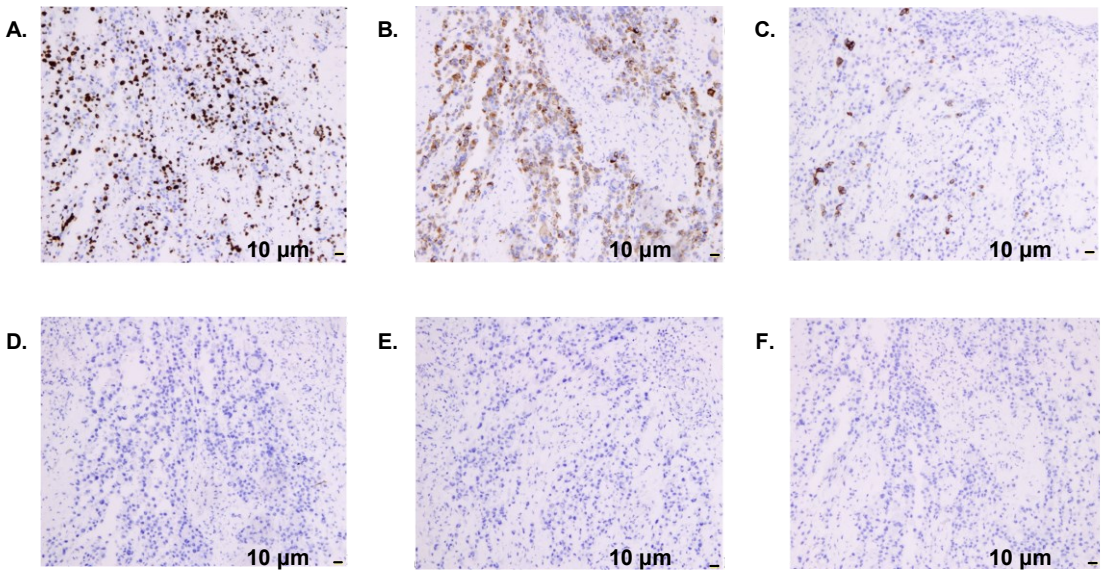

Figure 5.3. The results of the immunohistochemistry examination were as follows: (A) Ki67 (+++), (B) Melan-A (+++), (C) human melanoma black 45 (+), (D) CD20 (-), (E) CK7 (-), (F) CK5/6 (-). CK, cytokeratin; all magnifications, ×20.

The evidence mentioned above was consistent with the diagnosis of AMM. The patient was subjected to partial amputation of the left foot and plastic reconstructive surgery on January 4, 2019, and the pathological examination of the surgical specimen further confirmed the diagnosis of AMM **(Figure. 5.4)**. The patient is currently followed up and awaiting positron emission tomography-computed tomography (PET-CT) examination to determine the presence of metastatic disease. The last follow-up was on January 23rd, 2019.

Figure 5.4. The patient was subjected to partial amputation of the left foot and plastic reconstructive surgery.

3 Discussion

MM is a highly malignant tumor, accounting for 6.8-20% (third in incidence) of cutaneous malignant tumors, that mostly occurs in the skin, although rare cases of non-cutaneous melanoma may be encountered in the eyes and internal organs [168]. Primary acral AMM is an aggressive rare neoplasm, with only few cases reported to date. AMM does not produce melanin, therefore it may easily be misdiagnosed as foot ulcer or/and squamous cell carcinoma [166, 167]. When the patient was first referred to our hospital, he had stage T4b disease. A PET-CT scan was suggested; however, there were no readily identifiable metastases around the MM lesions, and the patient refused. Without a PET-CT scan, the presence or absence of visceral metastases could not be certainly confirmed. The etiology of AMM remains unclear, although it was previously hypothesized that the decreased tyrosinase activity and/or melanin transport disorders may constitute possible reasons [169]. AMM has been reported in the skin and the mucosa of the digestive tract and/or the genitourinary tract [168]. AMM is a clinically diverse entity without specific characteristics; early lesions are atypical and usually appear as pinkish papules, either as a single lesion or as a cluster [168, 170]. Invasive

growth during the later stages may manifest as red plaques with granulomatous nodules or ulcers; therefore, it is important to be aware of the diagnostic difficulties of primary acral AMM. In the present case, the diagnosis of AMM was confirmed by histopathology and immunohistochemistry. The immunohistochemistry staining may help diagnose AMM using common immunological markers, including HMB-45, Melan-A, S-100 and Ki-67 [171]. Ohnishi et al have reported that Melan-A is the most precise marker in terms of sensitivity and specificity [171]; in the present case, the immunohistochemical results revealed that the tumor was positive for HMB-45, Melan-A and Ki-67, while it was negative for CD20, CK7 and CK5/6.

The characteristics of AMM occurring in the limbs and body differ from those of other tumors, such as squamous cell carcinoma [171], basal cell carcinoma and lymphoma. AMMs are characterized by a higher proportion of nodular and acral lentiginous melanoma subtypes compared with pigmented melanomas. AMMs are also characterized by a greater Breslow thickness, higher mitotic rate, more frequent ulceration, higher tumor stage at diagnosis, and lower survival rates compared with pigmented melanoma [172]. Early surgical resection is the first choice of curative treatment and chemotherapy is the most commonly used palliative treatment. Although there have been advances in MM immunotherapy for patients with late-stage disease and metastasis, such as PD-1/CTLA-4 antibodies and IL-2 targeted therapy, due to the prognosis, early detection and treatment remain crucial for prolonging survival.

This chapter represents a modified version of the paper already published: Zhang J.J. et al., Primary acral amelanotic melanoma: A rare case report. Molecular and Clinical Oncology, 2020; 59. https://doi.org/10.3892/mco.2020.2129.

Chapter 5 Conclusion

Background: Amelanotic MM (AMM) is a rare clinical type of melanoma with non-specific clinical characteristics. The diagnosis of AMM is difficult, and easily misdiagnosed as other cutaneous diseases.

Methods: Biopsy check, histopathological examination immunohistochemical staining by common markers (HMB-45, Melan-A, S-100 and Ki-67) were performed.

Results: The chest X-ray, electrocardiogram and abdominal B-ultrasound of patient were normal. After surgical resecting the tumor mass, the histopathological examination revealed loss of epidermis with ulcer formation, abundant tumor cells throughout the whole thickness of the dermis (characterized by deeply stained nuclei, reddish cytoplasm and visible multinucleated giant cells), heterogeneous nuclear division, partial formation of nests and bundled distribution, and lack of pigment particles, while the immunohistochemical staining for Ki67 (+++), Melan-A (+++), human melanoma black (+), CD20 (-), cytokeratin (CK)7 (-) and CK5/6 (-)

Conclusion: The diagnosis was confirmed as AMM based on the findings of the histopathological examination and immunohistochemical staining.

CHAPTER 6.

Chapter 6. The main conclusions, innovations, and prospects of this dissertation

1 The main conclusions

The current melanoma investigation aimed to evaluate cancersuppression on different platforms. Firstly, common phytochemical RSV was evaluated to target the potential biomarkers, like Cyclin D1, PCDH9, RAC1of melanoma. Secondly, according to previous studies and *in silico* screening, PCDH9 and RAC1 were pinpointed for further investigation. The vector tool like lentivirus was used to overexpress and interfere PCHD9 expression in melanoma cells (A375 and G361). Then *in vitro* melanoma-cell-culture models and Specimen were studied. We demonstrated that PCDH9 could suppress melanoma cells. Third, after LC-MS/MS, the proteins and peptides that bind to PCDH9 were separated, then we used UniProt to analyse and demonstrate the functions of PCDH9. Forth, a rare case of amelanotic malignant melanoma (AMM) was reported that broaden the understanding of melanoma. The conclusions of current dissertation are as follows:

(1) RSV is a typical phytochemical and secondary metabolite of plant. Because of its antitumor properties, the effect of RSV on melanoma cells (A375) was tested. The ability of RSV to suppress melanoma by disrupting cell cycle and inducing apoptosis was assessed. We have found the influences of RSV were duration and concentration dependent, as increasing these two factors the rate become acuter. The two factors of RSV (duration and concentration) also influenced the degrees of RSV-induced apoptosis, and duration was the principal factor. RSV can influence A375 cells by affecting cell cycle: it downregulated Cyclin D1 and PCDH9, while the influence of RSV to Rac1 was not obvious.

(2) Specimen investigations of IHC assay displayed lower PCDH9 expressions in benign nevus tissue or/and normal skin than in malignant melanoma specimens, which suggested the indicative function of PCDH9. The study also revealed that PCDH9 was

mainly expressed in the cytoplasm rather than in nuclei. The results of a series of investigations-including cell viability assay, apoptosis assay and PCR of overexpression and interference of PCDH9 by GV358-PCDH9 lentivirus and GV358-SiRNA lentivirus respectively in melanoma cells (A375 and G361)- displayed overexpressed PCDH9 triggered upregulated expressions of CCND1 (Cyclin D1), while RAC1 and MMP2 were downregulated, and apoptosis of melanoma cell lines was promoted. Interfered PCDH9 induced downregulation of CCND1 (Cyclin D1), while RAC1 and MMP2 were upregulated and decreased apoptosis. The survival analysis of MMP2 showed that lower expression could increase prognostic survival, presumably overexpression of PCDH9 might increase melanoma survival. Though the cell regulator Cyclin D1 has been altered by PCDH9, the expression changes of PCDH9 did not affect melanoma cell regulation in a significant manner, indicating that Cyclin D1 may affect melanoma cells by another way. We hypothesized that Cyclin D1 might play important role in trafficking of PCDH9 than in cell regulation. RAC1 as a GTPase is involving in various cell biological processes and influences ROS generation that triggers oncogenesis. PCDH9 negatively correlated with RAC1, whose character furtherly proved the suppressed mechanism of PCDH9 on melanoma cells. To conclude, alteration of PCDH9 could affect melanoma cell viability. To make a hypothesis, overexpression of PCDH9 suppressed melanoma cells and might increase prognostic survival.

(3) Mapping PCDH9-binding proteins interaction by mass spectrometry was processed. Firstly, LC-MS/MS were processed to separate and analyze PCDH9-binding proteins. Then bioinformatic analyses were applied, popular bioinformatic platforms were selected for analyzing. After performing KEGG pathway, Gene-Enrichment and Functional Annotation Analysis, we found that most PCDH9-binding proteins in A375 cells are enriched in nuclear acid regulation, while in G361 cells are in homeostasis control. The biological processes were similar in two cells (A375 and G361 cells). After Cytoscape analysis, we found that the PPIs in A375 were focused on regulation of nucleic acid, while in G361 cells in homeostasis control. Herein, the conclusion are as

follows: the analyses of PCDH9-binding proteins by bioinformatic platforms exhibited PPI of PCDH9 to inhibit melanoma cells by different biological processes and suppress different melanoma cells by various methods.

(4) The rare amelanotic malignant melanoma (AMM) that was previously diagnosed as cutaneous squamous cell carcinoma (cSCC) was reported. This AMM case shows the various phenotypes of melanoma.

2 The innovations

(1) Investigate melanoma by eastern population.

(2) Explore this disease through different platform: First, use normal natural anti-tumor compound (resveratrol) to find potential bio-targets of melanoma; second, with the literature checking and bioinformatic study, the novel marker PCHD9 were selected. Third, *in vitro* study with immunohistochemical analysis through skin tissues were processed.

(3) Bioinformatics platforms were applied to investigate PPI mapping of PCDH9.

(4) A rare case -primary acral amelanotic melanoma- was reported.

3 The prospects

Melanoma is one the most dangerous cancers and the detected stage of melanoma is the key to cure this disease and the most relevant prognostic factor for survival [173]. As the developments and applications of Single Cell Sequencing, we could use this technology for reveal melanoma key molecules. During the whole melanoma study, we have found that PCDH9 suppressed different melanoma cell lines by various pathways. It will be helpful to process melanoma study through Single Cell Sequencing, even Spatial Transcriptomics (ST). As artificial intelligence (AI) developing, AI is capable to differentiate melanoma from benign nevi by images recognition with dermatologist-level precision [174]. Nano particles are easier absorbed by cancer cells and biocompatible as well. We could use Nano carrier as vector to bring PCDH9 for melanoma treatments.

Lists of publication about melanoma

1. Hui-Zhi Yang[#], **Jiaojiao Zhang**[#], Jie Zeng, Shengbo Liu, Fang Zhang, Francesca Giampieri, Danila Cianciosi, Tamara Y. Forbes-Hernandez, Johura Ansary, RongYi Chen1*, Maurizio Battino*, Resveratrol inhibits the proliferation of melanoma cells by modulating cell cycle. International Journal of Food Sciences and Nutrition. 2020 Jan 2; 71(1): 84-93.
2. **Jiaojiao Zhang**[#], Huizhi Yang[#], Fang Zhang, Jianqiang Shi, Rongyi Chen, Primary acral amelanotic melanoma: A rare case report. Molecular and Clinical Oncology. 2020 Aug 11; MS No. 11342-223491.
3. **Jiaojiao Zhang**, Jiahao Xie, Chunchan Zheng, Ruitao Zou, Guiyue Cai, Xiaoxuan Chen, Rongyi Chen*, PCDH9-Pyk2-CyclinD1 interaction target RAC1/ROS-NADPH-oxidase complex to inhibit melanoma cells, Poster in the 5th Annual Meeting of Chinese Society of Dermatology (CSID).
4. **Jiaojiao Zhang**, Zuhua Wang, Hui-Zhi Yang, Danila Cianciosi, Rongyi Chen*, Maurizio Battino*, Resveratrol suppresses melanoma by modulating cell cycle, Poster in the 9th ISHS International Strawberry Symposium.

REFERENCES

1. Series, W.H.O.T.R. *Global Health Observatory.* [cited 2018 June 21]; Available from: http://www.who.int/gho/database/en/.
2. Bono, A., et al., *Clinical and dermatoscopic diagnosis of early amelanotic melanoma.* Melanoma Research, 2001. **11**(5): p. 491-494.
3. Pizzichetta, M., et al., *Amelanotic/hypomelanotic melanoma: clinical and dermoscopic features.* British Journal of Dermatology, 2004. **150**(6): p. 1117-1124.
4. China, N.B.o.S.o., *China Statistical Yearbook*. 2010, China Statistics Press: Beijing, China.
5. Jiang, Z., et al., *Resveratrol and cancer treatment: updates.* Ann N Y Acad Sci, 2017. **1403**(1): p. 59-69.
6. Li, D.X., et al., *Inhibitory effect of berberine on human skin squamous cell carcinoma A431 cells.* Genet Mol Res, 2015. **14**(3): p. 10553-68.
7. Birch-Johansen, F., et al., *Does hormone replacement therapy and use of oral contraceptives increase the risk of non-melanoma skin cancer?* Cancer Causes & Control, 2012. **23**(2): p. 379-388.
8. Ouyang, Y.-H. *Skin cancer of the head and neck*. in *Seminars in plastic surgery*. 2010. Thieme Medical Publishers.
9. Cramer, S., *The origin of epidermal melanocytes. Implications for the histogenesis of nevi and melanomas.* Archives of pathology & laboratory medicine, 1991. **115**(2): p. 115.
10. Rebecca, V.W., R. Somasundaram, and M. Herlyn, *Pre-clinical modeling of cutaneous melanoma.* Nature Communications, 2020. **11**(1): p. 1-9.
11. Series, W.H.O.T.R., *World Cancer Report 2014*. 2014, World Health Organization. p. Chapter 5.14.
12. Series, N.C.I.C.T.R., *Melanoma Treatment–for health professionals* 2015.
13. Samarasinghe, V. and V. Madan, *Nonmelanoma skin cancer.* J Cutan Aesthet Surg, 2012. **5**(1): p. 3-10.
14. Aronow, M.E., A.K. Topham, and A.D. Singh, *Uveal Melanoma: 5-Year Update on Incidence, Treatment, and Survival (SEER 1973-2013).* Ocul Oncol Pathol, 2018. **4**(3): p. 145-151.
15. Society, A.C., *American Cancer Society: Cancer Facts and Figures 2019.* Atlanta, Ga: American Cancer Society, 2019.
16. Zhu, X., et al., *Proline-Rich Protein Tyrosine Kinase 2 in Inflammation and Cancer.* Cancers (Basel), 2018. **10**(5): p. 139.
17. UK, C.R., *Melanoma: statistics and outlook.* 2010.
18. Howlader, N., et al., *SEER cancer statistics review, 1975–2010.* Bethesda, MD: National Cancer Institute, 2013. **12**.
19. Weinstein, D., et al., *Diagnostic and prognostic biomarkers in melanoma.* J Clin Aesthet Dermatol, 2014. **7**(6): p. 13-24.

20. Schmidberger, H., et al., *Long-term survival of patients after ipilimumab and hypofractionated brain radiotherapy for brain metastases of malignant melanoma: sequence matters.* Strahlentherapie und Onkologie, 2018. **194**(12): p. 1144-1151.
21. Arheden, A., et al., *Real-world data on PD-1 inhibitor therapy in metastatic melanoma.* Acta Oncologica, 2019. **58**(7): p. 962-966.
22. Watts, C.G., et al., *Clinical features associated with individuals at higher risk of melanoma: a population-based study.* JAMA dermatology, 2017. **153**(1): p. 23-29.
23. Rastrelli, M., et al., *Melanoma: epidemiology, risk factors, pathogenesis, diagnosis and classification.* In Vivo, 2014. **28**(6): p. 1005-11.
24. Chi, Z., et al., *Clinical presentation, histology, and prognoses of malignant melanoma in ethnic Chinese: a study of 522 consecutive cases.* BMC Cancer, 2011. **11**(1): p. 85.
25. Jiaojie, L., K. Yunyi, and C. Xu, *Analysis of KIT gene mutation in melanoma patients.* China Oncology, 2016. **26**(5): p. 399-403.
26. Xavier-Junior, J.C.C. and J.P. Ocanha-Xavier, *WHO (2018) Classification of Skin Tumors*. 2019, LWW.
27. Schuchter, L., *Melanoma and nonmelanoma skin cancers*, in *Goldman's Cecil Medicine*. 2012, Elsevier. p. 1329-1334.
28. Linares, M.A., A. Zakaria, and P. Nizran, *Skin Cancer.* Primary care, 2015. **42**(4): p. 645-659.
29. Egger, M.E., et al., *Outcomes and prognostic factors in nodular melanomas.* Surgery, 2012. **152**(4): p. 652-660.
30. Parish, L.C., *Andrews' Diseases of the Skin: Clinical Dermatology.* JAMA, 2011. **306**(2): p. 213-213.
31. Kallini, J.R., S.K. Jain, and A. Khachemoune, *Lentigo maligna: review of salient characteristics and management.* Am J Clin Dermatol, 2013. **14**(6): p. 473-80.
32. McKENNA, J.K., et al., *Lentigo Maligna/Lentigo Maligna Melanoma: Current State of Diagnosis and Treatment.* Dermatologic Surgery, 2006. **32**(4): p. 493-504.
33. Xiong, M., A. Charifa, and C.S.J. Chen. *Lentigo Maligna Melanoma*. StatPearls [Internet] 2020 2020 Jun 29 [cited 2020; Available from: https://www.ncbi.nlm.nih.gov/books/NBK482163/.
34. Chang, D.Z., et al., *Clinical significance of BRAF mutations in metastatic melanoma.* Journal of translational medicine, 2004. **2**(1): p. 1-5.
35. Eskandarpour, M., et al., *Frequency of UV-inducible NRAS mutations in melanomas of patients with germline CDKN2A mutations.* Journal of the National Cancer Institute, 2003. **95**(11): p. 790-798.
36. Hodis, E., et al., *A landscape of driver mutations in melanoma.* Cell, 2012. **150**(2): p. 251-263.
37. Vidwans, S.J., et al., *A melanoma molecular disease model.* PloS one, 2011. **6**(3): p. e18257.

38. Wellbrock, C. and I. Arozarena, *The Complexity of the ERK/MAP-Kinase Pathway and the Treatment of Melanoma Skin Cancer.* Frontiers in Cell and Developmental Biology, 2016. **4**(33).
39. Gajos-Michniewicz, A. and M. Czyz, *Modulation of WNT/β-catenin pathway in melanoma by biologically active components derived from plants.* Fitoterapia, 2016. **109**: p. 283-292.
40. Beaumont, K.A., N. Mohana-Kumaran, and N.K. Haass. *Modeling melanoma in vitro and in vivo*. in *Healthcare*. 2014. Multidisciplinary Digital Publishing Institute.
41. Bhadury, J., et al., *Hypoxia-regulated gene expression explains differences between cell line-derived xenografts and patient-derived xenografts*. 2016, AACR.
42. Li, L., M. Fukunaga-Kalabis, and M. Herlyn, *The three-dimensional human skin reconstruct model: a tool to study normal skin and melanoma progression.* JoVE (Journal of Visualized Experiments), 2011(54): p. e2937.
43. Jenkins, R.W., et al., *Ex vivo profiling of PD-1 blockade using organotypic tumor spheroids.* Cancer Discovery, 2018. **8**(2): p. 196-215.
44. Patton, E.E., et al., *BRAF mutations are sufficient to promote nevi formation and cooperate with p53 in the genesis of melanoma.* Current Biology, 2005. **15**(3): p. 249-254.
45. White, R.M., et al., *Transparent adult zebrafish as a tool for in vivo transplantation analysis.* Cell stem cell, 2008. **2**(2): p. 183-189.
46. Nakamura, Y., *The Role and Necessity of Sentinel Lymph Node Biopsy for Invasive Melanoma.* Front Med (Lausanne), 2019. **6**: p. 231.
47. Ali, Z., N. Yousaf, and J. Larkin, *Melanoma epidemiology, biology and prognosis.* European Journal of Cancer Supplements, 2013. **11**(2): p. 81-91.
48. Wilson, M.A. and L.M. Schuchter, *Chemotherapy for melanoma*, in *Melanoma*. 2016, Springer. p. 209-229.
49. Kim, C., et al., *Long-Term Survival in Patients with Metastatic Melanoma Treated with DTIC or Temozolomide.* The Oncologist, 2010. **15**(7): p. 765-771.
50. Baker, S.D., et al., *Absorption, metabolism, and excretion of 14C-temozolomide following oral administration to patients with advanced cancer.* Clinical Cancer Research, 1999. **5**(2): p. 309-317.
51. Miklavčič, D., et al., *Electrochemotherapy: technological advancements for efficient electroporation-based treatment of internal tumors.* Medical & Biological Engineering & Computing, 2012. **50**(12): p. 1213-1225.
52. Testori, A., S. Ribero, and V. Bataille, *Diagnosis and treatment of in-transit melanoma metastases.* European Journal of Surgical Oncology, 2017. **43**(3): p. 544-560.
53. Matthiessen, L.W., et al., *Management of cutaneous metastases using electrochemotherapy.* Acta Oncologica, 2011. **50**(5): p. 621-629.
54. Austin, E., et al., *Laser and light-based therapy for cutaneous and soft-tissue metastases of malignant melanoma: a systematic review.* Archives of Dermatological Research, 2017. **309**(4): p. 229-242.

55. Yin, R., et al., *Photodynamic therapy with decacationic [60]fullerene monoadducts: Effect of a light absorbing electron-donor antenna and micellar formulation.* Nanomedicine: Nanotechnology, Biology and Medicine, 2014. **10**(4): p. 795-808.
56. Baldea, I. and A. Filip, *Photodynamic therapy in melanoma—an update.* Journal of Physiology and pharmacology, 2012. **63**(2): p. 109.
57. Huang, Y.-Y., et al., *Melanoma resistance to photodynamic therapy: new insights.* Biological Chemistry, 2013. **394**(2): p. 239.
58. Biteghe, F.A.N. and L.M. Davids, *A combination of photodynamic therapy and chemotherapy displays a differential cytotoxic effect on human metastatic melanoma cells.* Journal of Photochemistry and Photobiology B: Biology, 2017. **166**: p. 18-27.
59. Bastian, B.C., *The molecular pathology of melanoma: an integrated taxonomy of melanocytic neoplasia.* Annu Rev Pathol, 2014. **9**: p. 239-71.
60. Rossi, E., et al., *Pembrolizumab as first-line treatment for metastatic uveal melanoma.* Cancer Immunology, Immunotherapy, 2019. **68**(7): p. 1179-1185.
61. Dummer, R., et al., *Overall survival in patients with BRAF-mutant melanoma receiving encorafenib plus binimetinib versus vemurafenib or encorafenib (COLUMBUS): a multicentre, open-label, randomised, phase 3 trial.* The Lancet Oncology, 2018. **19**(10): p. 1315-1327.
62. Johnpulle, R.A., D.B. Johnson, and J.A. Sosman, *Molecular targeted therapy approaches for BRAF wild-type melanoma.* Current oncology reports, 2016. **18**(1): p. 6.
63. Rogiers, A., et al., *Long-term survival, quality of life, and psychosocial outcomes in advanced melanoma patients treated with immune checkpoint inhibitors.* Journal of oncology, 2019. **2019**.
64. Hodi, F.S., et al., *Improved Survival with Ipilimumab in Patients with Metastatic Melanoma.* New England Journal of Medicine, 2010. **363**(8): p. 711-723.
65. Hauschild, A., et al., *Dabrafenib in BRAF-mutated metastatic melanoma: a multicentre, open-label, phase 3 randomised controlled trial.* The Lancet, 2012. **380**(9839): p. 358-365.
66. McArthur, G.A., et al., *Safety and efficacy of vemurafenib in BRAFV600E and BRAFV600K mutation-positive melanoma (BRIM-3): extended follow-up of a phase 3, randomised, open-label study.* The Lancet Oncology, 2014. **15**(3): p. 323-332.
67. Robert, C., et al., *Improved Overall Survival in Melanoma with Combined Dabrafenib and Trametinib.* New England Journal of Medicine, 2014. **372**(1): p. 30-39.
68. Jerby-Arnon, L., et al., *A cancer cell program promotes T cell exclusion and resistance to checkpoint blockade.* Cell, 2018. **175**(4): p. 984-997. e24.
69. Hromic-Jahjefendic, A. and K. Lundstrom, *Viral Vector-Based Melanoma Gene Therapy.* Biomedicines, 2020. **8**(3): p. 60.
70. Conry, R.M., et al., *Talimogene laherparepvec: First in class oncolytic virotherapy.* Hum Vaccin Immunother, 2018. **14**(4): p. 839-846.

71. Stone, D., *Novel viral vector systems for gene therapy.* Viruses, 2010. **2**(4): p. 1002-7.
72. Brenner, M.K., et al., *Gene-marking to trace origin of relapse after autologous bone-marrow transplantation.* The Lancet, 1993. **341**(8837): p. 85-86.
73. Lundstrom, K., *Oncolytic alphaviruses in cancer immunotherapy.* Vaccines, 2017. **5**(2): p. 9.
74. Lundstrom, K., *Viral vectors in gene therapy.* Diseases, 2018. **6**(2): p. 42.
75. Vähä-Koskela, M.J.V., et al., *Oncolytic Capacity of Attenuated Replicative Semliki Forest Virus in Human Melanoma Xenografts in Severe Combined Immunodeficient Mice.* Cancer Research, 2006. **66**(14): p. 7185-7194.
76. Määttä, A.-M., et al., *Evaluation of cancer virotherapy with attenuated replicative Semliki forest virus in different rodent tumor models.* International Journal of Cancer, 2007. **121**(4): p. 863-870.
77. Galanis, E., et al., *Phase II Trial of Intravenous Administration of Reolysin® (Reovirus Serotype-3-dearing Strain) in Patients with Metastatic Melanoma.* Molecular Therapy, 2012. **20**(10): p. 1998-2003.
78. Niu, Z., et al., *Recombinant Newcastle Disease virus Expressing IL15 Demonstrates Promising Antitumor Efficiency in Melanoma Model.* Technology in Cancer Research & Treatment, 2015. **14**(5): p. 607-615.
79. Liang, W., et al., *Application of autologous tumor cell vaccine and NDV vaccine in treatment of tumors of digestive traet.* World Journal of Gastroenterology, 2003. **9**(3): p. 495.
80. Shafren, D.R., et al., *Systemic Therapy of Malignant Human Melanoma Tumors by a Common Cold-Producing Enterovirus, Coxsackievirus A21.* Clinical Cancer Research, 2004. **10**(1): p. 53-60.
81. Andtbacka, R.H., et al., *Phase II calm extension study: Coxsackievirus A21 delivered intratumorally to patients with advanced melanoma induces immune-cell infiltration in the tumor microenvironment.* Journal for ImmunoTherapy of Cancer, 2015. **3**(Suppl 2): p. P343.
82. Andtbacka, R.H.I., et al., *Patterns of Clinical Response with Talimogene Laherparepvec (T-VEC) in Patients with Melanoma Treated in the OPTiM Phase III Clinical Trial.* Annals of Surgical Oncology, 2016. **23**(13): p. 4169-4177.
83. Puzanov, I., et al., *Talimogene Laherparepvec in Combination With Ipilimumab in Previously Untreated, Unresectable Stage IIIB-IV Melanoma.* Journal of Clinical Oncology, 2016. **34**(22): p. 2619-2626.
84. Bommareddy, P.K., et al., *Talimogene Laherparepvec (T-VEC) and Other Oncolytic Viruses for the Treatment of Melanoma.* American Journal of Clinical Dermatology, 2017. **18**(1): p. 1-15.
85. Silk, A.W., et al., *Abstract CT026: phase 1b study of intratumoral Coxsackievirus A21 (CVA21) and systemic pembrolizumab in advanced melanoma patients: interim results of the CAPRA clinical trial*. 2017, AACR.
86. Lundstrom, K., *Biology and application of alphaviruses in gene therapy.* Gene Therapy, 2005. **12**(1): p. S92-S97.

87. Shin, J.A., et al., *Apoptotic effect of Polygonum Cuspidatum in oral cancer cells through the regulation of specificity protein 1.* Oral diseases, 2011. **17**(2): p. 162-170.
88. Sales, J.M. and A.V. Resurreccion, *Resveratrol in peanuts.* Crit Rev Food Sci Nutr, 2014. **54**(6): p. 734-70.
89. Jasinski, M., L. Jasinska, and M. Ogrodowczyk, *Resveratrol in prostate diseases - a short review.* Cent European J Urol, 2013. **66**(2): p. 144-9.
90. Back, J.H., et al., *Resveratrol-mediated downregulation of Rictor attenuates autophagic process and suppresses UV-induced skin carcinogenesis.* Photochem Photobiol, 2012. **88**(5): p. 1165-72.
91. Hao, Y.Q., et al., *[Study of apoptosis related factors regulatory mechanism of resveratrol to human skin squamous cell carcinoma A431 xenograft in nude mice].* Zhonghua Yi Xue Za Zhi, 2013. **93**(6): p. 464-8.
92. Kim, S.M. and S.Z. Kim, *Biological Activities of Resveratrol against Cancer.* 2018.
93. Ishiyama, M., et al., *A highly water-soluble disulfonated tetrazolium salt as a chromogenic indicator for NADH as well as cell viability.* Talanta, 1997. **44**(7): p. 1299-1305.
94. Tominaga, H., et al., *A water-soluble tetrazolium salt useful for colorimetric cell viability assay.* Analytical Communications, 1999. **36**(2): p. 47-50.
95. Doonan, F. and T.G. Cotter, *Morphological assessment of apoptosis.* Methods, 2008. **44**(3): p. 200-4.
96. Wickham, H., *ggplot2: Elegant Graphics for Data Analysis*. 2016: Springer-Verlag New York.
97. Team, R.C. *A language and environment for statistical*. 2013; Available from: http://www.R-project.org/.
98. Bartlett, M.S., *Tests of significance in factor analysis.* British Journal of statistical psychology, 1950. **3**(2): p. 77-85.
99. Elmore, S., *Apoptosis: a review of programmed cell death.* Toxicol Pathol, 2007. **35**(4): p. 495-516.
100. Sunarpi, H., et al., *Apoptosis: A review of programmed cell death.* Journal of Biological Sciences, 2017. **18**(8): p. 7-30.
101. Fesik, S.W., *Promoting apoptosis as a strategy for cancer drug discovery.* Nature Reviews Cancer, 2005. **5**(11): p. 876.
102. Yuan, Y., et al., *Targeted theranostic platinum(IV) prodrug with a built-in aggregation-induced emission light-up apoptosis sensor for noninvasive early evaluation of its therapeutic responses in situ.* J Am Chem Soc, 2014. **136**(6): p. 2546-54.
103. MacLachlan, T.K., N. Sang, and A. Giordano, *Cyclins, cyclin-dependent kinases and cdk inhibitors: implications in cell cycle control and cancer.* Crit Rev Eukaryot Gene Expr, 1995. **5**(2): p. 127-56.
104. Pucci, B., M. Kasten, and A. Giordano, *Cell cycle and apoptosis.* Neoplasia, 2000. **2**(4): p. 291-9.
105. Fagerberg, L., et al., *Analysis of the human tissue-specific expression by*

genome-wide integration of transcriptomics and antibody-based proteomics. Mol Cell Proteomics, 2014. **13**(2): p. 397-406.
106. Didsbury, J., et al., *rac, a novel ras-related family of proteins that are botulinum toxin substrates.* J Biol Chem, 1989. **264**(28): p. 16378-82.
107. Jordan, P., et al., *Cloning of a novel human Rac1b splice variant with increased expression in colorectal tumors.* Oncogene, 1999. **18**(48): p. 6835-9.
108. McAllister, S.S., *Got a light? Illuminating lung cancer.* Sci Transl Med, 2012. **4**(142): p. 142fs22.
109. Hulpiau, P. and F. van Roy, *Molecular evolution of the cadherin superfamily.* Int J Biochem Cell Biol, 2009. **41**(2): p. 349-69.
110. He, Y., et al., *Expression and significance of Wnt signaling components and their target genes in breast carcinoma.* Molecular medicine reports, 2014. **9**(1): p. 137-143.
111. Bauer, N.N., et al., *Rac1 activity regulates proliferation of aggressive metastatic melanoma.* Exp Cell Res, 2007. **313**(18): p. 3832-9.
112. Hodis, E., et al., *A landscape of driver mutations in melanoma.* Cell, 2012. **150**(2): p. 251-63.
113. Krauthammer, M., et al., *Exome sequencing identifies recurrent somatic RAC1 mutations in melanoma.* Nat Genet, 2012. **44**(9): p. 1006-14.
114. Lv, J., et al., *PCDH9 acts as a tumor suppressor inducing tumor cell arrest at G0/G1 phase and is frequently methylated in hepatocellular carcinoma.* Molecular medicine reports, 2017. **16**(4): p. 4475-4482.
115. Bennett, R.N. and R.M. Wallsgrove, *Secondary metabolites in plant defence mechanisms.* New phytologist, 1994. **127**(4): p. 617-633.
116. Athar, M., et al., *Multiple molecular targets of resveratrol: Anti-carcinogenic mechanisms.* Arch Biochem Biophys, 2009. **486**(2): p. 95-102.
117. Niles, R.M., et al., *Resveratrol is a potent inducer of apoptosis in human melanoma cells.* Cancer letters, 2003. **190**(2): p. 157-163.
118. Hsieh, T.-c., et al., *Inhibition of melanoma cell proliferation by resveratrol is correlated with upregulation of quinone reductase 2 and p53.* Biochemical and biophysical research communications, 2005. **334**(1): p. 223-230.
119. Gatouillat, G., et al., *Resveratrol induces cell-cycle disruption and apoptosis in chemoresistant B16 melanoma.* J Cell Biochem, 2010. **110**(4): p. 893-902.
120. Goswami, S.K. and D.K. Das, *Resveratrol and chemoprevention.* Cancer Lett, 2009. **284**(1): p. 1-6.
121. Wu, Z., et al., *Resveratrol inhibits the proliferation of human melanoma cells by inducing G1/S cell cycle arrest and apoptosis.* Mol Med Rep, 2015. **11**(1): p. 400-4.
122. Utikal, J., J.C. Becker, and S. Ugurel, *Diagnostic and prognostic biomarkers in melanoma: current state of play*, in *Diagnostic and Prognostic Biomarkers and Therapeutic Targets in Melanoma*. 2012, Springer. p. 9-18.
123. Chen, R., et al., *A time course-dependent metastatic gene expression signature predicts outcome in human metastatic melanomas.* Diagn Pathol, 2014. **9**(1): p. 155.

124. Chen, R., et al., *Rac1 regulates skin tumors by regulation of keratin 17 through recruitment and interaction with CD11b+ Gr1+ cells.* Oncotarget, 2014. **5**(12): p. 4406.
125. Dinehart, M.S., et al., *Immunohistochemistry utilization in the diagnosis of melanoma.* J Cutan Pathol, 2020. **47**(5): p. 446-450.
126. Hodis, E., et al., *A landscape of driver mutations in melanoma.* cell, 2012. **150**(2): p. 251-263.
127. Wang, C., et al., *Downregulation of PCDH9 predicts prognosis for patients with glioma.* J Clin Neurosci, 2012. **19**(4): p. 541-5.
128. Bidoki, S.H., et al., *Assessing Expression of TGF-B2 and PCDH9 Genes in Breast Cancer Patients.* Age, 2018. **7**: p. 20.
129. Wang, C., et al., *Characterizing the role of PCDH9 in the regulation of glioma cell apoptosis and invasion.* J Mol Neurosci, 2014. **52**(2): p. 250-60.
130. Chen, Y., et al., *Loss of PCDH9 is associated with the differentiation of tumor cells and metastasis and predicts poor survival in gastric cancer.* Clinical & experimental metastasis, 2015. **32**(5): p. 417-428.
131. Espina, C., et al., *A critical role for Rac1 in tumor progression of human colorectal adenocarcinoma cells.* Am J Pathol, 2008. **172**(1): p. 156-66.
132. Aznar, S., et al., *Rho GTPases: potential candidates for anticancer therapy.* Cancer Lett, 2004. **206**(2): p. 181-91.
133. del Pulgar, T.G., et al., *Rho GTPase expression in tumourigenesis: evidence for a significant link.* Bioessays, 2005. **27**(6): p. 602-613.
134. Vega, F.M. and A.J. Ridley, *Rho GTPases in cancer cell biology.* FEBS Lett, 2008. **582**(14): p. 2093-101.
135. Davis, M.J., et al., *RAC1P29S is a spontaneously activating cancer-associated GTPase.* Proc Natl Acad Sci U S A, 2013. **110**(3): p. 912-7.
136. Ellenbroek, S.I. and J.G. Collard, *Rho GTPases: functions and association with cancer.* Clin Exp Metastasis, 2007. **24**(8): p. 657-72.
137. Bae, Y.S., et al., *Regulation of reactive oxygen species generation in cell signaling.* Mol Cells, 2011. **32**(6): p. 491-509.
138. Wu, W.S., *The signaling mechanism of ROS in tumor progression.* Cancer Metastasis Rev, 2006. **25**(4): p. 695-705.
139. Bedard, K. and K.H. Krause, *The NOX family of ROS-generating NADPH oxidases: physiology and pathophysiology.* Physiol Rev, 2007. **87**(1): p. 245-313.
140. Harfouche, R., et al., *Roles of reactive oxygen species in angiopoietin-1/tie-2 receptor signaling.* FASEB J, 2005. **19**(12): p. 1728-30.
141. Ushio-Fukai, M. and R.W. Alexander, *Reactive oxygen species as mediators of angiogenesis signaling. Role of NAD (P) H oxidase.* Molecular and cellular biochemistry, 2004. **264**(1-2): p. 85-97.
142. Binker, M.G., et al., *EGF promotes invasion by PANC-1 cells through Rac1/ROS-dependent secretion and activation of MMP-2.* Biochemical and biophysical research communications, 2009. **379**(2): p. 445-450.
143. Steinbrenner, H., et al., *Tumor promoter TPA stimulates MMP-9 secretion from*

human keratinocytes by activation of superoxide-producing NADPH oxidase. Free Radic Res, 2005. **39**(3): p. 245-53.

144. Overall, C.M. and C. Lopez-Otin, *Strategies for MMP inhibition in cancer: innovations for the post-trial era.* Nat Rev Cancer, 2002. **2**(9): p. 657-72.
145. Napoli, S., et al., *Functional roles of matrix metalloproteinases and their inhibitors in melanoma.* Cells, 2020. **9**(5): p. 1151.
146. Marusak, C., et al., *The thiirane-based selective MT1-MMP/MMP2 inhibitor ND-322 reduces melanoma tumor growth and delays metastatic dissemination.* Pharmacol Res, 2016. **113**(Pt A): p. 515-520.
147. Kim, J.K. and J.A. Diehl, *Nuclear cyclin D1: an oncogenic driver in human cancer.* J Cell Physiol, 2009. **220**(2): p. 292-6.
148. Tang, Z., et al., *GEPIA: a web server for cancer and normal gene expression profiling and interactive analyses.* Nucleic Acids Research, 2017. **45**(W1): p. W98-W102.
149. Chang, K., et al., *The Cancer Genome Atlas Pan-Cancer analysis project.* Nature Genetics, 2013. **45**(10): p. 1113-1120.
150. *The Genotype-Tissue Expression (GTEx) pilot analysis: Multitissue gene regulation in humans.* Science, 2015. **348**(6235): p. 648.
151. Livak, K.J. and T.D. Schmittgen, *Analysis of relative gene expression data using real-time quantitative PCR and the 2− ΔΔCT method.* methods, 2001. **25**(4): p. 402-408.
152. Wang, C., et al., *Dual inhibition of PCDH9 expression by miR-215-5p up-regulation in gliomas.* Oncotarget, 2017. **8**(6): p. 10287-10297.
153. Xie, Z., et al., *Lnc-PCDH9-13: 1 is a hypersensitive and specific biomarker for early hepatocellular carcinoma.* EBioMedicine, 2018. **33**: p. 57-67.
154. Zhu, P., et al., *Protocadherin 9 inhibits epithelial–mesenchymal transition and cell migration through activating GSK-3β in hepatocellular carcinoma.* Biochemical and biophysical research communications, 2014. **452**(3): p. 567-574.
155. Pu, S., et al., *Up-to-date catalogues of yeast protein complexes.* Nucleic Acids Research, 2008. **37**(3): p. 825-831.
156. Lee, S.-W., et al., *Direct mass spectrometric analysis of intact proteins of the yeast large ribosomal subunit using capillary LC/FTICR.* Proceedings of the National Academy of Sciences, 2002. **99**(9): p. 5942-5947.
157. Ngounou Wetie, A.G., et al., *Protein–protein interactions: switch from classical methods to proteomics and bioinformatics-based approaches.* Cellular and Molecular Life Sciences, 2014. **71**(2): p. 205-228.
158. Luo, W. and C. Brouwer, *Pathview: an R/Bioconductor package for pathway-based data integration and visualization.* Bioinformatics, 2013. **29**(14): p. 1830-1831.
159. Yu, G., et al., *clusterProfiler: an R package for comparing biological themes among gene clusters.* Omics: a journal of integrative biology, 2012. **16**(5): p. 284-287.
160. Zar, J.H., *Biostatistical analysis*. 1999, NJ: Prentice Hall. 523.

161. Hochberg, Y. and Y. Benjamini, *More powerful procedures for multiple significance testing.* Statistics in medicine, 1990. **9**(7): p. 811-818.
162. Cohen, J., *A coefficient of agreement for nominal scales.* Educational and psychological measurement, 1960. **20**(1): p. 37-46.
163. Fabregat, A., et al., *Reactome diagram viewer: data structures and strategies to boost performance.* Bioinformatics (Oxford, England), 2018. **34**(7): p. 1208-1214.
164. Benjamini, Y. and Y. Hochberg, *On the adaptive control of the false discovery rate in multiple testing with independent statistics.* Journal of educational and Behavioral Statistics, 2000. **25**(1): p. 60-83.
165. Zhou, Y., et al., *Metascape provides a biologist-oriented resource for the analysis of systems-level datasets.* Nat Commun, 2019. **10**(1): p. 1523.
166. Yeşil, S., et al., *Amelanotic melanoma misdiagnosed as a diabetic foot ulcer.* Journal of Diabetes and its Complications, 2007. **21**(5): p. 335-337.
167. Hakamifard, A., et al., *The heel amelanotic melanoma, a rare subtype of skin cancer misdiagnosed as foot ulcer: A case report.* International Wound Journal, 2020. **17**(3): p. 819-822.
168. Kobayashi, J., et al., *A report of amelanotic malignant melanoma of the esophagus diagnosed appropriately with novel markers: A case report.* Oncology letters, 2018. **15**(6): p. 9087-9092.
169. Park, H.C., H.S. Kang, and J.S. Kim, *An amelanotic malignant melanoma of the lip: unusual shape and atypical location.* Cutis, 2013. **92**(5): p. 250-252.
170. Srivastava, P., et al., *Primary amelanotic malignant melanoma of cervix masquerading as squamous cell carcinoma presenting with extensive metastases.* Case Reports, 2018. **2018**: p. bcr-2018-224723.
171. Ohnishi, Y., et al., *A rare case of amelanotic malignant melanoma in the oral region: Clinical investigation and immunohistochemical study.* Oncology letters, 2015. **10**(6): p. 3761-3764.
172. Gong, H.-Z., H.-Y. Zheng, and J. Li, *Amelanotic melanoma.* Melanoma Research, 2019. **29**(3): p. 221-230.
173. Schadendorf, D., et al., *Melanoma.* The Lancet, 2018. **392**(10151): p. 971-984.
174. Brinker, T.J., et al., *Deep neural networks are superior to dermatologists in melanoma image classification.* European Journal of Cancer, 2019. **119**: p. 11-17.

FUNDING

This research was supported by Guangdong Provincial Natural Science Foundation of China 2016A030313682, Guangdong Provincial Natural Science Foundation of China 2020A1515010281, Guangdong Provincial Natural Science Foundation of China 2020A1515011218, and Guangzhou Civic Natural Science Foundation of China 202002030106.

ACKNOWLEDGMENTS

Time passed fast. The days when I entered Italy, Marche, Ancona and this university are still vivid. Thanks to Professor Battino Maurizio for his constant concern, support and supervision. Without his mentor, the "doctoral student" of Europe could have been a daydream, let alone receive a first-class education on Italy's Adriatic coast of Ancona. As a PhD candidate three years ago, I was confused about research, a lack of scientific research planning, and had no confidence. Under careful guidance of Prof. Battino and Dr. Francesca Giampieri, I have been gradually building confidence and becoming to clarify the research direction and goals. Without his supervision and encouragement, my PhD research project would not be successfully completed. I would like to express my highest sincere thanks. Prof. Battino's humorous and rigorous academic attitude and extremely charming personality also deeply influences me. In addition to the careful guidance in study and scientific research, he has given me meticulous care in life. Additionally, Prof. Battino also teaches me a lot of life principles and keeps inspiring me.

Sincerely thanks to Prof. Rongyi Chen of the Dermatology Hospital (Southern Medical University) for his guidance and help, Ms. Hui-zhi Yang of Guangdong Medical University for her experiment support and Dr. Francesca Giampieri of the Marche Polytechnic University, Italy for her patient guidance; Prof. Zhao-jun Wei of Hefei University of Technology, China for his kindly support; Dr. Patricia Reboredo-Rodriguez of the University of Vigo, Spain for their selfless help; and the care and help of Dr. Danila Cianciosi, Dr. Sadia Afrin, Dr. Massimiliano Gasparrini, Dr. Johura Ansary and Dr. Tamara Y. Forbes-Hernandez. Special thanks to Prof. Stefeno Bompadre for his enthusiastic help and selfless guidance during my studies and research at the Marche Polytechnic University.

Thanks to my friends, Dr. Amnah Nasim, Dr. Zuhua Wang and Dr. Bin Zhang who gave me great supports and encouragements when I was frustrated and confused.

Thanks to all the friends who have cared, paid attention, and helped me in my life.

Thanks to my families for their company and supports. Their supports and encouragements are my spiritual pillar and my strongest back forever.

I also want to thank all the professors, colleagues, friends, and loved ones who have not mentioned here and who have cared for and helped me. Thank reviewers and defense committee experts for spending time on checking and reviewing this thesis.

Jiaojiao Zhang

April 8th, 2021 in SH, China